CRANFIELD UNIVERSITY

Yirong Leng

Understanding the fundamentals of bio-struvite biomineralization in wastewater

School of Water, Energy and Environment
Research degree

PhD
Academic Year: 2014 - 2018

Supervisor: Ana Soares
March 2018

CRANFIELD UNIVERSITY

School of Water, Energy and Environment
Research degree

PhD

Academic Year 2014 - 2018

Yirong Leng

Understanding the fundamentals of bio-struvite biomineralization in wastewater

Supervisor: Ana Soares
March 2018

This thesis is submitted in partial fulfilment of the requirements for the degree of Doctor of Philosophy

ABSTRACT

Biomineralization can be exploited to recover phosphorus from liquid streams and wastewater through struvite (i.e. bio-struvite) production. However, there is a lack of knowledge regarding the attributes of the microorganisms involved, the mechanisms of bio-struvite production and possible benefits, compared with traditional struvite recovery. Five microorganisms (*Bacillus pumilus*, *Brevibacterium antiquum, Halobacterium salinarum, Myxococcus xanthus and Idiomarina loihiensis*) were investigated in this PhD thesis. Investigation of the biochemical properties and growth conditions indicated that all the microorganisms were able to use proteins as carbon source and produced urease (except *I. loihiensis*). Although *B. pumilus*, *M. xanthus* and *I. loihiensis* were identified as facultative anaerobes, bio-struvite biomineralization only occurred under aerobic conditions. In synthetic solution, all the microorganisms grew to increase the pH and release ammonia to create supersaturated conditions for struvite crystallization. Bio-struvite crystals occurred when supersaturation index of struvite achieved 0.6 to 0.8. The bio-struvite produced in *B. antiquum* and *I. loihiensis* cultures presented high homogeneity (both morphology and size) and intracellular vesicle-like structures, packed with electron-dense granules/materials, were observed, indicating a biological controlled mineralization process. On the other side, bio-struvite formation by *B. pumilus*, *H. salinarum and M. xanthus* was identified as a biological induced mineralization process. The same biomineralization mechanisms were identified in municipal wastewater. However the wastewater limited microbial growth and changed the dominant crystal morphology from coffin-lid to trapezoidal-platy shape. Compared with abiotic struvite precipitation, bio-struvite could be produced at low initial phosphorus concentrations in wastewater (≥19.7 mg/L), expanding the type and quality of waste streams that could be applied for nutrient recovery. Furthermore, the recovered bio-struvite presented high purity and met heavy metal limits set for inorganic fertilizers regulation. Overall, bio-struvite production presented important advantages, in comparison with abiotic struvite, and the process should be further developed for implementation at pilot and full scale.

Keywords:

bio-struvite; biomineralization; mechanism; biochemical property; growth rate; intracellular granule; crusted cell; morphology; municipal wastewater; nutrient recovery; inorganic phosphorus fertilizer; *Bacillus pumilus*; *Brevibacterium antiquum; Halobacterium salinarum; Myxococcus xanthus; Idiomarina loihiensis*

ACKNOWLEDGEMENTS

First and foremost, I would like to express my sincere and respectful gratitude to Dr Ana Soares for the patient guidance, the tremendous support, the insightful comments and the enthusiastic encouragement during this research project. I am thankful to her for always being approachable, and helping me out from various crises, scientific or otherwise. It is an honour and a privilege for me to share of her exceptional scientific knowledge and extraordinary human qualities. I am thankful to Professor Elise Cartmell and Dr Andrew McLeod for providing professional advices and valuable sources of knowledge. My appreciation is extended to Dr Raffaella Villa, for her kindly support and encouragement to help dispel the dark moments in my PhD journey.

I would like to gratefully acknowledge the team of laboratory technicians, Jane Hubble, Richard Andrews, Paul Barton, Nuannat Simmons and Xianwei Liu, for offering me with useful instrumental expertise and great practical assistance. Without their support I could not have accomplished the data collection necessary to do this research.

Thanks also to Francisco, Hanlin, Sarah, Ekwu, Kasia, Kanming, Lloyd, Matthew, Stephanie, Joana and Sabrina, for all the helps with my lab works, and for sharing with me the knowledge, creative ideas, happiness and enthusiasm. The same extends to everyone else in the Water Science Institute, for making my time here such a great experience.

To finish, I would like to especially appreciate my family, for always being there and believing in me. Although they are thousands miles away, they have made me feel their accompanying throughout my study.

TABLE OF CONTENTS

LIST OF FIGURES

LIST OF TABLES

LIST OF EQUATIONS

LIST OF ABBREVIATIONS

ATP	Adenosine triphosphate
AAS	Atomic absorption spectroscopy
BCM	Biologically induced mineralization
BIM	Biologically controlled mineralization
BNR	Biological nutrient removal
BSA	Bovine serum albumin
Ca-P	Calcium phosphate
CIs	Confidence intervals
COO^-	Carboxylate groups
DI water	Deionized water
DMSO	Dimethyl sulfoxide
DNA	Deoxyribonucleic acid
DO	Dissolved oxygen
Dv	Volume based particle size distribution
Dv_{50}	The value of the particle diameter at 50% in the cumulative distribution on the basis of volume
Dv_{90}	The value of the particle diameter at 90% in the cumulative distribution on the basis of volume
DW	Dry weight
EBPR	Enhanced biological phosphorus removal
EDX	Energy dispersive X-ray
EPS	Extracellular polymeric substances
ESPP	European sustainable phosphorus platform
EURASYP	European association for specialty yeast products
FFD	Full factorial experiment
FOMA	Organic and organo-mineral fertiliser manufacturers´ Spanish association
FWG	Fertilisers working group
ICP-MS	Inductively coupled plasma mass spectrometry
K_{sp}	Solubility product constant

N	Nitrogen
P	Phosphorus
PAOs	Phosphorus accumulating organisms
PE	Population equivalent
PI	Propidium Iodide
PO_4-P	Ortho-phosphate
poly-P	Polyphosphate
QA	Qualitative assessment
RCF	Relative centrifugal force
RNA	Ribonucleic acid
RSM	Response surface methodology
S-layer	Surface layer
SCOD	Soluble chemical oxygen demand
SDL	Sludge dewatering liquor
SEM	Scanning electron microscope
SI	Supersaturation index
$SI_{struvite}$	Supersaturation index of struvite
SG	SYBR® Green I
SSA	Sewage sludge ash
TEM	Transmission electron microscopy
UWWTD	Urban wastewater treatment directive
wt%	Weight percent
% w/v	Percent weight/volume
WWTP	Wastewater treatment plant
WWTPs	Wastewater treatment plants
XRD	X-ray powder diffractometer

1 Introduction

1.1 Background

Biomineralization is a widespread phenomenon in nature. It refers to a series of processes involving selective extraction, uptake and incorporation of elements from the local environment into functional structures under strict biological control (e.g. specific enzymes) (Mann, 2001). Organisms can exert their influences on construction and synthesis of minerals through changes in local chemistry and different shaping strategies (Weiner and Dove, 2003). Compared with inorganic minerals, biologically produced minerals (i.e. biominerals) are often characterized with more intricacy and morphological diversity, and generally associated with biological functions such as structural support, mechanical strength, protection, storage, etc. (Mann, 2001; Weiner and Dove, 2003). The biomineralization process plays an important role in the life science (Mann, 2001), and now attracts growing interest in materials chemistry (Arakaki et al., 2015), cleaning technology and resources recovery (Ike, Yamashita and Kuroda, 2017; Nancharaiah and Lens, 2015; Soares et al., 2014).

Phosphorus (P) is an essential element for all living organisms. About 25% of the biominerals contain phosphate (PO_4), and calcium (Ca^{2+}), magnesium (Mg^{2+}) and iron ($Fe^{2+/3+}$) are the three major metal elements found in P biominerals (e.g. brushite, struvite) (Weiner and Dove, 2003). Soares et al. (2014) reported the biological struvite (i.e. bio-struvite) in municipal wastewater, where *Brevibacterium antiquum* and *Bacillus pumilus* not only removed P to final orthophosphate (PO_4-P) of 1.5-2.1 mg/L, but also recovered P as struvite (28.6 mg P/L wastewater by *B. antiquum*), relating biomineralization with P recovery in wastewater.

1.1.1 Significance of phosphorus recovery

P plays a positive role in driving biochemical reactions involved in formation and function of deoxyribonucleic acid (DNA), adenosine triphosphate (ATP), cell membranes, bone, teeth, etc., and there is no substitute for P in nature (Elser, 2012). In agriculture industry, for decades, P has been widely used in

commercial fertilizer, and the phosphate rock is currently the main source for fertilizer production, with 62 billion tons of deposits in the ground, of which only about 16% is mineable (Gilbert, 2009). U.S. Geological Survey (2017) on phosphate rock showed that currently about 240-260 million tons of phosphate rock are mined globally each year. It in turns raised concerns about exhaustion of phosphate rock in both quality and quantity, and the requirement of reducing the reliance on phosphate rock by providing potential substitutes for the current commercial P fertilizer.

On the other hand, the wasted P entering surface water (e.g. lake, river, reservoir, coastal and marine environment) may lead to eutrophication problems, i.e., the enrichment of nutrients water booms the algae growth, leading to intensive consumption of dissolved oxygen, and thus affects the ecosystem (Conley et al., 2009). The Urban Wastewater Treatment Directive (UWWTD) imposes regulation about P limit in the wastewater discharged to sensitive areas (i.e. catchment of waters where wastewater from treatment plants beyond 10000 population equivalent (PE) has to undergo nutrient removal), either below 2 mg/L (plants of 10000-100000 PE) or 1 mg/L (plants >100000 PE) (UWWTD, 2013). The permitted P discharge concentrations can be achieved in traditional sludge-based P removal process, either by chemical precipitation (e.g. iron or aluminum salts) or through biological incorporation (e.g. polyphosphate-accumulating organisms) resulting in P accumulation in sludge (Cornel and Schaum, 2009). Both chemical and biological approaches resulted in P accumulation (90%) into the sewage sludge and increased sludge volume (Cornel and Schaum, 2009; Doyle and Parsons, 2002). However, the direct land application of sewage sludge and incinerated sewage sludge ash is still controversial due to the limited P bioavailability, co-precipitation induced heavy metals contamination (e.g. chromium, mercury, arsenic), and/or organic contaminants (e.g. pharmaceuticals, pathogens, viruses) (Melia et al., 2017).

The concentrated P in waste streams can promote P mineral scaling, for example struvite, within pipelines at wastewater treatment plant (WWTP), especially in high P-load side streams such as dewatering liquor of anaerobically digested sludge (75-300 mg PO_4-P/L) (Desmidt et al., 2015) and

centrate returned to the head of the WWTP (50-200 mg P/L) (Ivanov et al., 2005).

1.1.2 Struvite and bio-struvite as solution for P recovery

Struvite ($MgNH_4PO_4.6H_2O$) is an orthorhombic mineral with low water solubility and thermodynamic instability (Table 1-1) (Le Corre et al., 2009; Frost, Weier and Erickson, 2004). Struvite precipitation has been proved a promising technology to help recover P from concentrated wastewater streams and to affordably deliver a high-purity, plant available and market ready product (Cornel and Schaum, 2009; Egle, Rechberger and Zessner, 2015). A proposed acceptable purity range of struvite, as inorganic fertilizer, requires the nutrients' content equivalent to 10.0-13.9% P, 4.6-6.3% N and 13.1-18.1% magnesium oxide (MgO) (ESPP, 2015). Struvite is recognized as an ideal alternative to most phosphate fertilizers (Gantenbein and Khadka, 2009). It can be used as slow-release fertilizer in agriculture industry due to its low solubility in water (De-Bashan and Bashan, 2004). Besides high quantity of readily plant-available nutrients and constant composition that protecting the soil from excess mineral poisoning, the application of struvite has many other advantages including easy storage, transportation and handling, no heavy metal (theoretically) and no foul odor (Gantenbein and Khadka, 2009).

Table 1-1 Physiochemical properties of struvite

Nature	Description
Chemical Name	magnesium ammonium phosphate hexahydrate
Chemical Formula	$MgNH_4PO_4.6H_2O$
Specific Gravity	245.4 g/mol
Density	1.711 g/cm^3 (measured); 1.705 g/cm^3 (calculated) (Mindat, 2018)
Hardness	1.5 – 2 (Mindat, 2018)
Color	colorless, white, yellow, brownish, light grey (Mindat, 2018)
Crystal system	orthorhombic (Mindat, 2018)
Decomposition point	<40 °C (Frost, Weier and Erickson, 2004)
Solubility	insoluble in alkali; low in water: 0.18 mg/L at 25 °C; high in acid: 1.78 mg/L in 0.01 M hydrochloric acid (25 °C), 3.3 mg/L in 0.001 M hydrochloric acid (25 °C) (Le Corre et al., 2009)
Solubility product constant	$10^{-13.26}$ (Ohlinger, Young and Schroeder, 1998)

Conventional abiotic struvite precipitation applied P-rich waste streams (P >100 mg/L), pH adjustment (8-10) and seeding (e.g. sand, struvite powder) to achieve economical rewarding P recovery (Liu et al., 2013; Rittmann et al., 2011). However, bio-struvite, as an innovation way to remove and recover P from wastewater, has potential use at lower P concentration (7.5-30.5 mg PO_4-P/L) with no requirement to adjust pH (Soares et al., 2014). The bio-struvite recovered from wastewater was observed the same orthorhombic crystal as standard struvite (Soares et al., 2014). Furthermore, *B. antiquum* was reported to be capable of using organic and condensed P resources in wastewater, besides inorganic P, for bio-struvite production, which expanded the ranges of potential wastewater sources for phosphorus recovery (Simoes, 2017).

Bio-struvite was firstly identified in the 19th century (Robinson, 1889). Naturally occurred bio-struvite has been observed associating with various organic

substances in a state of biodegradation as in kidney stones, guano deposits, manures, animal excreta and sediments rich in organic remains (Jimenez-Lopez et al., 2007). At WWTP, the pH, temperature and availability of nutrients make it possible to apply microorganisms for P recovery by bio-struvite (Table 1-2).

Table 1-2 Typical characteristics of municipal wastewater

	Description
pH	5.9-8.2 (Jaffer et al., 2002); 6.5-8.5 (Henze and Comeau, 2008).
Temperature	13-27°C (Jaffer et al., 2002)
Chemical oxygen demand	Low in raw municipal wastewater (200-480 mg/L), but high in digester supernatant (200-2000 mg/L) and in reject water (600-3000 mg/L) (Henze and Comeau, 2008)
Phosphorus	Raw municipal wastewater typically contains 6-25 mg/L total P, of which 4-15 mg/L is inorganic PO_4-P, and the rest is organic P and polyphosphate (Henze and Comeau, 2008). About 90% of total P was removed to sludge (Cornel and Schaum, 2009). The PO_4-P in sludge centrate varied with raw resource and treatment process, from 44-167 mg/L (Jaffer et al., 2002) to 44-300 mg/L (Munch and Barr, 2001) and to 75-300 mg/L (Desmidt et al., 2015). The centrate returned to plant headwork contained 50-200 mg P/L (Ivanov et al., 2005).
Ammonium	Raw municipal wastewater typically contains 20-74 mg/L NH_4-N (Henze and Comeau, 2008). Considerable amount of NH_4-N can be produced in the digester. Typically there are plenty of NH_4-N in digester supernatant (100-500 mg/L) and in reject water (95-450 mg/L) (Henze and Comeau, 2008).
Magnesium	Most Mg^{2+} concentrated in sludge, only 6.7-44 mg/L in liquor (Jaffer et al., 2002). The centrate of sludge contain 7-26 mg/L Mg^{2+} (Munch and Barr, 2001).

However, the mechanisms involved in bio-struvite biomineralization may vary with organisms, and such variation reflects different levels of regulations on the biomineralization process (Mann, 2001). Based on the degree of biological control, biomineralization are traditionally grouped as biologically induced mineralization (BIM) and biologically controlled mineralization (BCM) (Frankel and Bazylinski, 2003). Specific minerals, such as magnetite, can be produced via both BIM and BCM processes, depending on the organism applied (e.g. iron-reducing bacteria for BIM, magnetotactic bacteria for BCM) (Frankel and Bazylinski, 2003).

1.1.3 Biologically induced mineralization and biologically controlled mineralization processes

BIM process takes place in an open environment, and occurs as a result of interactions between metabolic activity and local environment, typically by various metabolic products (e.g. pH, carbon dioxide, nitrogen compounds) extruding across the cell membrane via active pumping or passive diffusion to interact with ions and compounds presented in the environment (Frankel and Bazylinski, 2003). The lack of cellular control in BIM process often leads to adventitiously precipitation of minerals with poorly defined mineral specificity and crystallinity (e.g. inclusion of impurity), and heterogeneity in mineral morphology and size (Frankel and Bazylinski, 2003). BIM minerals were frequently observed with similar crystallochemical features as their inorganic counterparts precipitated by chemical reactions (Mann, 2001). The microbial cell surfaces and polymeric materials (e.g. extracellular polymeric substances-EPS) are negative charged groups (e.g. peptidoglycan, lipopolysaccharide), and are often recognized as important sites for surface-mediated mineralization by non-specific electrostatic interactions between such negatively charged groups and cations (e.g. calcium, iron, magnesium) (Arias, Cisternas and Rivas, 2017; Decho, 2000; Frankel and Bazylinski, 2003). Such electrostatic interactions can increase the local supersaturation for mineral nucleation, therefore lead to mineralization along the cell surface where the resulting mineral particles may remain firmly attached. This process is referred as epicellular mineralization (Mann, 2001). In open waters, cells encrusted completely in the mineral

deposits can settle to form sediments when gravitation overcomes buoyancy (Mann, 2001). BIM minerals typically nucleate and grow epicellularly (e.g. oxidation of manganese (II) by cyanobacteria) or extracellularly (e.g. struvite by *Proteus* bacteria) (Frankel and Bazylinski, 2003; Prywer and Torzewska, 2010). In contrast, in BCM, the organisms create isolated compartments (e.g. intracellular lipid vesicle, extracellular organic matrix) under certain conditions, to allow a great degree of control on the synthesis of minerals (Bazylinski and Frankel, 2003; Mann, 2001). The mineralization sites are sealed off from the general environment, allowing application of specialized regulations, including chemistry, space, morphology, structure and construction, on the crystallochemical property of minerals (Mann, 2001). The structures and compositions of these compartmentalized microenvironments are genetically programmed. More specifically, the lipid vesicle usually has a bilayer membrane where the lipid molecules are embedded with precisely regulated functional proteins (e.g. selective transport of molecules). In the case of BCM through a specifically designed organic matrix (e.g. protein, polysaccharide), these are precisely regulated to form a three-dimensional framework, where local supersaturation can be achieved by ion diffusion or ion transportation (e.g. cation-loaded vesicles) to the site of mineralization (Mann, 2001; Weiner and Dove, 2003). As a result of genetic and many levels of specialized control, the biomineral formation is not as sensitive to open environmental parameters as in BIM process, and allows self-assembly to form higher order structures/crystals (Weiner and Dove, 2003). These BCM minerals are characterized structurally as well-ordered crystals with species-specific crystallochemical properties and homogeneity of size and morphology, whereby they are distinguished from BIM minerals (Bazylinski and Frankel, 2003; Mann, 2001). Typical BCM process occurs intracellularly (e.g. magnetosome in magnetotactic bacteria) and extracellularly (e.g. bone formation) (Weiner and Dove, 2003).

1.1.4 Bio-struvite biomineralization

A wide spectrum of microorganisms, mainly bacteria, was identified to be involved in bio-struvite biomineralization in controlled condition (e.g. synthetic media) or real wastewater (Table 1-3).

Table 1-3 Microorganisms described to be able to form bio-struvite

Microorganisms	Strain	Domain	Source
Arthrobacter sp	Not specified	Bacteria	Synthetic media (Pérez-García et al., 1990)
Bacillus pumilus	GB 34	Bacteria	Wastewater (Soares et al., 2014)
Brevibacterium antiquum	DSM 21545	Bacteria	Wastewater (Simoes et al., 2017; Soares et al., 2014); synthetic media (Smirnov et al., 2005)
Chromohalobacter marismortui	ATCC 17056	Bacteria	Synthetic media (Rivadeneyra et al., 2006b)
Enterobacter sp.	EMB19	Bacteria	Synthetic media (Sinha et al., 2014)
Halobacterium salinarum	DSM 671	Archaea	Wastewater (Soares et al., 2014); synthetic media (Smirnov et al., 2005)
Halobacterium distributum	VKM-1739	Archaea	Synthetic media (Smirnov et al., 2005)
Idiomarina abyssalis	ATCC BAA-312	Bacteria	Marine media (González-Muñoz et al., 2008)
Idiomarina baltica	DSM 15154	Bacteria	Marine media (González-Muñoz et al., 2008)
Idiomarina loihiensis	DSM 15497; MAH1	Bacteria	Marine media (González-Muñoz et al., 2008)
Myxococcus coralloides	D	Bacteria	Synthetic media (Gonzalez-Muñoz et al., 1993)
Myxococcus xanthus	CECT 422	Bacteria	Wastewater (Soares et al., 2014); synthetic media (Omar, Gonzalez-Muñoz and Peñalver, 1998; Da Silva et al., 2000)
Paramecium tetraurelia	51s	Eukarya	Synthetic media (Grover, Rope and Kaneshiro, 1997)
Proteus mirabilis	Not specified	Bacteria	Artificial urine (Prywer and Torzewska, 2010)
Pseudomonas sp	Not specified	Bacteria	Synthetic media (Pérez-García et al., 1990)
Staphylococcus aureus	Not specified	Bacteria	Nutrient agar (Beavon and Heatley, 1963)
Streptomyces acidiscabies	E13	Bacteria	Synthetic media (Haferburg et al., 2008)

As a crystallization-based process, the nucleation and crystal growth of bio-struvite is firstly driven by chemical principles such as solubility, supersaturation and interfacial free energy, where energy barrier for homogeneous nucleation (i.e. in uniform phase) in supersaturated solution (supersaturated zone) can be reduced with presence of external substrate (e.g. insoluble particles, EPS), to allow onset of heterogeneous nucleation and crystal growth within metastable zone until thermodynamic liquid/solid equilibrium (struvite phase) is achieved (DeYoreo and Vekilov, 2003; Flemming and Wingender, 2010) (Figure 1-1). A reduced solubility (e.g. by cooling), an increased supersaturation (e.g. by raising pH or reactant concentrations) and a reduced interfacial free energy (e.g. by adding insoluble particles or EPS) can increase the nucleation rate and shorten the induction time (DeYoreo and Vekilov, 2003) (Figure 1-1). However, it might be difficult to use chemical reaction-based software (e.g. PHREEQC) (Charlton and Parkhurst, 2011) to predict the bio-struvite production in wastewater due to the significant difference between bio-struvite crystallization and abiotic struvite precipitation, especially in the case of BCM, where more complex conditions can be anticipated owing to several levels of regulations other than control only from chemistry (Mann, 2001).

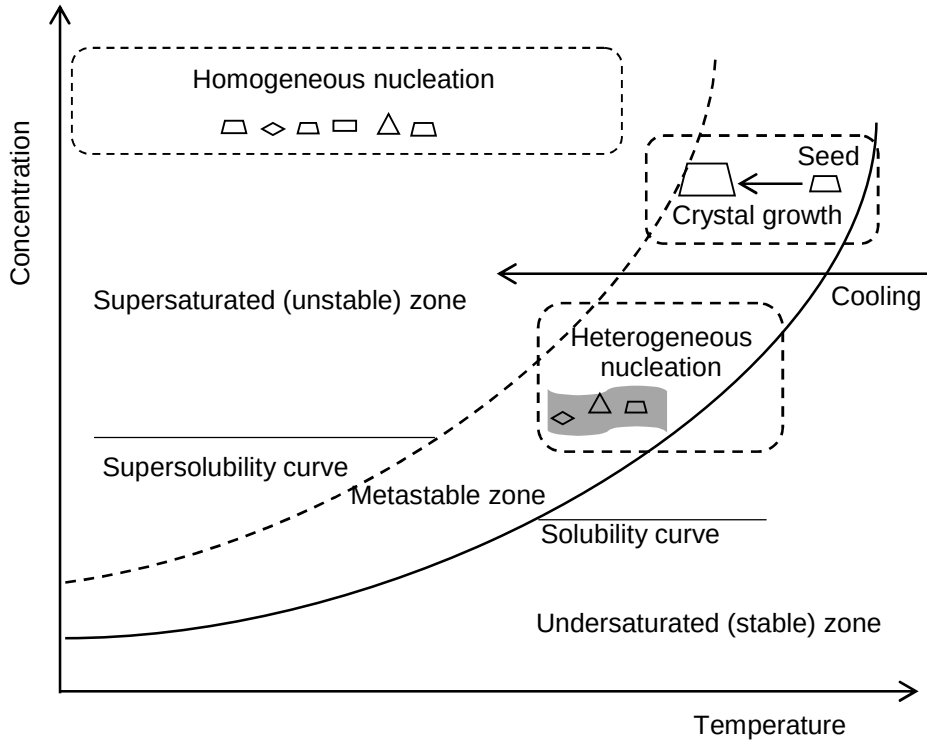

Figure 1-1 Schematic representation of a two-dimensional phase diagram of crystallization (adapted from Le Corre et al., 2009)

Microbial activities were reported to play important roles in bio-struvite crystallization and morphology fine-tuning. The *B. antiquum* was reported to accumulate P within cells (Simoes et al., 2017), and the observation of intercellular bio-struvite within *B. antiquum* and *P. tetraurelia* cells (Grover, Rope and Kaneshiro, 1997; Smirnov et al., 2005), is two of the rare reports associate with BCM process, which indicates the bio-struvite of more controlled structure and composition (Mann, 2001). The *Enterobacter sp.* is another bacterium suggested to be involved in bio-struvite BCM production due to the homogeneity of crystallochemical property (Sinha et al., 2014). Many microorganisms, especially urease-producing bacteria, were reported to be capable to metabolically breakdown nitrogenous organic compounds (e.g. urea, proteins, amino acids) to release NH_4-N, and increase the solution pH, together with the presence of PO_4-P and Mg^{2+} in the environment, to create supersaturated solution for bio-struvite crystallization (Sinha et al., 2014; Udert,

Larsen and Gujer, 2003). Furthermore, the accumulations of cations (e.g. Mg^{2+}) on the negatively charged organic substance (e.g. cell out-layer, EPS) via molecular interaction can lead to heterogeneous nucleation where the barrier energy is reduced (González-Muñoz et al., 2010), although it may lead to poor crystallinity of mineral if the non-specific interaction occurs in fluid with high complexity (e.g. wastewater) (Mann, 2001).

The previously reported morphology of bio-struvite crystals varied form coffin-lid shape (Prywer and Torzewska, 2009) to long-bar shape (González-Muñoz et al., 2008) and to trapezoidal-platy shape (Kemacheevakul et al., 2015). Crystal morphology is dominantly determined by the slow-growing surfaces (DeYoreo and Vekilov, 2003). Although the equilibrium shape of a crystal can be predicted from the surface structures and their bonding interactions, many low and high molecule weight additives can induce habit modification by changing the relative growth rates of different crystal faces via narrowing the growth range or through molecular-specific interactions (DeYoreo and Vekilov, 2003; Sadowski, Prywer and Torzewska, 2014). For example, the electrostatic interaction between negative charged polysaccharide in *P. mirabilis* cell membrane framework and molecular structures of the crystal surface was reported to allow the microbial cells to change the struvite morphology by enhancing specific crystal faces (Prywer and Torzewska, 2009, 2010).

The mechanism involved in the bio-struvite biomineralization in wastewater, are still not documented or understood. The capability of the microorganisms to produce bio-struvite needs to be linked to their biochemical property to improve understanding of the fundamentals. Furthermore, bio-struvite biomineralization needs to be compared with abiotic struvite precipitation, especially the mineral quality and the potential application in wastewater within wide range of PO_4-P, to reveal the benefits of bio-struvite. Consequently, further research on how the microorganisms remove and recover nutrients from wastewater by bio-struvite, and the influence of wastewater on the biomineralization process, has to be investigated to prompt the application of bio-struvite biomineralization in wastewater.

1.2 Aims and objectives

This project aimed at understanding the fundamentals of bio-struvite mineralization by five selected microorganisms in synthetic media and municipal wastewater. A comparison between bio-struvite and abiotic struvite production in municipal wastewater lead to the understanding of biomineralization application to the wastewater industry.

The project key objectives were to:

A. Identify the factors that impact the growth of the selected microorganisms and bio-struvite production.

B. Understand the mechanisms of bio-struvite mineralization in synthetic solutions and municipal wastewater and investigate the influence of wastewater on bio-struvite biomineralization.

C. Evaluate the potential application of bio-struvite biomineralization process to wastewater treatment plants and potential use of bio-struvite as inorganic fertilizer.

1.3 Thesis plan

This thesis is presented in a paper format. A summary of the thesis chapter structure and connection between chapters is presented in Figure 1-2. All thesis sections have been written by the first author, Yirong Leng and supervisor's comments provided by Dr. Ana Soares. Laboratory work and all data analysis were undertaken by Yirong Leng.

Chapter 2 investigates the biochemical properties of the selected microorganisms, and the capability of the selected microorganisms to produce bio-struvite under aerobic and anaerobic conditions. The outcome of Chapter 2 was used to support the experimental planning of Chapter 3, 4 and 5. This chapter is written up in preparation for submission to the journal *Chemosphere*.

Chapter 3 identifies the mechanisms involved in bio-struvite production in controlled conditions (i.e. synthetic solution). This chapter also investigates the influence of microbial activity on the crystal morphology. The outcome of Chapter 3 was used to compare with the mechanisms involved in bio-struvite

biomineralization in wastewater in Chapter 4. This chapter is written up in preparation for submission to the journal *Bioresource Technology*.

Chapter 4 identifies the mechanisms of bio-struvite production in wastewater. This chapter also examines the influence of wastewater on P recovery and the crystal morphology, size and purity, by comparison with the outcome of Chapter 3. The outcome of Chapter 4 was used to support the experimental plan for Chapter 5. This chapter is written up in preparation for submission to the journal *Bioresource Technology*.

Chapter 5 compares bio-struvite mineralization with abiotic struvite spontaneous precipitation in terms of crystal production, necessary solution supersaturation and crystal purity and heavy metal contents. This chapter also investigates the significance of initial PO_4-P and NH_4-N in municipal wastewater for PO_4-P removal and bio-struvite production among the selected microorganisms. This chapter is written up in preparation for submission to the journal *Water Research*.

Chapter 6 details and generates overall synthesis of the PhD research outputs and discussed the contributions to knowledge and the areas for future work.

Chapter 7 brings together the overall conclusions of the project in relation to the objectives.

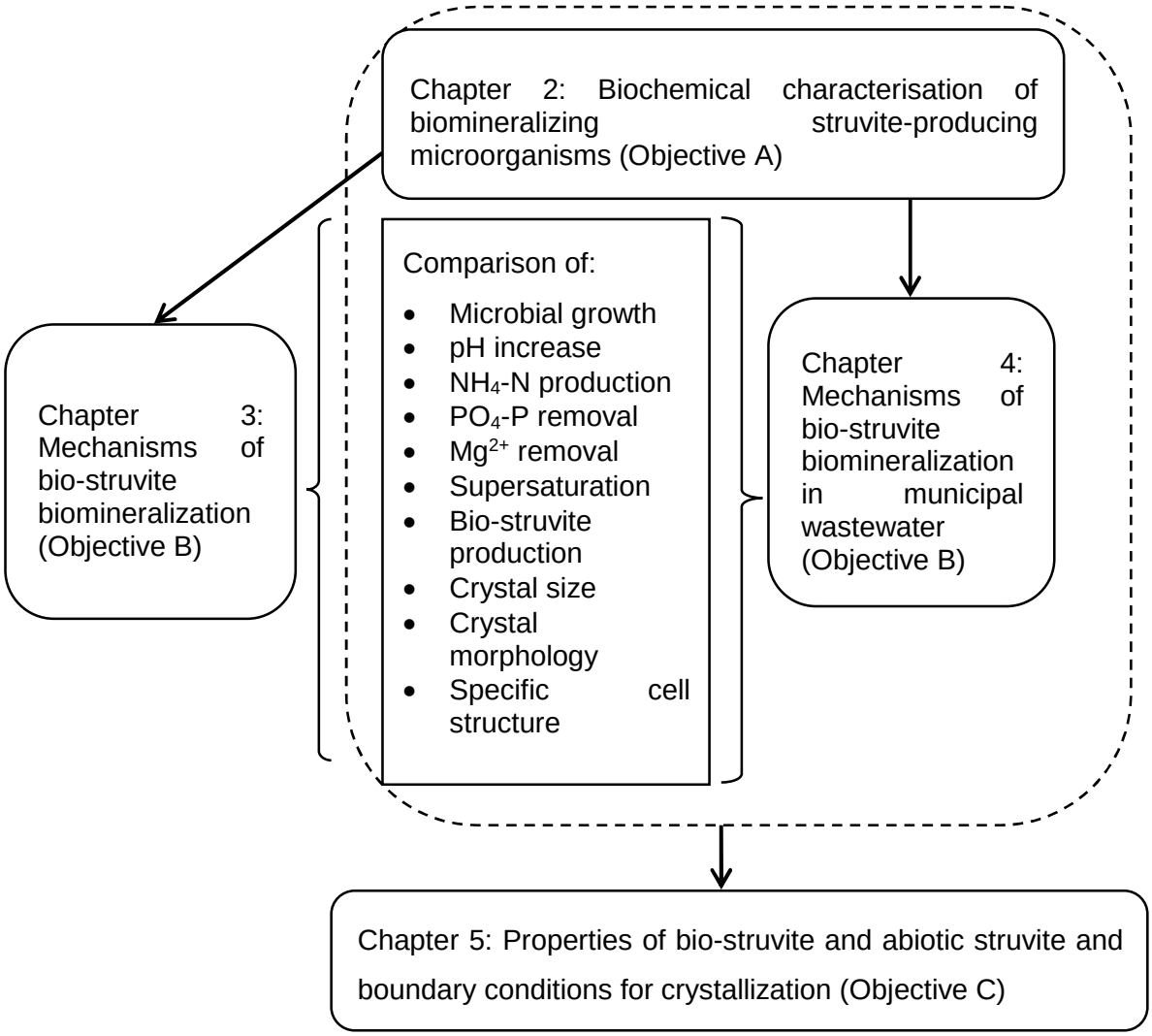

Figure 1-2 Schematic representation of thesis structure and chapter interaction

1.4 References

Arakaki, A. et al. (2015) 'Biomineralization-inspired synthesis of functional organic/inorganic hybrid materials: organic molecular control of self-organization of hybrids', *Organic & biomolecular chemistry*, 13(4) Royal Society of Chemistry, pp. 974–989.

Arias, D. et al. (2017) 'Biomineralization mediated by ureolytic bacteria applied to water treatment: a review', *Crystals*, 7(11), p. 345.

Bazylinski, D. A. and Frankel, R.B. (2003) 'Biologically controlled mineralization in prokaryotes', *Reviews in Mineralogy and Geochemistry*, 54(1), pp. 217–247.

Beavon, J. and Heatley, N.G. (1963) ‘The occurrence of struvite (magnesium ammonium phosphate hexahydrate) in microbial cultures’, *Journal of General Microbiology*, 31(1), pp. 167–169.

Charlton, S.R. and Parkhurst, D.L. (2011) ‘Modules based on the geochemical model PHREEQC for use in scripting and programming languages’, *Computers and Geosciences*, 37(10), pp. 1653–1663.

Conley, D.J. et al. (2009) ‘Controlling eutrophication: nitrogen and phosphorus’, *Science*, 323, pp. 1014–1015.

Cornel, P. and Schaum, C. (2009) ‘Phosphorus recovery from wastewater: needs, technologies and costs’, *Water Science and Technology*, 59(6), pp. 1069–1076.

Le Corre, K.S. et al. (2009) ‘Phosphorus recovery from wastewater by struvite crystallization: a review’, *Critical Reviews in Environmental Science and Technology*, 39(6), pp. 433–477.

De-Bashan, L.E. and Bashan, Y. (2004) ‘Recent advances in removing phosphorus from wastewater and its future use as fertilizer (1997-2003)’, *Water Research*, 38(19), pp. 4222–4246.

Decho, A.W. (2000) ‘Microbial biofilms in intertidal systems: an overview’, *Continental Shelf Research*, 20(10–11), pp. 1257–1273.

Desmidt, E. et al. (2015) ‘Technology global phosphorus scarcity and full-scale P- recovery techniques : a review’, *Critical Reviews in Environmental Science and Technology*, 45(4), pp. 336–384.

DeYoreo, J.J. and Vekilov, P.G. (2003) ‘Principles of crystal nucleation and growth’, *Reviews in Mineralogy and Geochemistry*, 54(1), pp. 57–93.

Doyle, J.D. and Parsons, S. a. (2002) ‘Struvite formation, control and recovery’, *Water Research*, 36(16), pp. 3925–3940.

Egle, L. et al. (2015) ‘Overview and description of technologies for recovering phosphorus from municipal wastewater’, *Resources, Conservation and Recycling*, 105, pp. 325–346.

Elser, J.J. (2012) ‘Phosphorus: a limiting nutrient for humanity?’, *Current Opinion in Biotechnology*, 23(6), pp. 833–838.

ESPP (2015) *Proposed E.U., fertiliser regulation criteria for recovered struvite*. Available at: https://phosphorusplatform.eu/images/download/ESPP struvite FR criteria proposal sent 24-4-15.pdf (Accessed: 1 February 2018).

Flemming, H.C. and Wingender, J. (2010) ‘The biofilm matrix’, *Nature Reviews Microbiology*, 8(9), pp. 623–633.

Frankel, R.B. and Bazylinski, D. a (2003) ‘Biologically induced mineralization by bacteria’, *Reviews in Mineralogy and Geochemistry*, 54(1), pp. 95–114.

Frost, R.L. et al. (2004) ‘Thermal decomposition of struvite: implications for the decomposition of kidney stones’, *Journal of Thermal Analysis and Calorimetry*, 76(3), pp. 1025–1033.

Gantenbein, B. and Khadka, R. (2009) *Struvite recovery from urine at community scale in Nepal. Final Project Report Phase I*. Duebendorf, Switzerland.

Gilbert, N. (2009) ‘The disappearing nutrient’, *Nature*, 461(7265), pp. 716–718.

Gonzalez-Muñoz, M.T. et al. (1993) ‘Struvite production by *Myxococcus coralloides D*’, *Chemosphere*, 26(10), pp. 1881–1887.

González-Muñoz, M.T. et al. (2008) ‘Ca-Mg kutnahorite and struvite production by *Idiomarina* strains at modern seawater salinities’, *Chemosphere*, 72(3), pp. 465–472.

González-Muñoz, M.T. et al. (2010) ‘Bacterial biomineralization: new insights from *Myxococcus*-induced mineral precipitation’, *Geological Society, London, Special Publications*, 336(1), pp. 31–50.

Grover, J.E. et al. (1997) ‘The occurrence of biogenic calcian struvite, $(Mg,Ca)NH_4PO_4.6H_2O$, as intracellular crystals in *Paramecium*’, *Journal of Eukaryotic Microbiology*, 44(4), pp. 366–373.

Haferburg, G. et al. (2008) ‘Ni-struvite - A new biomineral formed by a nickel resistant *Streptomyces acidiscabies*’, *Chemosphere*, 72(3), pp. 517–523.

Henze, M. and Comeau, Y. (2008) ‘Wastewater characterization’, in *Biological wastewater treatment: principles modelling and design*. IWA publishing, pp. 33–52.

Ike, M. et al. (2017) ‘Microbial removal and recovery of metals from wastewater’, in Yoshida, T. (ed.) *Applied Bioengineering: Innovations and Future Directions*. Weinheim, Germany: Wiley-VCH Verlag GmbH & Co. KGaA, pp. 573–595.

Ivanov, V. et al. (2005) ‘Phosphate removal from the returned liquor of municipal wastewater treatment plant using iron-reducing bacteria’, *Journal of Applied Microbiology*, 98(5), pp. 1152–1161.

Jaffer, Y. et al. (2002) ‘Potential phosphorus recovery by struvite formation’, *Water Research*, 36(7), pp. 1834–1842.

Jimenez-Lopez, C. et al. (2007) ‘Biomineralization induced by *Myxobacteria*’, *Communicating Current Research and Educational Topics and Trends in Applied Microbiology*, 1, pp. 143–154.

Kemacheevakul, P. et al. (2015) ‘Effect of magnesium dose on amount of pharmaceuticals in struvite recovered from urine’, *Water Science and Technology*, 72(7), pp. 1102–1110.

Liu, Y. et al. (2013) ‘Magnesium ammonium phosphate formation, recovery and its application as valuable resources: a review’, *Journal of Chemical Technology*

and Biotechnology, 88(2), pp. 181–189.

Mann, S. (2001) *Biomineralization : principles and concepts in bioinorganic materials chemistry*. Oxford University Press.

Melia, P.M. et al. (2017) 'Chemosphere trends in the recovery of phosphorus in bioavailable forms from wastewater', *Chemosphere*, 186 Elsevier Ltd, pp. 381–395.

Mindat (2018) *Struvite*., *Mindat.org* Available at: https://www.mindat.org/min-3811.html (Accessed: 5 February 2018).

Munch, E. V. and Barr, K. (2001) 'Controlled struvite crystallisation for removing phosphorus from anaerobic digester sidestreams', *Water Research*, 35(1), pp. 151–159.

Nancharaiah, Y. V. and Lens, P.N.L. (2015) 'Selenium biomineralization for biotechnological applications', *Trends in Biotechnology*, 33(6), pp. 323–330.

Ohlinger, K.N. et al. (1998) 'Predicting struvite formation in digestion', *Water Research*, 32(12), pp. 3607–3614.

Omar, N. Ben et al. (1998) 'Struvite crystallization on *Myxococcus* cells', *Chemosphere*, 36(3), pp. 475–481.

Pérez-García, I. et al. (1990) 'Struvite formation by *Arthrobacter* sp. and *Pseudomonas* sp.: the influence of agitation', *Chemosphere*, 20(1–2), pp. 243–251.

Prywer, J. and Torzewska, A. (2010) 'Biomineralization of struvite crystals by *Proteus mirabilis* from artificial urine and their mesoscopic structure', *Crystal Research and Technology*, 45(12), pp. 1283–1289.

Prywer, J. and Torzewska, A. (2009) 'Bacterially induced struvite growth from synthetic urine: experimental and theoretical characterization of crystal morphology', *Crystal Growth and Design*, 9(8), pp. 3538–3543.

Rittmann, B.E. et al. (2011) 'Capturing the lost phosphorus', *Chemosphere*, 84(6), pp. 846–853.

Rivadeneyra, M.A. et al. (2006) 'Carbonate and phosphate precipitation by *Chromohalobacter marismortui*', *Geomicrobiology Journal*, 23(2), pp. 89–101.

Robinson, H. (1889) 'On the formation of struvite by microorganisms', *Proceedings of Cambridge Philosophical Society*., Vol.6, pp. 360–362.

Sadowski, R.R. et al. (2014) 'Morphology of struvite crystals as an evidence of bacteria mediated growth', *Crystal Research and Technology*, 49(7), pp. 478–489.

Da Silva, S. et al. (2000) 'Effect of culture conditions on the formation of struvite by *Myxococcus xanthus*', *Chemosphere*, 40(12), pp. 1289–1296.

Simoes, F. (2017) *A new route to recover phosphorus from waste water: biological struvite production School*. Cranfield University.

Simoes, F. et al. (2017) ‘Understanding the growth of the bio-struvite production Brevibacterium antiquum in sludge liquors’, *Environmental Technology*, Taylor & Francis, pp. 1–10.

Sinha, A. et al. (2014) ‘Microbial mineralization of struvite: a promising process to overcome phosphate sequestering crisis’, *Water Research*, 54, pp. 33–43.

Smirnov, A. et al. (2005) ‘Formation of insoluble magnesium phosphates during growth of the archaea *Halorubrum distributum* and *Halobacterium salinarium* and the bacterium *Brevibacterium antiquum*’, *FEMS Microbiology Ecology*, 52(1), pp. 129–137.

Soares, A. et al. (2014) ‘Bio-Struvite: A new route to recover phosphorus from wastewater’, *Clean - Soil, Air, Water*, 42(7), pp. 994–997.

U.S. Geological Survey (2017) *Mineral commodity summaries 2017: U.S. Geological Survey*. Reston, Virginia.

Udert, K.M. et al. (2003) ‘Biologically induced precipitation in urine-collecting systems’, *Water Science and Technology: Water Supply*, 3(3), pp. 71–78.

UWWTD (2013) *Phosphorous Standard for Wastewater Treatment Works*.

Weiner, S. and Dove, P.M. (2003) ‘An overview of biomineralization processes and the problem of the vital effect’, *Reviews in mineralogy and geochemistry*, 54(1), pp. 1–29.

2 Biochemical characterization of bio-mineralizing struvite-producing microorganisms

Authors: Y Leng, A Soares

Cranfield Water Science Institute, Vincent Building, Cranfield University, Bedfordshire, MK43 0AL, UK

Abstract

The biochemical properties of selected microorganisms (*Bacillus pumilus, Brevibacterium antiquum, Myxococcus xanthus, Halobacterium salinarum* and *Idiomarina loihiensis*) known for their ability to produced struvite through biomineralization were investigated. All five microorganisms grew at mesophilic temperatures (22–34°C), were able to produce urease (except *I. loihiensis*), and use bovine serum albumin as a carbon source. *I. loihiensis* was characterized as a facultative anaerobe able to use oxygen and nitrate as electron acceptors. Growth rate 0.15 1/h was measured for *I. loihiensis* at pH 8.0, NaCl 3.5% w/v, and calcium 28 mg/L. The growth rates for the other microorganisms tested were 0.14-0.43 1/h, and the preferred conditions were pH 7–7.3, NaCl ≤1% w/v, and no calcium. All the microorganisms produced struvite, as identified by morphological and XRD analysis, only under aerobic conditions. The biological struvite yield was between 1.5–1.7 g/L, the ortho-phosphate removal and recovery was 55–76% and 46–54%, respectively, the magnesium removal and recovery was 92–98% and 83–95%, respectively. Large crystals (>300 μm) were observed, and with coffin-lid and long-bar shapes being the dominant morphology of the biological struvite crystals. The characterization of the biochemical properties of the selected microorganisms is critical for reactor and process design, as well as operational conditions, to promote phosphorus recovery from waste streams.

Keywords: biomineralization, struvite, biochemical properties, phosphorus recovery

2.1 Introduction

Many microorganisms are of industrial importance and their application for human benefit depends on their unique biochemical properties, such as the capability to produce industrially important organic substances including alcohols, ketones, enzymes, and antibiotics (Castillo Martinez et al., 2013). The temperature, pH, electron acceptor, and organic carbon source are among the most important environmental parameters affecting microbial growth and organic substance synthesis (Silva et al., 2016). For industrial exploitation of microorganisms, the investigation of biochemical characterization makes it possible to design appropriate processes and control the operational conditions to meet microbial requirements.

Biological struvite (bio-struvite) has been identified as a new way to recover phosphorus (P) from municipal wastewater streams (Soares et al., 2014). Microorganisms play an important role in bio-struvite mineralization through different metabolic activity (Sinha et al., 2014) and by construction or synthesis of specific structures and substances (Arias, Cisternas and Rivas, 2017). Five microbial strains, *Halobacterium salinarum, Bacillus pumilus, Brevibacterium antiquum, Myxococcus xanthus,* and *Idiomarina loihiensis*, have been reported to be involved in bio-struvite formation in liquid streams (González-Muñoz et al., 2008; Soares et al., 2014). Some biochemical characteristics of these microbial strains are presented in Table 2-1.

The Gram-positive bacteria *B. pumilus* and *B. antiquum* distinguish themselves from the other three microorganisms by their thick peptidoglycan cell membrane. *B. pumilus* and *M. xanthus* can form endospores under stress conditions (González-Muñoz et al., 2010; Robinson, 2014). *M. xanthus, I. loihiensis* and *H. salinarum* were reported to produce extracellular polymeric substances (EPS), which may fix cations and contribute to mineral heterogeneous nucleation and precipitation (González-Muñoz et al., 2008, 2010; Merroun et al., 2003). Most of the selected microorganisms can use oxygen (O_2) as an electron acceptor (Table 2-1). *H. salinarum* has been reported to be able to use dimethyl sulfoxide (DMSO) as an electron acceptor

under anaerobic conditions, and use photophosphorylation in the presence of light (Losensky et al., 2017). *B. pumilus* ATCC 27142 (Koh, Morehouse and Chandler, 1956) and a novel strain Gisella Alcaraz- *B. pumilus* (Alcaraz, 2015) were suggested to be facultative anaerobes, but the electron acceptor was not mentioned. *B. pumilus* and *M. xanthus* can use carbohydrates as a carbon source but this does not apply to *B. antiquum* and *H. salinarum* (Mesbah and Wiegel, 2005; Poza, Sieiro and Villa, 2004; Robinson, 2014; Shivaji et al., 2006). According to the literature, all the selected microorganisms can use protein/amino acids as a carbon source (González-Muñoz et al., 2010; Hou et al., 2004; Mesbah and Wiegel, 2005; Poza, Sieiro and Villa, 2004; Robinson, 2014; Shivaji et al., 2006; Trujillo and Goodfellow, 2015). The utilization of organic carbon sources depended on enzyme production, and the rates of enzyme-catalyzed reactions optimally perform under an appropriate range of temperature, pH and salinity (James, Edwards and Dawson, 1991; Silva et al., 2016). The selected microbial strains have been reported to grow at pH between 5.5 and 9, and mesophile /thermophilic temperature ranging from 20–45 °C (González-Muñoz et al., 2008; Janssen, Wireman and Dworkin, 1977; Mesbah and Wiegel, 2005; Robinson, 2014; Shivaji et al., 2006). The halotolerant microorganisms *B. antiquum, H. salinarum* and *I. loihiensis* can live in environments containing high sodium chloride (NaCl) (Gavrish et al., 2004; González-Muñoz et al., 2008; Mesbah and Wiegel, 2005), particularly *H. salinarum*, which can survive at extremely high NaCl concentrations (17.4~30.16 %) (Mesbah and Wiegel, 2005) (Table 2-1).

However, although some of the biochemical properties and growth conditions of selected microorganism have been reported in the literature, some of the values are controversial and further verification and characterization is required.

Statistical design is recognized as an approach widely used in parameter screening and optimization studies (Massey et al., 2009). By using such design, Simoes et al. (2017) investigated the significant factors required for *B. antiquum* growth, and maximized the microbial growth rate in wastewater streams by screening and optimizing a number of factors.

This study aims to investigate the biochemical properties of microorganisms selected owing to their capability to produce bio-struvite in synthetic solutions. Knowledge of such parameters will allow the design of reactors/processes and operational conditions to ensure proliferation of the selected microorganisms, and even out-compete other microorganisms in mixed cultures, for eventual enhanced P recovery by bio-struvite from waste streams.

Table 2-1 Biochemical properties of the five tested microorganisms

		B. pumilus	*M. xanthus*	*B. antiquum*	*I. loihiensis*	*H. salinarum*
Strain		MTCC 1640	CECT 422	DSM 21545	MAH1 /CECT 5996	DSM 671
Type		Bacteria	Bacteria	Bacteria	Bacteria	Archaea
Gram reaction		+	-	+	-	-
Cell shape		rod	rod	short rod/ coccoid	rod	rod
Size		0.6~0.7 x 2.0~3.0 µm	0.5 x 6 µm	0.6~1 µm	0.3~0.5 x 0.6–2 µm	0.5-1 x 1–6 µm
Motility		+	+	-	+	+
Endospore forming		+	+	-	-	-
O_2 requirement/tolerance		aerobic	aerobic	aerobic	aerobic	facultative anaerobic, photophosphorylation at low oxygen concentration with light
Electron acceptor		O_2	O_2	O_2	O_2	O_2, dimethyl sulfoxide
Extracellular polymeric substances synthesis		not documented	+	not documented	+	+
Preferred organic carbon source	carbohydrate	arabinose, mannitol, xylose, glucose, lactose, acetone	glucose	not able to directly use	not documented	not able to directly use
	protein/amino acid	casein, lysine,	amino acids	casein, amino acid	amino acid	lysine, ornithine, arginine
	Other	citrate, sucrose, D-trehalose, starch, D-glucose, D-arabinose, D-xylose, gelatin	not documented	gluconate, urea, gelatin, salicin, sorbitol	L-alaninamide	gelatin
Growth temperature		20~40 °C, optimum 30~35 °C	14~40°C, optimum 34~36°C	7°C, <37°C; optimum 24~26°C	2 ~ 43°C; optimum 28 ~37 °C	20~55°C, optimum 35~50°C
Growth pH		6~8, optimum at 7	5.5–9.0, optimum at 7	5.5~10, optimum at 7	not documented	5.5~8, optimum at 7
Growth in NaCl		0~2 %	not documented	0~18 %, optimum 3%	0.7~20 %, optimum 2~6 %	17.4~30.16 %, optimum 20.3 %
References		(Robinson, 2014; Shivaji et al., 2006)	(González-Muñoz et al., 2010; Janssen, Wireman and Dworkin, 1977; Merroun et al., 2003; Poza, Sieiro and Villa, 2004; Shimkets, 2000)	(Gavrish et al., 2004; Robinson, 2014; Simoes et al., 2017; Trujillo and Goodfellow, 2015)	(González-Muñoz et al., 2008)	(Losensky et al., 2017; Mesbah and Wiegel, 2005; Mormile et al., 2003; Oren et al., 1995; Zinder and Dworkin, 2006)

2.2 Methodology

2.2.1 Microbial strains and culture solution

Five microbial strains were used in this study: *H. salinarum* (DSM 671, German Resource Centre for Biological Material, Germany), *B. pumilus* (GB43, LGC Standards, Middlesex, UK), *B. antiquum* (DSM 21545, German Resource Centre for Biological Material, Germany), *M. xanthus* (CECT 422, Spanish Type Culture Collection, University of Valencia, Paterna, Spain) and *I. loihiensis* (MAH1 /CECT 5996, Spanish Type Culture Collection, University of Valencia, Paterna, Spain). The microorganism were grown in synthetic B41 solution comprising 4 g/L yeast extract, 2 g/L magnesium sulfate heptahydrate ($MgSO_4.7H_2O$) and 2 g/L di-potassium hydrogen phosphate (Da Silva et al., 2000). The solution was autoclaved at 121°C for 20 min and cooled to room temperature (22–24°C). For inoculation of each microbial strain, 100 ml synthetic B41 solution in a 250 ml E-flask was inoculated with 0.9% w/v NaCl pre-washed pure cultures of the selected microorganisms that were grown for 96 h. The E-flasks were sealed with foam stoppers and incubated on an orbital shaker (Stuart model SSL1, Fisher Scientific, UK) at 150 RPM at room temperature. The halophile *I. loihiensis* was grown in B41 solution with 1% w/v NaCl (González-Muñoz et al., 2008).

2.2.2 Gram staining and enzyme production

Microorganisms in their early exponential phase of growth (8 h) were characterized by the Gram-staining method (Claus, 1992).

A KB002™ HiAssorted Biochemical Test Kit (HiMedia Laboratories Pvt. Ltd, India) was used to characterize the pure cultures, according to the manufacturer's instructions. All tests were completed in triplicate and a non-inoculated control was maintained under identical conditions.

2.2.3 Statistical design of experiments

To investigate the impact of growth conditions on microorganisms, a full factorial experiment (FFD) was designed with five factors: temperature, initial pH, NaCl, calcium (Ca^{2+}, by calcium chloride) and bovine serum albumin (BSA) as an additional carbon source (Table 2-2). The tests were completed at temperatures

varying from 6–34°C and pH 5.5–8.5 to cover the range of temperatures and pH of municipal wastewater (Tchobanoglous et al., 2003). Calcium concentration was adjusted to 28 mg/L to mimic the Ca^{2+} concentrations in municipal wastewater (Gassama et al., 2015). The NaCl content varied between 0.5–3.5% w/v based on previously reported data (Table 2-1).

Table 2-2 Factors and variable values used in the full factorial design experiment

		Levels		
Factors		low	mediate	high
Temperature (°C)		6	20	34
NaCl (% w/v)	*M. xanthus*	0	0.5	1
	B. pumilus	0	1	2
	B. antiquum	0.5	2	3.5
	I. loihiensis	0.5	2	3.5
	H. salinarum	0.5	2	3.5
Initial pH		5.5	7	8.5
BSA (g/L)		0		4
Ca^{2+} (mg/L)		0		28

Three factors (temperature, NaCl and initial pH) at the 3-level and two factors (Ca^{2+} and BSA) at the 2-level corresponded to $3^3 \times 2^2$ combinations of recipes, which were studied in duplicate and thus generated $3^3 \times 2^2 \times 2 = 216$ tests for each microorganism. The initial and final intact cell counts were examined to generate the overall cell increase that was used as a response to the factors investigated. The experimental data were fitted to a first-order linear regression model or second-order polynomial regression model considering linear and quadratic forms of the independent factors. The response surface methodology (RSM) (Bezerra et al., 2008) was applied to examine the significant relationship ($p<0.01$) between cell increase and the five growth factors, as well as the significant two-factor interactions ($p<0.01$). The RSM was also used to determine the optimal conditions that jointly maximize the cell increase by applying a multiple response optimization. All statistical design and analysis was performed using Minitab 17 (Minitab, 2010).

2.2.4 Microbial cultivation under investigated growth conditions

Microorganisms were grown in 96-well (12x8) sterile microplates with working volume about 250 µL per well (Corning™, Fisher scientific, UK). Each well contained 234 µL solution and 26 µL inoculum. To prepare the solutions corresponding to the FFD recipes (Table 2-2), synthetic B41 solution with different NaCl concentration was autoclaved and mixed with 0.22 µm sterile filtered (Sartorius Stedim Biotech, Germany) BSA and $CaCl_2$ concentrated solutions. The initial pH was adjusted by 0.1 M sodium hydroxide (NaOH) and 0.1 M hydrogen chloride (HCl) sterile solutions. To minimize liquid evaporation from each well, only the central wells (10 x 6) of the microplate were used for microbial inoculation, and the edge and corner wells of the microplate were used for the non-inoculated controls (Syberg, 2016). Breathable rayon film (VWR Collection, VWR, UK) was used to seal the microplates to stop cross-contamination and to achieve uniform air and gas exchange, while also reducing liquid evaporation for each well. The sealed microplates were then placed inside a cube humidity chamber with four ventilation holes at each bottom corner and with a water reservoir inside. The humidity chamber was covered with a lid for incubation at constant temperatures of 6, 20 and 34 °C for 106, 66 and 48h incubation time, respectively. The application of a humidity chamber was found to reduce liquid evaporation from 150 to 20–25 µL/well by the end of the incubation period.

2.2.5 Microbial cultivation at different dissolved oxygen levels

After applying those growth conditions which indicated the maximum increase of intact cell count, the microorganisms were inoculated into synthetic solutions at two dissolved oxygen (DO) levels using sacrificial glass vials. For microbial cultivation under aerobic conditions, 30 ml sacrificial glass vials containing 9 ml synthetic B41 solution pre-adjusted in terms of pH, NaCl, Ca^{2+} and BSA were inoculated with 1 ml inoculum and sealed with breathable film. The DO in the 30 mL vials varied between 6–8 mg/L. For microbial cultivation under anoxic/anaerobic conditions, synthetic B41 solution was pre-adjusted in terms of pH, NaCl and bubbled with nitrogen (N_2) gas after passing through a 0.22 µm sterile filter (Sartorius Stedim Biotech, Germany) at a rate of 30 min/L. The 10 ml sacrificial glass vials were sealed with a nontoxic butyl rubber stopper and autoclaved (121°C, 20 min). The DO in the 10 mL vials was close to 0 mg/L. Concentrated solution of calcium chloride and BSA, and 1 ml

inoculum were then added using a sterile disposable syringe and needle (VWR, UK). The capability of *I. loihiensis* to grow under anoxic conditions was examined in synthetic solutions with absence of oxygen but with 0.5 g/L sodium nitrate ($NaNO_3$). The glass vials were placed inside humidity chambers and incubated on an orbital shaker-incubator (MAXQ5000 M6, Thermo Scientific, UK) at 150 RPM for 120 h. Samples were taken for examination at regular intervals (4–24h) through sacrificial vials. All tests were completed in triplicate, and non-inoculated controls were maintained under identical conditions.

2.2.6 Abiotic struvite formation

Abiotic struvite was prepared by mixing 200 mL 0.05 M $MgSO_4 \bullet 7H_2O$ (pre-adjusted to pH 9 with 1 M NaOH) with 100 ml 0.2 M $NH_4H_2PO_4$ (pre-adjusted to pH 9 with 1 M NaOH) (Le Corre et al., 2005). Concentrated BSA solution was added to the mixture at a rate of 4 g/L and incubated on an orbital shaker at 150 RPM at room temperature for 24 h.

2.2.7 Crystal isolation, purification and determination

The microorganisms were inoculated in 500 mL B41 media in 1 L sterile Duran bottles, sealed by a breathable film, and incubated under the investigated optimal growth conditions at agitation rate 150 RPM for 120 h. At the end of the incubation period, the samples were filtered through a 10 µm nylon-mesh filter (Plastok, UK) and the crystals were washed with deionized (DI) water twice. The isolated crystals were air-dried at 37°C for 2 h and weighed to determine crystal yields. The pure crystals were then identified by use of an X-ray powder diffractometer (XRD, D5000, Siemens / Bruker, Germany).

2.2.8 Analytical methods

The intact cell count was examined by the SYBR Green I (SG) - propodium iodide (PI) co-staining method using a flow cytometer (BD accuri C6, BD Biosciences, US) (Nocker et al., 2017). Solution DO and pH values were determined with a portable dissolved oxygen meter (HQ40D, HACH, UK) and digital pH-meter (Jenway 3540, Bibby Scientific, UK). The concentrations of soluble chemical oxygen demand (SCOD), ortho-phosphates (PO_4-P), ammonium (NH_4-N) and nitrate (NO_3-N) were monitored with Merck Spectroquant® test kits. Magnesium (Mg^{2+}) was measured by atomic absorption spectroscopy (AAS, Analyst 800, PerkinElmer, UK) equipped with

flaming and electrothermal spectrometers. A high-resolution microscope (L-series upright compound microscope, Division of GT vision Ltd, UK) was applied for observation of Gram-stained cultures and crystal morphology in microbial cultures.

2.3 Results and discussion

2.3.1 Microbial properties and enzyme production

B. pumilus and B. antiquum were identified as Gram-positive and *M. xanthus, H. salinarum* and *I. loihiensis* as Gram-negative, which is in agreement with previously published information (Table 2-1). In particular, *B. pumilus* formed crusted two-cell clusters or tetrads in B41 media, which were not observed in the other four microbial cultures. Such cell structures did not grow in size but had the potential to aggregate together or onto the crystal surface. Similar cell structures were observed as mineralized *Thiomargarita* embryo-infesting cells (Bailey et al., 2007), and as silica spheroids onto the cell sheath in microbial silicification (Yee et al., 2003). Thus, the crusted cell structures observed during *B. pumilus* growth in this study is proposed associated with the biomineralization.

The cell outer layer of both Gram-positive and Gram-negative bacteria are mainly negatively charged, which enables the membrane to interact with and accumulate cations (e.g. Mg^{2+}, Ca^{2+}) onto the surface for mineral precipitation (Frankel and Bazylinski, 2003; Macaskie et al., 2000; Orange et al., 2009). Gram-positive microorganisms have been reported to have increased potential to form a thick mineral crust around the cell due to their thick outer layer (~ 25 nm thick) of peptidoglycan (Westall, 1999). Furthermore, EPS such as the secreted carboxylate (COO^-) groups or phosphate groups may bond into the peptidoglycan framework within the Gram-positive cell envelope to increase the electronegative charge density, robustness and interactions with dissolved metal ions (Schultze-Lam et al., 1996). It is suggested that *B. pumilus* can form mineral particles along the cell surface during exponential phase in solutions rich in PO_4-P and Mg^{2+}, and the mineral particles firmly attach to the cell surface to form completely encrusted cell minerals.

The biochemical characterization tests demonstrated varied enzyme production amongst the microorganisms investigated. Nevertheless, it was quite remarkable to

observe that *H. salinarum*, *B. antiquum, B. pumilus* and *M. xanthus* were capable of using ornithine as a carbon source and produce urease. Biomineralization of struvite by urease-producing microorganisms in the urinary tract has been reported, leading to the formation of kidney stones, that typically contain 15–20% struvite (Arias, Cisternas and Rivas, 2017; Coe, Evan and Worcester, 2005; Prywer and Torzewska, 2010). A wide range of microorganisms, particularly the bacteria, can produce many different types of enzymes, including exoenzymes to degrade proteins into molecules (small peptides and amino acids) and endoenzymes to further degrade and then metabolize these molecules, whereby they use proteins/amino acids as a carbon source to gain energy (Christy, Gopinath and Divya, 2014). Urease activity, as well as the degradation of proteins, can generate energy for microbial growth and produce ammonia as a by-product, which raises the pH and release NH_4-N to combine with PO_4-P and Mg^{2+} for struvite precipitation (Sadowski, Prywer and Torzewska, 2014).

I. loihiensis was the only microorganism investigated in this study that did not produce urease and also the only one that showed a positive reaction of NO_3^- reduction to nitrite (NO_2^-). The latter is a common phenomenon in anoxic respiration, where NO_3^- was used as an electron acceptor.

All five microorganisms showed neither positive nor negative results in terms of lysine utilization. They were also found to be negative for their ability to use citrate and carbohydrates (including glucose, arabinose, lactose, adonitol and sorbitol) as a carbon source, and for phenylalanine deamination and hydrogen sulfide production. The only exception was that *B. pumilus* showed a 33% positive result for glucose utilization. The results obtained in this study partially agree with the organic carbon source utilization presented in Table 2-1.

2.3.2 Identification of significant factors that impacted microbial growth

By applying the multi-response surface methodology, BSA was identified to have a significant positive linear correlation ($p<0.01$) with microbial growth. All selected microorganisms were able to use BSA as a carbon source (Table 2-3). Temperature, pH and NaCl were also identified as being significant for microbial growth for all selected microorganisms. A Ca^{2+} of 28 mg/L was identified to be required for growth of *I. loihiensis* but not for *M. xanthus* growth, and was a non-significant factor for the

other three microorganisms (Table 2-3). In addition, temperature correlated with other factors ($p<0.01$) within the investigated range of 6-34 °C. The growth of *B. pumilus, M. xanthus*, and *I. loihiensis* had a positive linear correlation with the temperature and reached a peak value at 34 °C, while the relationship between temperature and cell count for *H. salinarum* and *B. antiquum* fitted a quadratic trend and the growth peak occurred between 22–24 °C. Thus, the optimal growth temperature for the investigated microorganisms was within the mesophilic range of temperatures (Table 2-3). Quadratic relationships between pH and microbial growth were also observed. *B. pumilus, H. salinarum B. antiquum* and *M. xanthus* preferred neutral pH (7.1–7.3), while *I. loihiensis* was observed to adapt to a mild alkaline pH of 8.0 (Table 2-3). Furthermore, *I. loihiensis*, as a halophile, distinguished itself from the other four microorganisms by its ability to adapt to grow at high NaCl concentration (3.5% w/v); whereas the other four microorganisms preferred relatively low NaCl concentration (0.5–1% w/v) (Table 2-3). A coefficient of determination (R-sq) was introduced to display the degree of the regression model approximates of the real data points, with an R-sq >0.7 typically being considered good (Grace-Martin, 2012). In this study, the coefficient of determination was within the range of 0.71–0.94 (Table 2-3), and thus the regression model could well explain the variability of the response data.

Table 2-3 Significant growth factors (main effect, $p<0.01$) and preferred growing conditions defined by multi-response surface methodology

	Temperature (°C)	NaCl (% w/v)	pH	BSA (g/L)	Ca^{2+} (mg/L)	R-sq*
B. pumilus	34	0.5	7.3	4	Ns	0.94
H. salinarum	24	0.5	7.1	4	Ns	0.8
B. antiquum	22	0.5	7.3	4	Ns	0.85
M. xanthus	34	1	7.2	4	0	0.73
I. loihiensis	34	3.5	8.0	4	28	0.71

Ns - Non-significant correlation to microbial growth

* - R-sq ranges from 0 to 1, indicated the proportion of variation that can be explained by the regression model. R-sq =1 indicates that the regression line perfectly fits the data.

2.3.3 Optimized microbial growth at different dissolved oxygen levels

No lag phase of microbial growth was observed under aerobic conditions (DO = 6-8 mg/L) and the exponential phase occurred within 24/48 h incubation time. The growth rates (μ) for the different microorganisms under aerobic condition varied between 0.14 and 0.43 1/h (Figure 2-1). The relatively high growth rate of *B. pumilus* (0.35 1/h) and *M. xanthus* (0.24 1/h) under anaerobic conditions distinguished themselves from the other three microbial strains (μ ≤0.04 1/h) (Figure 2-1a). The growth rate of *I. loihiensis* under anoxic condition was 0.12 1/h (Figure 2-1a), and >99.5% of NO_3-N was reduced by the end of the incubation time. The final microbial intact cell counts for *B. pumilus, B. antiquum*, *M. xanthus, H. salinarum, I. loihiensis* were 80–94% lower under anaerobic conditions and 66% lower under anoxic conditions, than those under aerobic conditions (Figure 2-1 b). The SCOD removal was 20–27% under aerobic conditions, 0–2% under anaerobic conditions and only 6% by *I. loihiensis* under anoxic conditions (Figure 2-1 c). Aerobic respiration, using oxygen as an electron acceptor, is known to enable microorganisms to convert energy from carbon source to adenosine triphosphate (ATP) production more efficiently than using other electron acceptors (Kader & Saltveit, 2003). Hence, it was unsurprising that higher cell counts and SCOD removal were observed under aerobic conditions (Figure 2-1 b-c). None of the intact cell, microbial growth or SCOD removal was observed in non-inoculated controls.

I. loihiensis has been reported to be an aerobic organism (González-Muñoz et al., 2008). However, in this study it was identified as a facultative anaerobe, able to use both O_2 and NO_3 as an electron acceptor. Although *B. pumilus* and *M. xanthus* have been recognized as obligate aerobes (Robinson, 2014; Shimkets, 2000), in this study, they were found to be facultative anaerobes. Several *B. pumilus* strains have been reported as facultative anaerobes, yet the electron acceptor has not been identified (Alcaraz, 2015; Koh, Morehouse and Chandler, 1956). There was no report related to *M. xanthus* being a facultative anaerobe, although genome sequencing demonstrated that its common ancestor was a facultative anaerobe (Thomas et al., 2008). *B. antiquum* was observed to be a strict aerobe in this study with a specific growth rate of 0.14 1/h, the same order of magnitude than previously reported maximum growth rate (μ=0.14 1/h) in wastewater with presence of NaCl (3% w/v) and using acetate as the major carbon source (equivalent to 1124 mg chemical

oxygen demand/L) (Simoes et al., 2017). Besides carbon source and electron acceptor, exhaustion of macro/micro-nutrients (Maathuis, 2009; Mcardle and Ashworth, 1999) or formation of toxic metabolism by-products (Trinh and Srienc, 2009) cannot be excluded as factors affecting the microbial growth.

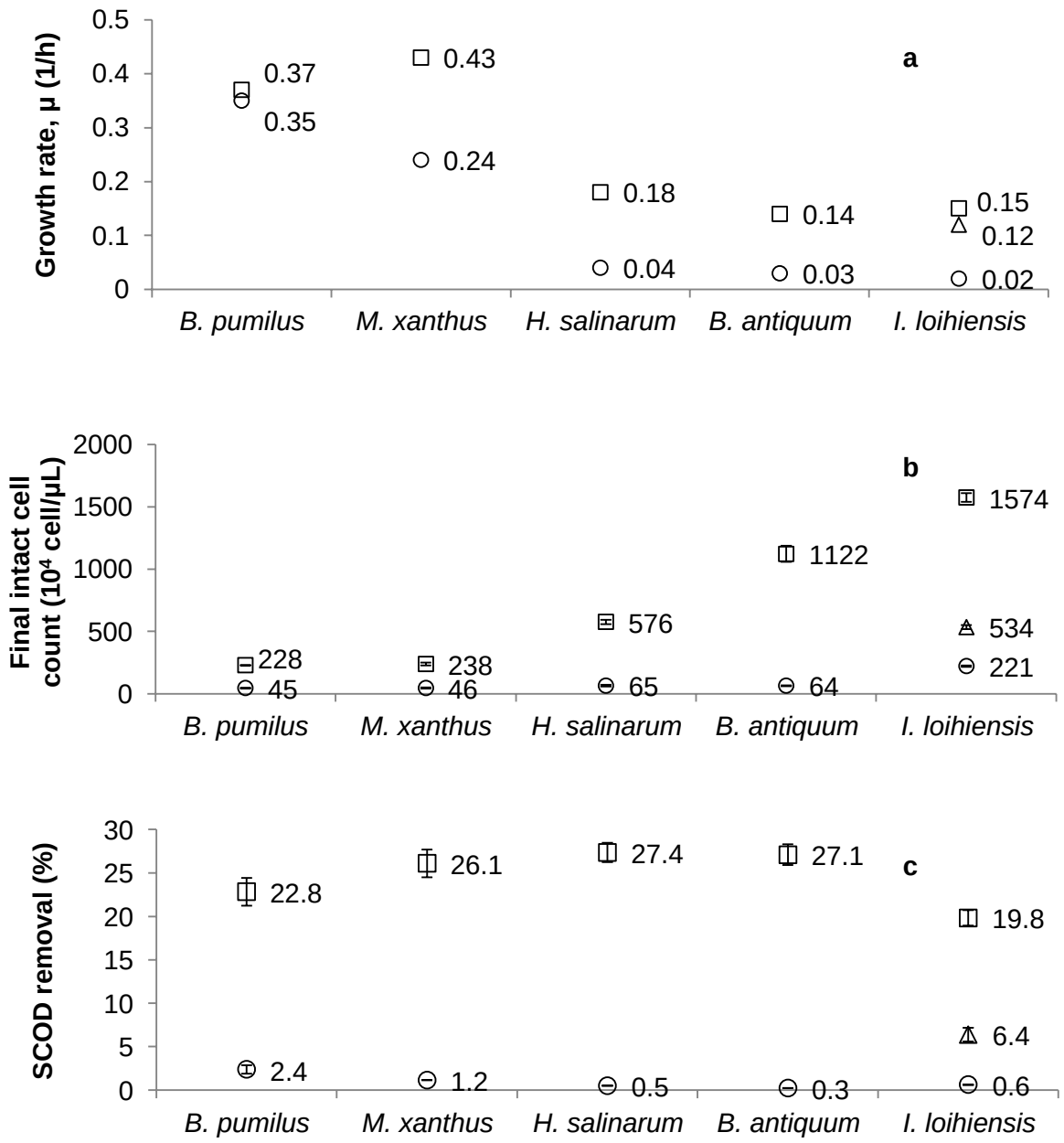

Figure 2-1 (a) Microbial growth rate (1/h) during exponential growth (0 - 24 /48 h), and intact cell counts (b) and SCOD removal (c) by the end of 120 h incubation period under aerobic (□), anoxic (Δ) and anaerobic conditions (○). Error bars represent standard deviation obtained from duplicates.

2.3.4 Bio-struvite crystal identification and morphology

All the selected microorganisms produced crystals under aerobic conditions. The XRD diffractions results showed that the curves of isolated purified crystal products met the peak profile of the standard struvite crystals curve (pattern: COD 9007674). The crystals produced by all the microorganisms tested were hence identified as bio-struvite. The bio-struvite and the abiotic struvite crystals presented with the same dominant faces [011], [111] and [00$\bar{1}$] (Table 2-4). Besides these three faces, [010] was also found predominant for the bio-struvite produced by *M. xanthus, H. salinarum, B. antiquum*, and *I. loihiensis* (Table 2-4).

Table 2-4 Predominant face of bio-struvite and abiotic struvite crystals

	B. pumilus	*M. xanthus*	*H. salinarum*	*B. antiquum*	*I. loihiensis*	abiotic struvite
[011]	X	X	X	X	X	X
[111]	X	X	X	X	X	X
[00$\bar{1}$]	X	X	X	X	X	X
[010]		X	X	X	X	

The dominant morphology of the bio-struvite crystals was coffin-lid shape (Figure 2-2 a-b, d-e) and long bar shape (Figure 2-2 c), which have been reported to be among the most typical struvite forms (Tansel, Lunn and Monje, 2018). The shape and size of these bio-struvite crystals were different from the relatively small dendritic abiotic struvite (Figure 2-2 h). Abiotic struvite of such dendritic X-shape is typically formed at high pH ≥9 (Ronteltap et al., 2010; Ye et al., 2014). In most microbial cultures grown under aerobic conditions, crystals were observed as early as after 4 h of incubation (Figure 2-2 g) and these grew larger to more than 300 μm during stationary phase (Figure 2-2 a-b, d-f). In *B. pumilus* culture, a considerable number of crusted tetrad clusters were observed aggregated on the specific bio-struvite crystal surface, particularly the [011] faces (Figure 2-2 g). Bacteria (e.g. *Proteus mirabilis*) was reported to exert control on the bio-struvite crystal morphology (Torzewska, Stączek and Rózalski, 2003). Prywer and Torzewska (2009) proposed a potential of specific molecular interactions, which related the *P. mirabilis* capability of binding to positively charged molecules (e.g. $Mg[H_2O]_6^{2+}$ octahedra) in the crystal surface structure. Such

molecular interactions varied with the composition of the microbial secreted biomolecules (e.g. polysaccharide) and its affinity for cations (Prywer and Torzewska, 2009), as well as the charged molecules' type and density on the crystal surface (Sadowski, Prywer and Torzewska, 2014). In this study, the microbial growth may have potential to enhance specific faces of the bio-struvite crystals (e.g. [011], [111], $[00\bar{1}]$ faces) and therefore lead to the different crystal morphology (e.g. coffin-lid shape).

The self-assembly of crystals such as contact twinning (Figure 2-3 a-b) and penetration twining (Figure 2-3 c) were observed, along with the parallel grouping of coffin-lid shaped crystals (Figure 2-3 d) and long-bar shaped crystals (Figure 2-3 e). Some bio-struvite crystals were observed with truncated apices, which was related to enhanced [111] end caps (Figure 2-3 f). Similar struvite crystals were observed at low or moderate pH (8–8.5) (Sadowski, Prywer and Torzewska, 2014).

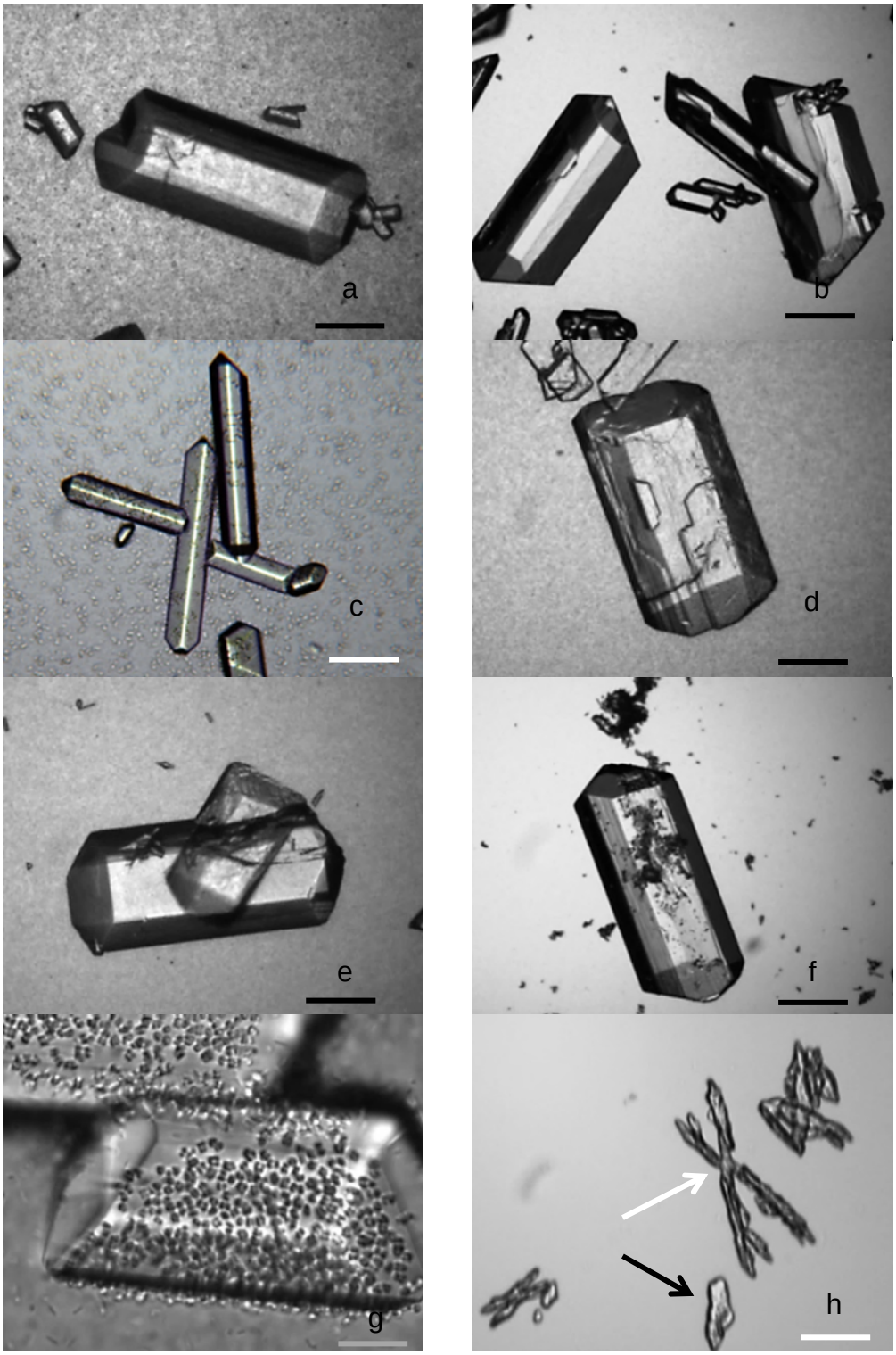

Figure 2-2 Coffin-lid and long-bar shaped bio-struvite produced in stationary phase by (a) - *B. pumilus;* (b, c) - *M. xanthus;* (d) - *H. salinarum;* (e) - *B. antiquum* and (f) - *I. loihiensis*. (g) Crusted cell cluster aggregated on *B. pumilus* bio-struvite crystal surface (4 h incubation); (h) - dendritic abiotic struvite crystals, single (black arrow) and X-shape (white arrow). Black bar scale – 88.32 µm, white bar scale – 35.93 µm, grey bar scale – 10.19 µm.

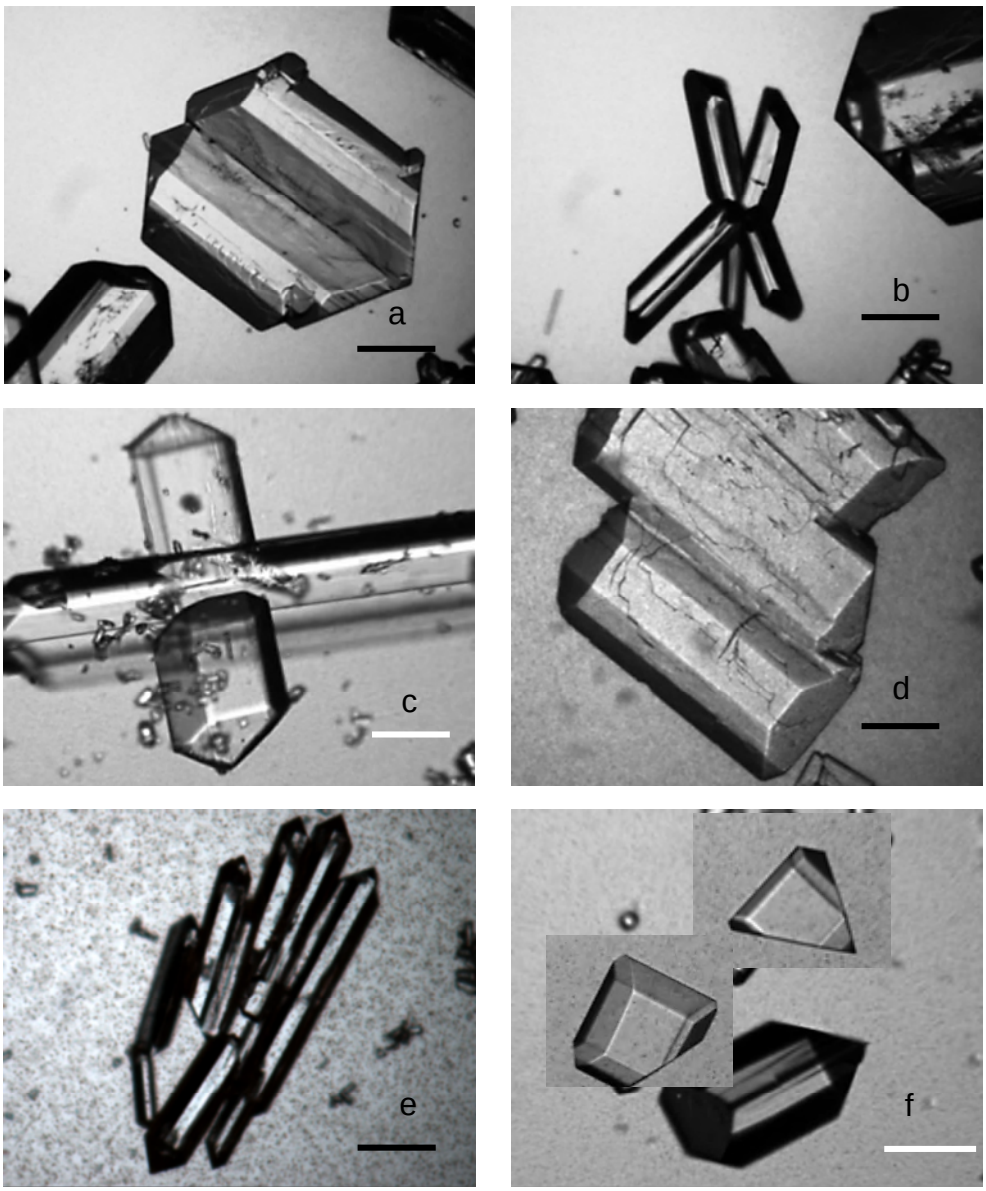

Figure 2-3 Bio-struvite crystals contact twinning (a - c), parallel grouping (d - e), bio-struvite crystals with truncated apices (f). Black bar scale – 88.32 µm, white bar scale – 35.93 µm.

2.3.5 Bio-struvite production and removal and recovery of phosphate and magnesium

The bio-struvite crystal yields under aerobic conditions varied between 1521 and 1746 mg crystals per liter synthetic solution (Table 2-5). No crystal was collected under oxygen-limiting conditions (Table 2-5). The removal of PO_4-P and Mg^{2+} by the end of the 120 h incubation time varied with DO levels. Under aerobic conditions, the removal of PO_4-P and Mg^{2+} was between 55–76% and 92–98%, respectively. Under anaerobic conditions, the removal of PO_4-P and Mg^{2+} varied between 1–2% and 2–

8% of Mg^{2+}, respectively. Under anoxic conditions, *I. loihiensis* was able to remove 2% of PO_4-P and 32% of Mg^{2+}, from the synthetic media (Table 2-5).

A mass balance to the nutrients in solution (liquid and crystals >10 μm) demonstrated that considerable amounts of PO_4-P and Mg^{2+} were recovered as bio-struvite (46–54% and 83–95%, respectively (Table 2-5). Although *B. antiquum* removed a relatively high content of PO_4-P (314 mg/L, 76%) from the synthetic solution, the PO_4-P recovery (48%) by bio-struvite crystals was lower than those for *B. pumilus*, *M. xanthus* and *H. salinarum* (52–54%). Moreover, the Mg^{2+} recovery by *B. antiquum* (84%) and *I. loihiensis* (83%) was observed to be lower than for the other three microorganisms (92–95%).

The synthesis of bio-struvite and removal of PO_4-P and of Mg^{2+} have been reported to depend on microbial growth and metabolism pathways (Sinha et al., 2014). The significant difference of PO_4-P removal and bio-struvite crystal yields between aerobic and anaerobic conditions in this study indicates the importance of DO for P removal and bio-struvite production. Furthermore, the capability of the selected microorganisms, particularly *I. loihiensis,* to produce bio-struvite and remove PO_4-P in this study might be underestimated due to the NaCl concentration of 3.5% w/v. It was reported that the increased NaCl could increase the solubility of the struvite phase and therefore lead to inhibition of the bio-struvite size (Rivadeneyra et al., 2006a). A significant prevention of NaCl (3% w/v NaCl) on bio-struvite production was also observed in the sludge dewatering liquors (Simoes et al., 2017). The molar ratio of the removed PO_4-P to Mg^{2+} by *B. antiquum* under aerobic conditions ([PO_4-P]/[Mg^{2+}]=1.4) was relatively higher than the standard stoichiometric ratio [PO_4-P]/[Mg^{2+}] of struvite, indicating that *B. antiquum* may absorb considerable amounts of PO_4-P into cells. Such PO_4-P accumulation within *B. antiquum* cells was reported to be relative to the formation of intracellular bio-struvite (Smirnov et al., 2005).

Table 2-5 Removal and recovery of PO_4-P and Mg^{2+} at two DO levels by the end of 120-h incubation period

	DO (mg/L)	Bio-struvite [a] production (mg bio-struvite/L synthetic solution)	PO_4-P removal	Mg^{2+} removal	PO_4-P recovered by bio-struvite [a]	Mg^{2+} recovered by bio-struvite [a]
B. pumilus	7.2	1700	265 ± 3 mg/L 64%	176 ±1 mg/L 98%	215 mg/L 52%	167 mg/L 93%
	0	0	8 ± 3 mg/L 2%	5 ± 1 mg/L 2%	-	-
M. xanthus	7.2	1746	272 ± 1 mg/L 66%	177 ± 0 mg/L 98%	221 mg/L 54%	171mg/L 95%
	0	0	5 ± 1 mg/L 1%	9 ± 1 mg/L 5%	-	-
H. salinarum	7.8	1692	276 ± 1 mg/L 67%	170 ± 0 mg/L 94%	215 mg/L 52%	166 mg/L 92%
	0	0	7 ± 0 mg/L 2%	7 ± 1 mg/L 4%	-	-
B. antiquum	8.0	1550	314 ± 1 mg/L 76%	173 ± 0 mg/L 96%	196 mg/L 48%	152 mg/L 84%
	0	0	7 ± 3 mg/L 1%	10 ±1 mg/L 6%	-	-
I. loihiensis	6.2	1521	229 ± 1 mg/L 55%	166 ±0 mg/L 92%	192 mg/L 46%	149 mg/L 83%
	0	0	4 ± 2 mg/L 1%	14 ±5 mg/L 8%	-	-
	0[b]	0	9 ± 3 mg/L 2%	58 ±1 mg/L 32%	-	-
control	-	0	0	0	-	-

[a] - Bio-struvite crystals >10 μm

[b] - Anoxic condition with 0.5 g/L $NaNO_3$

2.3.6 Implication for wastewater industry

Similar to most biological processes in conventional wastewater treatment, bio-struvite production will be ideally applied in open, mixed-culture conditions. The microorganisms enrolled in bio-struvite production are required to out-compete others and become the dominant species in a mixed-microbial culture. The investigation of microbial capability and growth of the selected microorganisms in this study can help identify the suitable types of streams (e.g. municipal wastewater, urine, seawater) for resource recovery, reactor and process design, and the most appropriate operational conditions regarding temperature, pH, availability of certain nutrients, and concentrations of NaCl, Ca^{2+} and DO.

The findings of biochemical characterization in this study (Table 2-6) can be compared with existing information (Table 2-1). This study's findings indicate that *B. pumilus, M. xanthus, B. antiquum* and *H. salinarum* have the potential to grow in urine due to their ability to produce urease and adapt to lower pH (urine pH 5–7). The ability to grow under anoxic conditions, alkaline pH, high concentrations of NaCl and Ca^{2+} (e.g. seawater) can possibly be used as selective pressures for *I. loihiensis* competitive growth. *B. pumilus, M. xanthus* and *I. loihiensis* have the potential to grow in effluents from mesophilic digesters of temperature around 35 °C. Furthermore, specific wastewater streams characterized by high load of protein/amino acids (e.g. dairy processing wastewater) are proposed as preferred wastewater sources to grow the microorganisms. Nevertheless, a well-aerated environment was identified as being essential for bio-struvite production.

Table 2-6 Summary of biochemical properties of investigated microorganisms and comparison with existing literature (based on Table 2-1)

	New	Agreement
Enzyme production	• *B. pumilus, M. xanthus* and *H. salinarum* produce urease	• *B. antiquum* produce urease
Electron acceptor	• *I. loihiensis* – O_2 and NO_3-N (facultative anaerobe) • *B. pumilus* and *M. xanthus* are facultative anaerobes [c]	• All the tested microorganism can use O_2 as electron acceptor [a]
Carbon source	• *I. loihiensis* cannot directly use carbohydrates, but can use proteins • *B. pumilus* and *M. xanthus* cannot directly use carbohydrates [bc]	• *B. antiquum, I. loihiensis* and *H. salinarum* cannot directly use carbohydrates • *B. pumilus, M. xanthus, H. salinarum* and *B. antiquum* can use amino acids/proteins
Growth temperature	• *H. salinarum* prefer mesophilic temperature (24°C)[c]	• *B. pumilus M. xanthus* and *I. loihiensis* prefer high mesophilic temperature (34°C) • *B. antiquum* prefer mesophilic temperature (22°C)
Growth pH	• *I. loihiensis* can grow within pH 5.5–8.5, and prefer mild alkaline pH 8	• *B. pumilus, M. xanthus, B. antiquum* and *H. salinarum* prefer neutral pH (7.1–7.3)
Growth NaCl	• *M. xanthus* prefer 1% w/v NaCl • *B. antiquum* and *H. salinarum* prefer 0.5% w/v NaCl [c]	• *I. loihiensis* prefer 3.5% w/v NaCl • *B. pumilus* prefer 0.5 % w/v NaCl
Ca^{2+}	• Positive effect of Ca^{2+} of 28 mg/L on *I. loihiensis* growth • Negative effect of Ca^{2+} of 28 mg/L on *M. xanthus* growth	

[a] - Microorganisms produced bio-struvite only under aerobic conditions.

[b] - The *B. pumilus* were 33% positive for glucose utilization.

[c] - This finding is different from previous reports.

2.4 Conclusion

- Proteins/amino acids were the preferred organic carbon sources for the five microorganisms investigated.
- *B. pumilus, M. xanthus, H. salinarum* and *B. antiquum* were able to produce urease.
- *I. loihiensis* was found to be a facultative anaerobe able to use O_2 and NO_3-N as an electron acceptor.
- The preferred temperature for all selected microorganisms was within the mesophilic range (22–34 °C); most microorganisms preferred a neutral pH and NaCl concentrations less than 1% w/v, whereas *I. loihiensis* preferred a mild alkaline pH 8, high NaCl of 3.5% w/v and the presence of Ca^{2+}.
- The selected microorganisms produced bio-struvite crystals under aerobic conditions. The morphology of crystals produced was dominantly coffin-lid and long-bar shapes.
- The bio-struvite production and PO_4-P removal highly depended on the microbial growth and DO level. At the investigated optimal growing conditions, in the presence of DO, the bio-struvite crystal (>10 μm) yield and PO_4-P removal varied between 1,521–1,746 mg/L and 55–76%, respectively.

2.5 References

Alcaraz, G. (2015) *Gisella Alcaraz Bacillus Pumilus*. Available at: https://microbewiki.kenyon.edu/index.php/Gisella_Alcaraz-Bacillus_Pumilus (Accessed: 1 January 2018).

Arias, D. et al. (2017) 'Biomineralization mediated by ureolytic bacteria applied to water treatment: a review', *Crystals*, 7(11), p. 345.

Bailey, J. V. et al. (2007) 'Evidence of giant sulphur bacteria in Neoproterozoic phosphorites', *Nature*, 445(7124), pp. 198–201.

Bezerra, M.A. et al. (2008) 'Response surface methodology (RSM) as a tool for optimization in analytical chemistry', *Talanta*, 76(5), pp. 965–977.

Castillo Martinez, F.A. et al. (2013) 'Lactic acid properties, applications and production: a review', *Trends in Food Science and Technology*, 30(1), pp. 70–83.

Christy, P.M. et al. (2014) 'A review on anaerobic decomposition and enhancement of biogas production through enzymes and microorganisms',

Renewable and Sustainable Energy Reviews, 34, pp. 167–173.

Claus, D. (1992) 'A standardized Gram staining procedure', *World Journal of Microbiology & Biotechnology*, 8(4), pp. 451–452.

Coe, F.L. et al. (2005) 'Kidney stone disease', *Journal of Clinical Investigation*, 115(October), pp. 2598–2608.

Le Corre, K.S. et al. (2005) 'Impact of calcium on struvite crystal size, shape and purity', *Journal of Crystal Growth*, 283(3–4), pp. 514–522.

Frankel, R.B. and Bazylinski, D. a (2003) 'Biologically induced mineralization by bacteria', *Reviews in Mineralogy and Geochemistry*, 54(1), pp. 95–114.

Gassama, U.M. et al. (2015) 'Influence of municipal wastewater on rice seed germination, seedling performance, nutrient Uptake, and chlorophyll content', *Journal of Crop Science and Biotechnology*, 18(1), pp. 9–19.

Gavrish, E.I. et al. (2004) 'Three new species of brevibacteria, *Brevibacterium antiquum* sp. nov., *Brevibacterium aurantiacum* sp. nov. and *Brevibacterium permense* sp. nov.', *Mikrobiologiia*, 73(2), pp. 218–225.

González-Muñoz, M.T. et al. (2008) 'Ca-Mg kutnahorite and struvite production by *Idiomarina* strains at modern seawater salinities', *Chemosphere*, 72(3), pp. 465–472.

González-Muñoz, M.T. et al. (2010) 'Bacterial biomineralization: new insights from *Myxococcus*-induced mineral precipitation', *Geological Society, London, Special Publications*, 336(1), pp. 31–50.

Grace-Martin, K. (2012) *Can a regression model with a small R-squared be useful?*., *The Analysis Factor* Available at: http://www.theanalysisfactor.com/small-r-squared/ (Accessed: 1 February 2018).

Hou, S. et al. (2004) 'Genome sequence of the deep-sea γ-proteobacterium *Idiomarina loihiensis* reveals amino acid fermentation as a source of carbon and energy.', *Proceedings of the National Academy of Sciences of the United States of America*., Vol.101, pp. 18036–18041.

James, P.D. et al. (1991) 'The effects of temperature, pH and growth rate on secondary metabolism in *Streptomyces thermoviolaceus* grown in a chemostat.', *Journal of general microbiology*, 137(7), pp. 1715–1720.

Janssen, G.R. et al. (1977) 'Effect of temperature the growth of *Myxococcus xanthus*', *Journal of bacteriology*, 130(1), pp. 561–562.

Koh, W.Y. et al. (1956) 'Relative resistances of microorganisms to cathode rays: I. nonsporeforming bacteria', *Applied microbiology*, 4(3), p. 143.

Losensky, G. et al. (2017) 'Shedding light on biofilm formation of *Halobacterium salinarum* R1 by SWATH-LC/MS/MS analysis of planktonic and sessile cells', *Proteomics*, 17(7), pp. 1–13.

Maathuis, F.J. (2009) ‘Physiological functions of mineral macronutrients’, *Current Opinion in Plant Biology*, 12(3), pp. 250–258.

Macaskie, L.E. et al. (2000) ‘Enzymically mediated bioprecipitation of uranium by a *Citrobacter* sp.: A concerted role for exocellular lipopolysaccharide and associated phosphatase in biomineral formation’, *Microbiology*, 146(8), pp. 1855–1867.

Massey, M.S. et al. (2009) ‘Effectiveness of recovered magnesium phosphates as fertilizers in neutral and slightly alkaline soils’, *Agronomy Journal*, 101(2), pp. 323–329.

Mcardle, H.J. and Ashworth, C.J. (1999) ‘*Micronutrients in fetal growth and development*’, 55(3), pp. 499–510.

Merroun, M.L. et al. (2003) ‘Lanthanum fixation by *Myxococcus xanthus*: Cellular location and extracellular polysaccharide observation’, *Chemosphere*, 52(1), pp. 113–120.

Mesbah, N. and Wiegel, J. (2005) ‘Halophilic thermophiles: A novel group of extremophiles’, in *Microbial diversity: current perspectives and potential applications*. New Delhi: IK Publishing House, pp. 91–118.

Minitab (2010) *Minitab 17 Statistical Software* Minitab Inc., State College, Pennsylvania, USA

Mormile, M.R. et al. (2003) ‘Isolation of *Halobacterium salinarum* retrieved directly from halite brine inclusions’, *Environmental Microbiology*, 5(11), pp. 1094–1102.

Nocker, A. et al. (2017) ‘When are bacteria dead? A step towards interpreting flow cytometry profiles after chlorine disinfection and membrane integrity staining’, *Environmental Technology*, 38(7), pp. 891–900.

Orange, F. et al. (2009) ‘Experimental silicification of the extremophilic archaea *Pyrococcus abyssi* and *Methanocaldococcus jannaschii*: Applications in the search for evidence of life in early earth and extraterrestrial rocks’, *Geobiology*, 7(4), pp. 403–418.

Oren, A. et al. (1995) ‘*Halobaculum gomorrense* gen. nov., sp. nov., a novel extremely halophilic archaeon from the Dead Sea.’, *International journal of systematic bacteriology*, 45(4), pp. 747–754.

Poza, M. et al. (2004) ‘Cloning and expression of clt genes encoding milk-clotting proteases from *Myxococcus xanthus* 422’, *Applied and environmental microbiology*, 70(10), pp. 1–6.

Prywer, J. and Torzewska, A. (2010) ‘Biomineralization of struvite crystals by *Proteus mirabilis* from artificial urine and their mesoscopic structure’, *Crystal Research and Technology*, 45(12), pp. 1283–1289.

Prywer, J. and Torzewska, A. (2009) ‘Bacterially induced struvite growth from synthetic urine: experimental and theoretical characterization of crystal morphology’, *Crystal Growth and Design*, 9(8), pp. 3538–3543.

Rivadeneyra, M.A. et al. (2006) ‘Precipitation of minerals by 22 species of moderately halophilic bacteria in artificial marine salts media: Influence of salt concentration’, *Folia Microbiologica*, 51(5), pp. 445–453.

Robinson, R.K. (2014) *Encyclopedia of food microbiology*. Academic press.

Ronteltap, M. et al. (2010) ‘Struvite precipitation from urine - Influencing factors on particle size’, *Water Research*, 44(6), pp. 2038–2046.

Sadowski, R.R. et al. (2014) ‘Morphology of struvite crystals as an evidence of bacteria mediated growth’, *Crystal Research and Technology*, 49(7), pp. 478–489.

Schultze-Lam, S. et al. (1996) ‘Mineralization of bacterial surfaces’, *Chemical Geology*, 132, pp. 171–181.

Shimkets, L.J. (2000) ‘Growth, sporulation, and other tough decisions’, in *In Prokaryotic Development*. American Society of Microbiology, pp. 277–284.

Shivaji, S. et al. (2006) ‘*Bacillus aerius* sp. nov., *Bacillus aerophilus* sp. nov., *Bacillus stratosphericus* sp. nov. and *Bacillus altitudinis* sp. nov., isolated from cryogenic tubes used for collecting air samples from high altitudes’, *International Journal of Systematic and Evolutionary Microbiology*, 56(7), pp. 1465–1473.

Da Silva, S. et al. (2000) ‘Effect of culture conditions on the formation of struvite by *Myxococcus xanthus’*, *Chemosphere*, 40(12), pp. 1289–1296.

Silva, T.D. et al. (2016) ‘Effect of pH, temperature, and chemicals on the endoglucanases and β-glucosidases from the thermophilic fungus *Myceliophthora heterothallica* F.2.1.4. obtained by solid-state and submerged cultivation’, *Biochemistry Research International*, 2016

Simoes, F. et al. (2017) ‘Understanding the growth of the bio-struvite production *Brevibacterium antiquum* in sludge liquors’, *Environmental Technology*, Taylor & Francis, pp. 1–10.

Sinha, A. et al. (2014) ‘Microbial mineralization of struvite: a promising process to overcome phosphate sequestering crisis’, *Water Research*, 54, pp. 33–43.

Smirnov, A. et al. (2005) ‘Formation of insoluble magnesium phosphates during growth of the archaea *Halorubrum distributum* and *Halobacterium salinarium* and the bacterium *Brevibacterium antiquum*’, *FEMS Microbiology Ecology*, 52(1), pp. 129–137.

Soares, A. et al. (2014) ‘Bio-Struvite: A new route to recover phosphorus from wastewater’, *Clean - Soil, Air, Water*, 42(7), pp. 994–997.

Syberg, S. (2016) *Reducing the edge effect in cell culture microplates*., *Thermo Fisher Scientific* Available at: https://www.rdmag.com/article/2016/10/reducing-edge-effect-cell-culture-microplates (Accessed: 1 February 2018).

Tansel, B. et al. (2018) ‘Struvite formation and decomposition characteristics for ammonia and phosphorus recovery: A review of magnesium-ammonia-

phosphate interactions', *Chemosphere*, 194, pp. 504–514.

Tchobanoglous, G. et al. (2003) *Wastewater engineering: Treatment and reuse*. 4th edn. Tchobanoglous, G. et al. (eds.) McGraw-Hill Education.

Thomas, S.H. et al. (2008) 'The mosaic genome of *Anaeromyxobacter dehalogenans* strain 2CP-C suggests an aerobic common ancestor to the delta-proteobacteria', *PLoS ONE*, 3(5)

Torzewska, A. et al. (2003) 'Crystallization of urine mineral components may depend on the chemical nature of *Proteus endotoxin* polysaccharides', *Journal of Medical Microbiology*, 52(6), pp. 471–477.

Trinh, C.T. and Srienc, F. (2009) 'Metabolic engineering of *Escherichia coli* for efficient conversion of glycerol to ethanol', *Applied and Environmental Microbiology*, 75(21), pp. 6696–6705.

Trujillo, M.E. and Goodfellow, M. (2015) '*Brevibacterium*', in *Bergey's Manual of Systematics of Archaea and Bacteria*. John Wiley & Sons, Inc., in association with Bergey's Manual Trust, pp. 1–22.

Westall, F. (1999) 'The nature of fossil bacteria: A guide to the search for extraterrestrial life', *Journal of Geophysical Research*, 104451(25), pp. 437–16.

Ye, Z. et al. (2014) 'Phosphorus recovery from wastewater by struvite crystallization: Property of aggregates', *Journal of Environmental Sciences*, 26(5), pp. 991–1000.

Yee, N. et al. (2003) 'The effect of cyanobacteria on silica precipitation at neutral pH: Implications for bacterial silicification in geothermal hot springs', *Chemical Geology*, 199(1–2), pp. 83–90.

Zinder, S.H. and Dworkin, M. (2006) 'Morphological and physiological diversity', in *In The Prokaryotes*. Springer New York, pp. 185–220.

3 Understanding the mechanisms of bio-struvite biomineralization

Author: Y Leng*, F Simoes, A Soares*

* Cranfield Water Science Institute, Vincent Building, Cranfield University, Bedfordshire, MK43 0AL, UK

Abstract

The mechanisms of struvite production through biomineralization were investigated for five microorganisms (*Bacillus pumilus, Brevibacterium antiquum, Myxococcus xanthus, Halobacterium salinarum* and *Idiomarina loihiensis*) in synthetic solution. After 72–96 h of incubation, the microbial strains tested increased the pH from 7.5-7.7 to 8.4-8.7, removed ortho-phosphate (63–71%) and the magnesium (94–99%) by biomineralization. The minerals formed were identified as struvite (i.e. bio-struvite). Within the initial 24 h of incubation, microbial growth rates of 0.16 - 0.28 1/h were measured, and bio-struvite production was observed when the solution supersaturation achieved 0.6 - 0.8. The crystals produced by *B. pumilus, H. salinarum* and *M. xanthus* were trapezoidal-platy shaped and presented a gap size distribution (Dv_{90} - Dv_{50}) about 200 µm. *B. antiquum* and *I. loihiensis* produced crystals of coffin-lid/long-bar shape and a narrow gap size distribution around 100 µm, indicating homogeneous crystal size distribution. Intracellular supersaturation condition of struvite phase was achieved within *B. antiquum* and *I. loihiensis* cells, corresponding to observation of intracellular vesicle-like structures occupied with electron-dense granules/materials. This study suggests that *B. antiquum* and *I. loihiensis* produces bio-struvite through biologically controlled mineralization. This mechanism is preferred for recovering nutrients from streams such as wastewater because it allows a link between manipulation of microbial growth conditions and bio-struvite production, even in highly complex streams.

Keywords: biomineralization; bio-struvite; P recovery; intracellular cluster

3.1 Introduction

Phosphorus (P) is an essential element for all living organisms. It plays a vital role in genetic processes and storage, cycling and storage of bioenergy, and synthesis of functional biomolecules and structural components (Elser, 2012). Struvite (magnesium ammonium phosphate hexahydrate - $MgNH_4PO_4.6H_2O$) has received substantial attention from the wastewater industry as a route for both removal and recovery of P and nitrogen (N) from wastewater (Doyle and Parsons, 2002). Such removal prevents eutrophication of surface waters (Conley et al., 2009), and reduces the risk of uncontrolled formation of P-mineral scaling (e.g. struvite, calcium phosphate) along centrate return pipelines at wastewater treatment plants (WWTPs) (Doyle and Parsons, 2002). The recovered struvite can be applied to soil and slowly releases a source of nutrients (P, N and Mg^{2+}), and has potential use as an excellent substitute for commercial P and N fertilizers (Parsons and Smith, 2008). However, large-scale struvite production is still limited due to the costs of reagents and pH adjustment required by struvite precipitation (Kataki et al., 2016).

Soares et al. (2014) reported a new way to recover P and N by producing struvite biologically (i.e. bio-struvite), even from wastewater containing ortho-phosphate (PO_4-P) of 7.5 mg/L. The struvite occurrence via biomineralization was identified as a combination of ammonium (NH_4-N), released from the metabolism of nitrogenous organic substances, with PO_4-P and Mg^{2+} presented in the environment (Sinha et al., 2014). A wide spectrum of microorganisms were reported to be capable of producing bio-struvite in controlled conditions (synthetic media) and wastewater streams (González-Muñoz et al., 2008; Grover, Rope and Kaneshiro, 1997; Sinha et al., 2014; Soares et al., 2014), and the mechanisms of biomineralization varied with microbial strains. However, most of the studies to date have focused on pathological biomineralization of struvite in kidney stones, particularly with respect to its growth and morphological properties (Coe, Evan and Worcester, 2005; Li et al., 2015).

Biomineralization, based on cellular control in the process, is traditionally grouped into two distinct modes: biologically induced mineralization (BIM) and

biologically controlled mineralization (BCM) (Mann, 2001). BIM takes place in an open environment where the minerals are precipitated adventitiously and their chemical characteristics could be readily altered by interference from foreign substances and interactions between various metabolic pathways (Mann, 2001). BCM encompasses genetic control where the microorganisms can exert specific regulation in isolated compartments such as the controlled solution composition inside lipid vesicles (Mann, 2001; Weiner and Dove, 2003). One distinctive feature of BCM is the biominerals' species-specific crystallochemical properties and homogeneity with respect to morphology, size, and composition (Mann, 2001). Thus, BCM has potential to yield reproducible products of more controlled quality. Most biogenic P-minerals such as carbonated hydroxyapatite are recognized as BCM products (Omelon et al., 2013). Nevertheless, struvite formation through BCM has been scarcely reported. Only three microbial strains, *Paramecium tetraurelia*, *Brevibacterium antiquum* and *Enterobacter sp*, were reported to be involved in BCM bio-struvite formation, either by occurrence of intracellular bio-struvite (Grover, Rope and Kaneshiro, 1997; Smirnov et al., 2005), or by homogeneity regarding morphology, composition and mineralogy in the crystals (Sinha et al., 2014).

Theoretically, the crystallization of struvite only takes place if the concentrations of PO_4-P, NH_4-N and Mg^{2+} exceed the solubility product (Weiner and Dove, 2003). However, microbial activity may exert influence on the formation, growth and morphology of struvite. Many microorganisms can metabolically break down nitrogenous organic matter such as urease and protein molecules to release NH_4-N, and increase the solution pH, to create a supersaturated solution for bio-struvite crystallization (Sadowski, Prywer and Torzewska, 2014; Sinha et al., 2014). Furthermore, the interaction with and accumulation of cations on the negatively charged cell outer layer can lead to heterogeneous nucleation where the energy barrier is reduced for growth of biominerals (Frankel and Bazylinski, 2003; Macaskie et al., 2000). Additionally, bacteria *Proteus mirabilis* was reported to change the struvite size or morphology by interaction between negatively charged polysaccharides within cell membrane

and molecular structures of the crystal surface (Prywer and Torzewska, 2009, 2010).

All microorganisms investigated in this study have been proven to form bio-struvite in streams. *B. antiquum* was reported to grow in Mg^{2+}- and PO_4-rich synthetic solutions and produce bio-struvite crystals within the cytoplasm (Smirnov et al., 2005). The *Myxococcus xanthus* bio-struvite was found related to the autolysis of cellular membranes in synthetic solutions (Da Silva et al., 2000). *Halobacterium salinarum* and *Bacillus pumilus* bio-struvite were observed in wastewater streams (Soares et al., 2014), and *Idiomarina loihiensis* bio-struvite was observed in seawater synthetic solutions (González-Muñoz et al., 2008).

This study aims to understand the mechanisms involved in bio-struvite formation in synthetic solutions for the selected microorganisms through exploring the relationships between cell growth, solution composition, crystallization properties, microbial activity and specific cell structures.

3.2 Materials and methods

3.2.1 Microorganisms

Five microbial strains, initially isolated from soil or marine environments, were purchased from commercial culture collections: *H. salinarum* (DSM 671, German Resource Centre for Biological Material, Germany), *B. pumilus* (GB43, LGC Standards, Middlesex, UK), *B. antiquum* (DSM 21545, German Resource Centre for Biological Material, Germany), *M. xanthus* (CECT 422, Spanish Type Culture Collection, University of Valencia, Paterna, Spain) and *I. loihiensis* (MAH1 /CECT 5996, Spanish Type Culture Collection, University of Valencia, Paterna, Spain).

3.2.2 Microbial cultivation

I. loihiensis was grown in 300 ml glass bottles (Poulten Graf™, Fisher Scientific, UK) containing 90 ml synthetic B41 media (4 g/L yeast extract, 2 g/L magnesium sulfate heptahydrate - $MgSO_4 \bullet 7H_2O$ and 2 g/L di-potassium

hydrogen phosphate - K_2HPO_4) (Da Silva et al., 2000) with additional 1% sodium chloride (NaCl) (González-Muñoz et al., 2008). The other four microorganisms were grown in synthetic B41 media without NaCl. The autoclaved media (121°C, 20 min) were inoculated with 10 mL of pre-washed (0.9% w/v NaCl) microbial cultures grown for 96 h. The bottles were capped with foam stoppers and incubated on an orbital shaker (Stuart model SSL1, Fisher Scientific, UK) at agitation rate 150 RPM at room temperature (22–24°C) for 96 h. Samples (sacrificial bottles) were taken at regular intervals (approximately every 12 h), and the entire content of the bottles was analyzed to avoid biased analysis, specifically when completing the crystal size distribution analysis. All tests were completed in duplicate, and controls were maintained under identical conditions but without inoculation.

3.2.3 Isolation, purification and determination of precipitants; abiotic struvite preparation

At the end of the incubation period, the precipitated crystals were filtered through a 10 µm nylon-mesh filter (Plastok, UK) and washed with deionized (DI) water twice. The filter was air-dried at 37°C for 6 h and weighed to determine the crystal production yield.

Abiotic struvite was prepared by mixing 200 ml 0.05 M $MgSO_4 \bullet 7H_2O$ solution (pre-adjusted to pH 9 with 1 M sodium hydroxide) with 100 ml 0.2 M $NH_4H_2PO_4$ (pre-adjusted to pH 9 with 1 M sodium hydroxide) (Le Corre et al., 2005), and left shaking on an orbital shaker at 150 RPM at room temperature for 24 h.

3.2.4 Supersaturation index and intercellular crystals

Supersaturation index of struvite ($SI_{struvite}$) is used to evaluate the equilibrium between aqueous (soluble ions) and solid phase of struvite, and to quantify supersaturation with respect to struvite phase in fluids. $SI_{struvite}$ was determined by a computer application Visual MINTEQ ver. 3.1 (Gustafsson, 2000), which uses chemical equilibrium models based on the thermodynamic equilibrium and a solubility product constant (K_{sp}) of $10^{-13.26}$ (Ali, Schneider and Hudson, 2005). Assuming no loss of bio-struvite crystals in filtration, K_2HPO_4 was the only P

resource and $MgSO_4 \cdot 7H_2O$ was the only Mg^{2+} resource in solution for bio-struvite, cell structures and intracellular ions of PO_4-P and Mg^{2+}, and the intracellular ion concentrations of PO_4-P and Mg^{2+} were determined by a mass balance (Equation 3-1, 3-2):

$$\mathbf{PO_4\text{-}P_{\text{removed from solution}} = PO_4\text{-}P_{\text{crystals}} + P_{\text{cell structures}} + PO_4\text{-}P_{\text{intracellular}}} \quad \textbf{(Equation 3-1)}$$

$$\mathbf{Mg^{2+}_{\text{removed from solution}} = Mg^{2+}_{\text{crystals}} + Mg^{2+}_{\text{cell structures}} + Mg^{2+}_{\text{intracellular}}} \quad \textbf{(Equation 3-2)}$$

To estimate the intracellular $SI_{struvite}$, the volume and dry weight (DW) of each single cell were assumed to be between 0.5–2 × 10^{-15} L (Gao, 2008) and 1.6–2.8 × 10^{-13} g (Logan, 2005, 2008), respectively. Magnesium and P were assumed to account for 0.5% and 3% of microbial cells on a DW basis, respectively (Stolp, 1988). Furthermore, a constant NH_4-N concentration of 0.001 M within cells was assumed; as well as uniform concentration of PO_4-P and Mg^{2+} in the cytoplasm; a constant degree of intracellular $SI_{struvite}$ during the incubation period; and intracellular neutral pH of 7 for *H. salinarum, M. xanthus*, *B. antiquum* and *B. pumilus* and mild alkaline pH of 8 for *I. loihiensis* (Leng and Soares, 2018a).

For examining intracellular crystals, the microbial cells were harvested from cultures at stationary phase of growth (60 h) and diluted with DI water to achieve approx. 200–300 cell/µL. A drop of the diluted culture was transferred to a 400-mesh Formvar and carbon-coated copper grid, air-dried and examined by transmission electron microscopy (TEM, CM 20, Philips, Japan).

3.2.5 Analytical method

Over the incubation period, intact cell counts were estimated using a flow cytometer (BD accuri C6, BD Biosciences, US) by the SYBR Green I (SG) - propidium iodide (PI) co-staining method (Nocker et al., 2017). Solution pH values were determined by using a digital pH-meter (Jenway 3540, Bibby Scientific, UK). Followed by 0.22 µm sterile filtration (Sartorius Stadium Biotech, Germany), the concentrations of soluble chemical oxygen demand (SCOD) and PO_4-P and NH_4-N were analyzed using a Merck cell test kit according to the

manufacturer's instructions. Magnesium (Mg^{2+}) and potassium (K^{+}) were analyzed by atomic absorption spectroscopy (AAS, Analyst 800, PerkinElmer, UK) equipped with flaming and electrothermal spectrometers.

The crystal growth was investigated over time by frequent particle size distribution (D_v) analysis using a Mastersizer (Malvern 3000, Malvern Instruments Ltd, UK) with a Hydro EV dispersion unit (stirring speed of 1200 RPM). About 95 ml of sample was diluted, to meet the range of laser obscuration and stirring speed was maintained at around 1200 RPM. Microbial distribution and crystal morphology in fresh culture was recorded by microscopic analysis using a high-resolution microscope (L-series upright compound microscope, Division of GT vision Ltd, UK). The morphology and surface characteristics of the isolated purified crystals were investigated by using a scanning electron microscope equipped with energy dispersive X-ray spectroscopy (SEM-EDX, XL 30 SFEG, Philips, The Netherlands). The crystal characterizations of isolated purified crystals were identified by an X-ray powder diffractometer (XRD, D5000, Siemens / Bruker, Germany). The element analysis of the precipitants was implemented through dissolving 25 mg of the precipitations in 20 ml extra pure water (pre-adjusted to pH 2 by 1 M hydrogen chloride), followed by 0.22 µm filtration to determine PO_4-P, NH_4-N, Mg^{2+} and K^{+} in the crystal dissolution.

3.3 Results and discussion

3.3.1 Microorganism growth and activity in synthetic media

The five microbial strains investigated were observed to grow in synthetic solution (Figure 3-1). The microbial growth presented no lag phase and the growth rates (µ) were of 0.16 - 0.28 1/h, during the initial 24 h of incubation (exponential phase) (Table 3-1, Figure 3-1). These growth rates were higher than those previously estimated using turbidity measurements (µ <0.05 1/h) by Soares et al. (2014). The *B. antiquum* growth rate (µ=0.21 1/h) observed in this study was the same order of magnitude than previously reported a maximum growth rate (µ=0.14 1/h) in wastewater using acetic acid and oleic acid as the

major carbon sources (equivalent to 2000 mg chemical oxygen demand/L) (Simoes et al., 2017). The SCOD removal was 48–68% (initial SCOD of 3500 mg/L) by the end of the incubation time (Table 3-1). Neither intact cell counts nor SCOD reduction was observed in non-inoculated controls.

The major carbon source in synthetic solution B41 media was yeast extract that is rich in protein (50–75%) and carbohydrates (4–13%) (EURASYP, 2011). Protein was reported as the preferred carbon source for the tested microorganisms (Leng and Soares, 2018a). After 24 h incubation, the media still contained significant amounts of SCOD and the cultures reached steady state (Figure 3-1), therefore it was important to understand what was limiting the microbial growth. A concentrated yeast extract solution (10 mL, 50 g/L) of was added to the *B. pumilus* culture after 96 h of incubation and the intact cell count doubled in the subsequent 34 h incubation (data not shown). Yeast extract is known as a nutrient-rich complex, it not only serves as a carbon source, but also provides B-complex vitamins, nitrogen, amino acids, carbon and trace minerals (e.g. iron, selenium, zinc) necessary for microbial growth (EURASYP, 2014). A wide spectrum of microorganisms, particularly the bacteria, require the B-complex vitamins as functional coenzymes for many oxidation-reduction reactions needed for growth and energy transformation (Jurtshuk, 1996). Due to the high dissolved oxygen (maintained at 6–8 mg/L) and the amount of organic carbon source remaining (measured as SCOD after 24 h of incubation), when the stationary phase of growth was reached, the limitation in microbial growth might have resulted from lack of essential macro/micro nutrients.

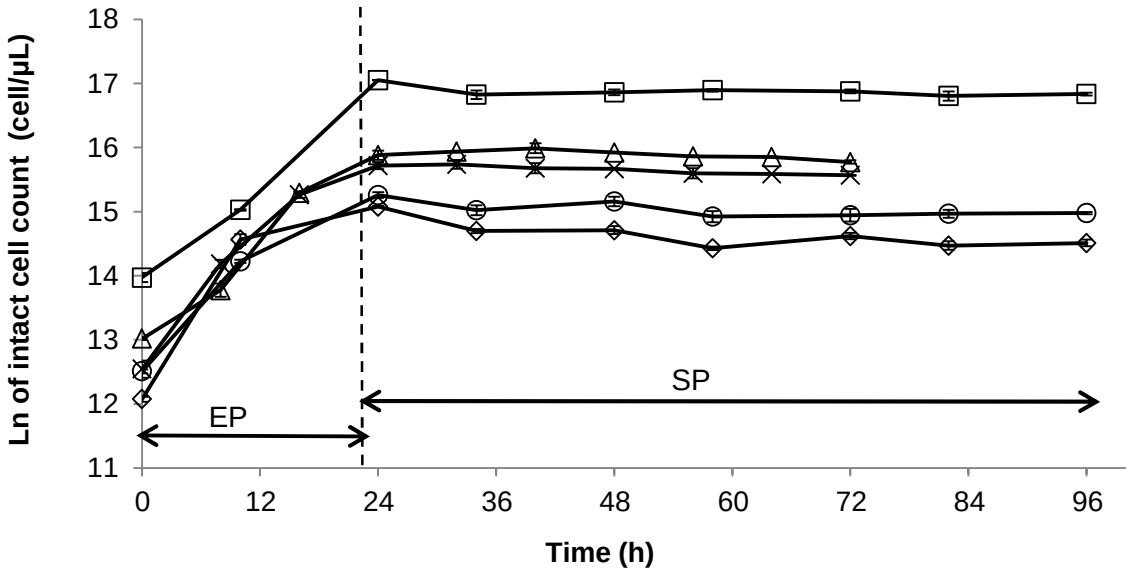

Figure 3-1 Natural logarithm of intact cell count of *H. salinarum* (×), *B. antiquum* (Δ), *B. pumilus* (◊), *M. xanthus* (○) and *I. loihiensis* (□) in synthetic media over the incubation period. Error bars indicate standard deviation of duplicates. (EP - exponential phase, SP - stationary phase of growth)

Table 3-1 Growth rates of pure microbial strains and SCOD removal in synthetic solution

	H. salinarum	*B. pumilus*	*B. antiquum*	*M. xanthus*	*I. loihiensis*
Growth rate, µ (1/h)	0.23	0.28	0.21	0.19	0.16
SCOD removal	2280 mg/L 65%	1920 mg/L 55%	2360 mg/L 68%	2180 mg/L 62%	1680mg/L 48%

Microbial cell clusters were frequently found around the crystal surface during the exponential phase of growth (Figure 3-2 a), and aggregated with small crystals (Figure 3-2 e). It was observed that small particles around 1 µm (Figure 3-2 b) occurred during the exponential phase of growth. These particles could aggregate to form bulk crystals (Figure 3-2 c) via rearrangement or recrystallization (De Yoreo et al., 2015). Some small particles around 4 µm were

observed with a crystalline structure (Figure 3-2 d). An evolution of crystal morphology from cell cluster to bulk crystal was observed (Figure 3-2 e-g), and the crystal coarse surface was smoothened by Ostwald ripening (Ratke and Voorhees, 2013). The crusted two-cell or tetrad clusters in *B. pumilus* culture (Figure 3-2 h) occurred in the early exponential phase of growth (0-10 h) and throughout the incubation period. Such structures did not grow in sphere size but had the potential to aggregate together or onto the crystal surface (Figure 3-2 i). Such specific cell structures observed in *B. pumilus* cultures were similar as previously reported for mineralized embryo-infesting *Thiomargarita* cells (Bailey et al., 2007) and silica spheroids attached onto the cell membrane in microbial silicification (Yee et al., 2003). Thus, the crusted cell structures observed during *B. pumilus* growth in this study were likely associated with the epicellular mineralization. The cell outer layers of both Gram-positive and Gram-negative are predominantly negatively charged, which enables the interaction with and accumulation of cations onto the surface to nucleate mineral particles (Frankel and Bazylinski, 2003; Macaskie et al., 2000; Orange et al., 2009). Gram-positive microorganisms have been reported to have potential to form a thick mineral crust around the cell due to their thick outer layer (≈25 nm thick) of peptidoglycan (Westall, 1999). Furthermore, extracellular polymeric substances (EPS) such as the secreted carboxylate groups (COO^-) or phosphate groups may bond into the peptidoglycan framework within the Gram-positive cell envelope to increase the electronegative charge density, and thus resulting in highly interactive cations (Schultze-Lam et al., 1996). It is suggested that *B. pumilus* can form mineral nucleus along the cell surface during rapid growth in solutions rich in PO_4-P and Mg^{2+}, and the nucleus can firmly attach to the cell surface to completely encrust the cell minerals.

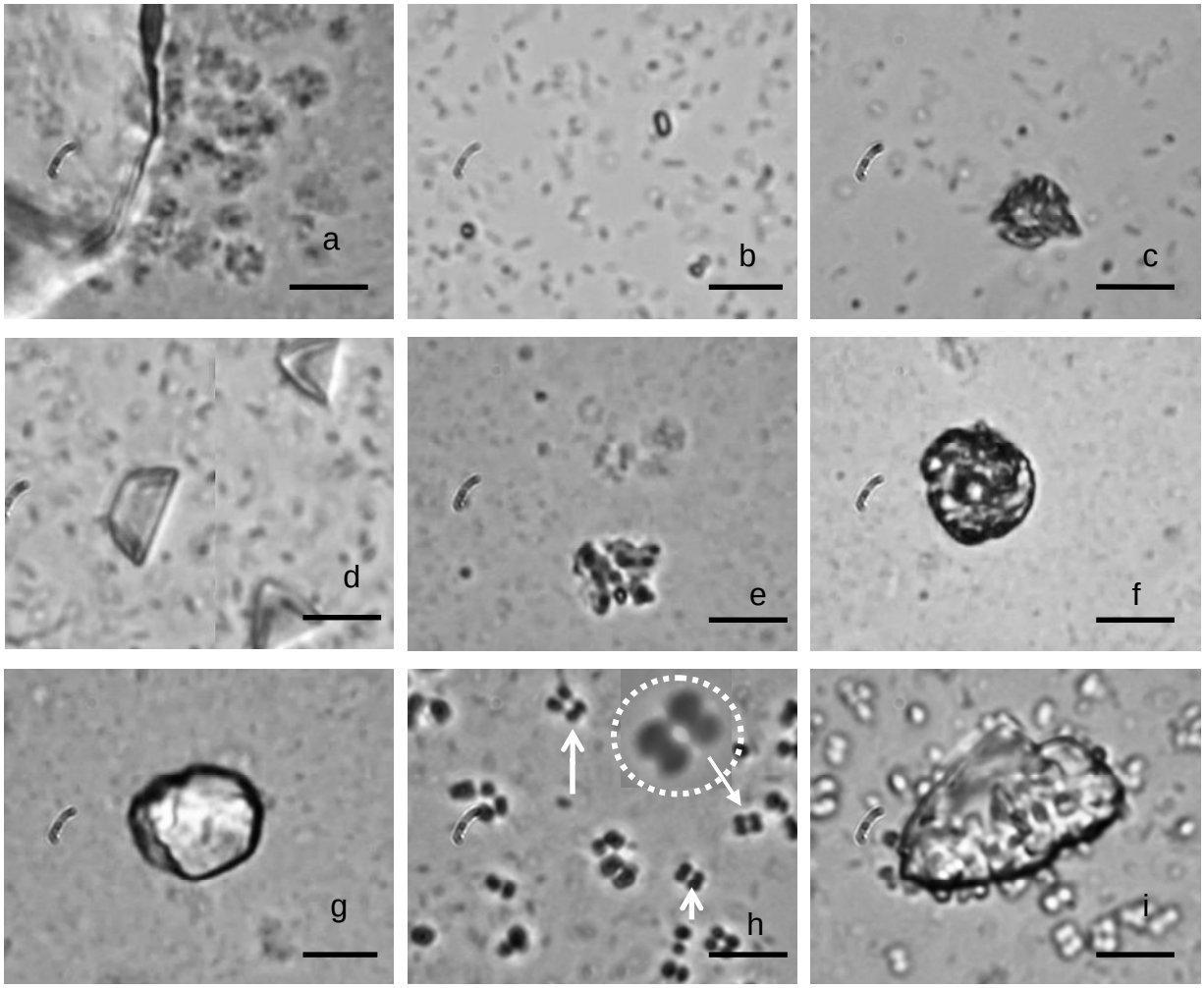

Figure 3-2 Optical microscope photograph observed in late exponential phase of growth (16–24 h): (a) cell clusters of *I. loihiensis* around crystal surface, (b) small particles about 1 μm in *M. xanthus* culture, (c) aggregate of small particles in *B. antiquum* culture, (d) triangle and trapezoidal crystals (approx. 4 μm) in *M. xanthus* culture, (e–g) a morphology evolution in *I. loihiensis* culture: from (e) aggregate of cell clusters and particles to (f)) large particle (approx. 5 μm) with clear boundary, and to (g) large particle of crystalline view. (h) Crusted two-cell or tetrad cell clusters (white arrow – crusted tetrad cell cluster) in *B. pumilus* culture, and (i) their aggregate onto crystal surface. Bar scale – 4.06 μm.

3.3.2 Crystal identification and morphology

All tested microorganisms produced crystals in synthetic solution, and no crystals were observed in the non-inoculated controls. The crystals produced by the microorganisms were identified by XRD analysis and compared with the standard struvite curve (pattern COD 9007674). The diffraction results showed

that all the crystal products met the peak profiles of the standard curve and they also presented the same orthorhombic crystal structure as struvite. The peak profile of the isolated purified crystals' XRD curves presented the same preferentially oriented directions with enhanced [011], [00$\bar{1}$] and [111] faces, as those of abiotic struvite (Table 3-2). Hence, it can be concluded that the crystals recovered from the solutions inoculated with the microorganisms were struvite. However, the bio-struvite diffraction peaks varied slightly between microbial strains and thus different crystal morphology was observed. The bio-struvite crystal morphology was mainly a trapezoidal-platy shape (Figure 3-3 a–c) (*H. salinarum, B. pumilus* and *M. xanthus*), coffin-lid shape (Figure 3-3 d) (*B. antiquum*) and long-bar shape (Figure 3-3 e) (*I. loihiensis*). The observed three morphology were among the typical forms of struvite (Tansel, Lunn and Monje, 2018). Coffin-lid shaped bio-struvite with truncated apices was observed in *B. antiquum* culture (Figure 3-3 d). The truncated apices were reported in crystals that lost the rectangular symmetry and new faces appear in solution at pH <8.5 (Sadowski, Prywer and Torzewska, 2014). The abiotic struvite appeared as thin and small crystals with a typical dendritic structure (Figure 3-3 f), which was previously reported to frequently occur at pH ≥9 (Ronteltap et al., 2010; Ye et al., 2014). The self-assembly of crystals by contact twining on [001] and [00$\bar{1}$] unite (Figure 3 g–h) or parallel growth (Figure 3-3 i) was observed in this study. The contact twining on [001] and [00$\bar{1}$] unite was reported among the most typical twinning types of struvite (Mindat, 2018). In particular, the contact twining of coffin-lid and long-bar shaped bio-struvite along the [00$\bar{1}$] direction (Figure 3-3 g) observed in this study may be associated with a trend to form homogeneous morphology via Ostwald ripening to fill the gap space and to smoothen the surface (Ratke and Voorhees, 2013).

Microorganisms have been reported to influence the crystal morphology by secreting/functioning specific substances such as polysaccharides and lipopolysaccharides with anionic nature, which are responsible for the selective interaction with the molecular structure of the crystal surface (Prywer, Torzewska and Płociński, 2012). Such interactions have been reported to slow

down the growth of specific crystal faces, and therefore change the crystal morphology (Sadowski, Prywer and Torzewska, 2014). The morphology of coffin-lid shaped bio-struvite crystal observed in this study resulted from large [00$\bar{1}$] faces as the bottom and small [001] faces as the top. Prywer, Torzewska and Płociński (2012) reported the occurrence of such coffin-lid shaped bio-struvite crystals in *P. mirabilis* cultures which were found to be due to the cells' selective binding to the [00$\bar{1}$] faces with high density of $Mg[H_2O]_6^{2+}$ octahedra, other than [001] faces terminated by NH_4^+ tetrahedra, and as a result the growth of [00$\bar{1}$] was slowed down and its face expression enhanced, whereas the [001] faces grow freely and consequently are smaller than the [00$\bar{1}$] faces. Thus, the microorganisms investigated in this study are suggested to be capable of synthesizing specific organic molecules that have preference to bind to [00$\bar{1}$], [111] and especially [011] faces of bio-struvite crystals, influencing the morphology.

Table 3-2 Predominant faces of bio-struvite and abiotic struvite crystals

Crystal Face expression	*H. salinarum*	*B. pumilus*	*B. antiquum*	*M. xanthus*	*I. loihiensis*	Abiotic struvite
[011]	X	X	X	X	X	X
[00$\bar{1}$]	X	X	X	X	X	X
[111]	X	X	X	X	X	X
[010]	X		X		X	

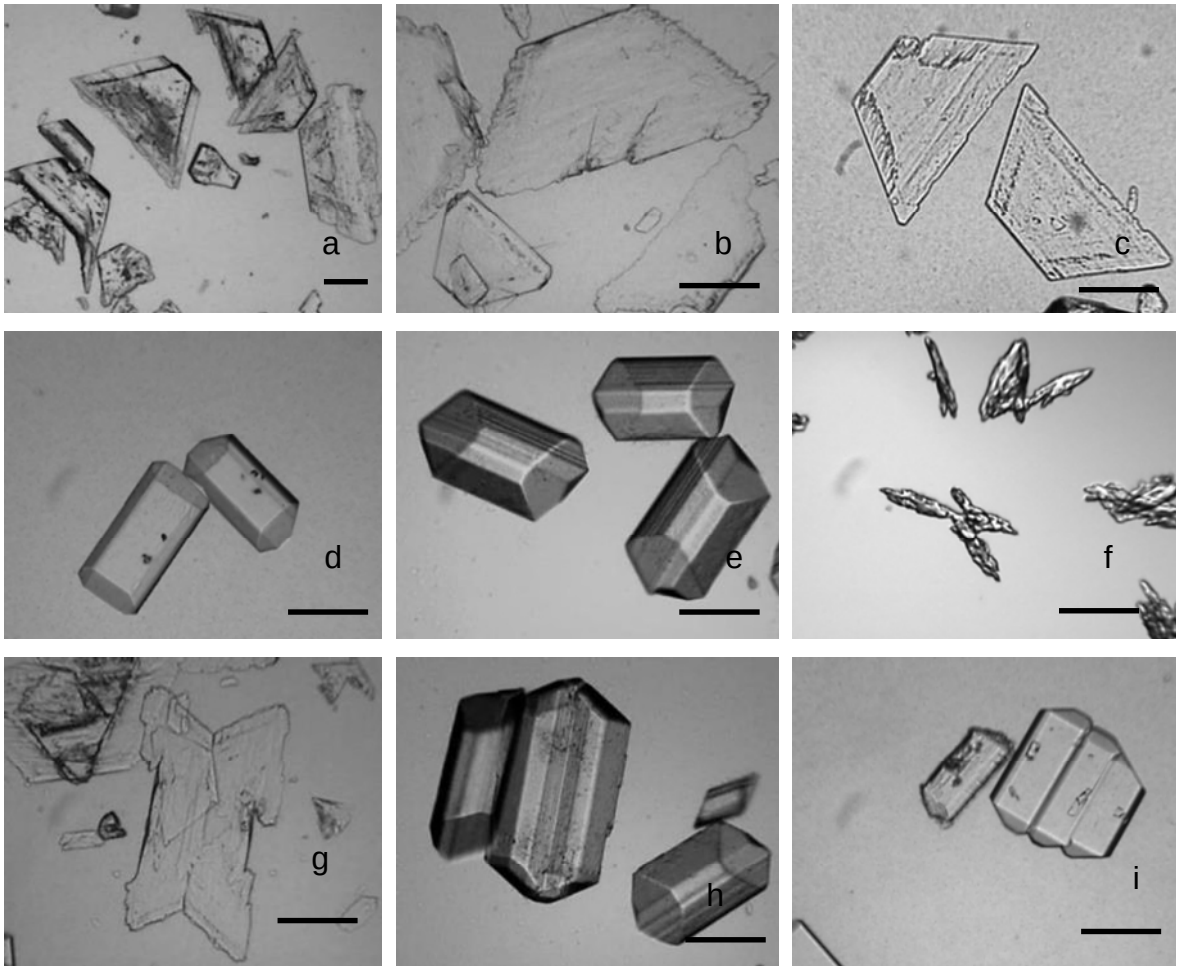

Figure 3-3 Optical microscope photographs of crystals observed during microbial stationary phase of growth: large trapezoidal-platy shaped and coffin-lid shaped bio-struvite crystals produced by (a) - *H. salinarum,* (b) *B. pumilus,* (c) - *M. xanthus* (d) - *B. antiquum* (e) - *I. loihiensis.* (f) Dendritic abiotic struvite crystal. Crystal contact twinning in (g) - *M. xanthus* culture and (h) - *I. loihiensis* culture. (i) Parallel grouping of *B. antiquum* bio-struvite. Scale bar – 35.93 µm.

The bio-struvite produced in the inoculated bottles was further identified by comparison with abiotic struvite standard produced by mixing chemical solutions. Similar stoichiometric ratios of the component elements of the bio-struvite and abiotic struvite were obtained: the molar ratio of [Mg]:[P]:[O]:[N] of the crystal surface structure was approximately 1:1:9:0.2, and the $[Mg^{2+}]$:$[PO_4$-P]:$[NH_4$-N] in crystal dissolution was 1:1:1. Therefore, the crystals produced by the selected microorganisms were similar to the abiotic struvite standard. An

observed loss of nitrogen and oxygen in the composition of the struvite and bio-struvite analyzed was due to the crystal air-drying method that caused volatilization of ammonia and water molecules within the crystalline frameworks, especially on the crystal surface, as previously described (Bhuiyan, Mavinic and Koch, 2008a; Frost, Weier and Erickson, 2004). Furthermore, K was only found in the bio-struvite: 0.8-1.1 % weight percent (wt%) on the crystal surface and 1.1–1.8 wt% in the crystal dissolution. As an essential macronutrient required for microbial growth, K accounts for 1% of microbial cells on a DW basis (Stolp, 1988). Sadowski, Prywer and Torzewska (2014) reported the electrostatic interaction between charged residues on the cell outer layer and crystal surface. In this study, it is suggested that through electrostatic interaction, the microbial cells can bond to the crystal surface and help settle additional K^+ onto this surface.

3.3.3 Bio-struvite production and uptake of nutrients

The microorganisms produced about 1500 mg bio-struvite (>10 µm) per liter of solution, corresponding to an approx. recovery of 190 mg/L PO_4-P and 150 mg/L Mg^{2+}, of the nutrients in solution (Table 3-3). The formation of bio-struvite resulted in the removal of PO_4-P (240-280 mg/L, 63-71%) and Mg^{2+} (150-190 mg/L, 94-99 %) from the synthetic media by the end of the incubation period (Table 3-3). The most significant reduction of PO_4-P and Mg^{2+} occurred during the microbial exponential phase (0–24 h), with removal of 37–50 % and 58–74%, respectively (Figure 3-4 a–b). The presence of Mg^{2+} has been reported to be vital for biological PO_4-P removal as bio-struvite (Smirnov et al., 2005). In this study, the lack of Mg^{2+} at the end of incubation may limit the bio-struvite production and PO_4-P removal that could be further promoted by adding more Mg^{2+} sources. It is noted that *B. antiquum* removed up to 71% of PO_4-P and 99% of Mg^{2+} by the end of 72 h incubation (Figure 3-4 a-b). Yet only 50% of the PO_4-P and 87% of Mg^{2+} was recovered by bio-struvite (>10 µm). Similarly, in *I. loihiensis* cultures, around 65% PO_4-P and 95% Mg^{2+} was removed from solution but only 46% PO_4-P and 73% Mg^{2+} was recovered as bio-struvite (>10 µm). Besides the loss potential of small bio-struvite crystals (<10 µm) during filtration, the data obtained suggests accumulation of PO_4-P and Mg^{2+} within

cytoplasm or cell structures, as reported in *P. tetraurelia* cells (Grover, Rope and Kaneshiro, 1997) and in *B. antiquum* cells (Simoes et al., 2017; Smirnov et al., 2005).

Overall, the concentration of NH_4-N and pH increased in the synthetic solution by the end of the incubation period (Figure 3-4 c–d), and the values varied between 69 to 105 mg/L and 0.7 to 1.0, respectively (Table 3-3). A rapid increase of NH_4-N was observed within the first 24 h of incubation (Figure 3-4c), corresponding to the rapid microbial growth in the exponential phase (Figure 3-1). A slight pH drop (≤0.3) was observed in the early exponential phase (0–10 h), which may be due to accumulation of carbon dioxide in the solution. Such a reduction was followed by a steady pH increase until the end of the incubation period (Figure 3-4 d). The *B. antiquum* and *I. loihiensis* were observed increasing overall pH by 1.0 units, which was higher than for the other three microorganisms (by 0.7–0.9 units), corresponding to the NH_4-N production (Table 3-3).

The synthesis of bio-struvite, particularly through the BIM process, has been reported to be related to the microbial capability to biodegrade nitrogenous-rich compounds (e.g. proteins) in culture media to release NH_4-N and raise pH (Sinha et al., 2014). The microbial growth hence created a mild alkaline environment where the Mg^{2+} was no longer soluble and integrated with PO_4-P and NH_4-N to precipitate as bio-struvite (Smirnov et al., 2005). The microorganisms investigated in this study were known to be capable of using proteins/amino acids as carbon sources (Leng and Soares, 2018a). Thus, the yeast extract applied in this study was not only providing microbial growth with a carbon source but also was used as the main source for NH_4-N production.

Table 3-3 Bio-struvite production and changes of PO_4-P, NH_4-N, Mg^{2+} and pH in the presence of microbial strains by the end of 72 h (*H. salinarum* and *B. antiquum*) and 96 h (*B. pumilus*, *M. xanthus* and *I. loihiensis*) incubation and in non-inoculated control (average ± standard deviation of duplicates).

	H. salinarum	*B. antiquum*	*M. xanthus*	*B. pumilus*	*I. loihiensis*	Control
Bio-struvite production (mg bio-struvite* per liter of synthetic solution)	1567	1509	1536	1515	1481	0
pH increase	0.7±0.0	1.0±0.0	0.8± 0.1	0.8±0.0	1.0±0.0	< 0.1
NH_4-N increase	71±6 mg/L	105±6 mg/L	71±8 mg/L	69±5 mg/L	105 ±4 mg/L	< 1 mg/L
PO_4-P removal	259±6 mg/L 68%	273±8 mg/L 71%	239±17 mg/L 63%	256±11 mg/L 65%	279±7 mg/L 67%	< 1 mg/L 0%
Mg removal	159±2 mg/L 94%	168±3 mg/L 99%	157±5 mg/L 94%	152±5 mg/L 96%	191±3 mg/L 95%	<1 mg/L 0%
PO_4-P recovered as bio-struvite crystals*	192 mg/L 50%	191 mg/L 50%	192 mg/L 51%	191 mg/L 48%	190 mg/L 46%	0 0%
Mg^{2+} recovered as bio-struvite crystals*	149 mg/L 88%	148 mg/L 87%	149 mg/L 89%	148 mg/L 93%	147 mg/L 73%	0 0%

* - Bio-struvite crystals >10 μm

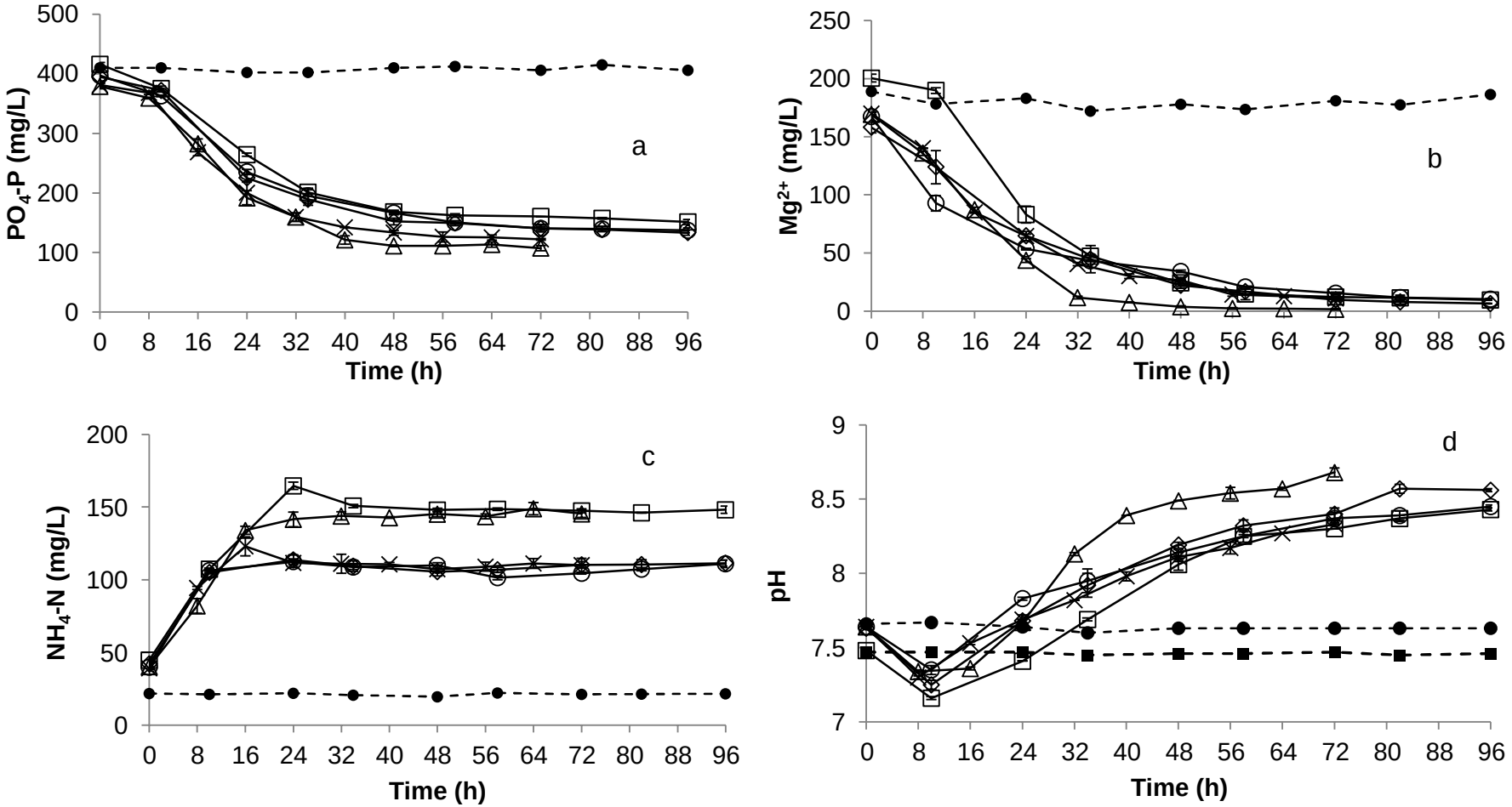

Figure 3-4 Variation of (a) PO_4-P, (b) Mg^{2+}, (c) NH_4-N and (d) pH in microbial cultures of *H. salinarum* (×), *B. antiquum* (Δ), *B. pumilus* (◊), *M. xanthus* (○) and *I. loihiensis* (□) and in non-inoculated controls without NaCl (●) and with 1% NaCl (■) during 72/96 h incubation time. Error bars indicate standard deviation of duplicates.

3.3.4 Extracellular and intracellular supersaturation

In the presence of microorganisms, the extracellular $SI_{struvite}$ (or solution $SI_{struvite}$) in synthetic solutions increased from an initial $SI_{struvite}$ of around 0.57 to values between 0.64 (*B. antiquum*, 24h) and 0.89 (*M. xanthu*s, 48h) within the 48 h incubation time, and then steadily dropped to values between 0.13 (*B. antiquum*, 72h) and 0.69 (*I. loihiensis*, 96h) by the end of the incubation time, while the solution $SI_{struvite}$ of the control was maintained at a constant level (0.52–0.56) (Figure 3-5 a). Solution $SI_{struvite}$ was recognized as the driving force for the crystallization process (De Yoreo et al., 2015). In particular, the bio-struvite crystals were observed during the microbial exponential phase (8–24 h) (Figure 3-1) when solution $SI_{struvite}$ achieved 0.6-0.8 (Figure 3-5 a). When comparing the solution $SI_{struvite}$ curve with those of pH and concentrations of NH_4-N, PO_4-P and Mg^{2+}, the extracellular $SI_{struvite}$ (except that of *B. antiquum* culture) was observed with relatively slight changes with time. It is suggested that the release of NH_4-N and pH increase played a key role in maintaining the solution $SI_{struvite}$ for the crystallization process until the end of the incubation even when the concentration of Mg^{2+} (3-30 mg/L) limited the solution $SI_{struvite}$ after 48 h incubation time (Figure 3-4 b). When comparing the solution $SI_{struvite}$ eligible for bio-struvite formation ($SI_{struvite}$ =0.6-0.8) in this study with those previously reported for abiotic struvite formation, for example a minimum $SI_{struvite}$ of 1.2 (Galbraith and Schneider, 2010) and technique scale-based optimal $SI_{struvite}$ between 2-6 (Bhuiyan, Mavinic and Koch, 2008b), the bio-struvite can nucleate in solution with relatively low $SI_{struvite}$ where the nucleation of abiotic struvite may not occur without seeding. This is related to another significant role microorganisms play in biomineralization: negatively charged specific organic structures (e.g. peptidoglycan layer) or substances secreted by organisms (e.g. EPS) may serve as heterogeneous nucleation sites by interacting/accumulating cations and entrapping crystal nucleus for precipitation (Arias, Cisternas and Rivas, 2017; Decho, 2000). The cell surface layer (S-layer) was recognized as the main crystalline bio-structure that can act as a nucleus (Braissant et al., 2003). In particular, González-Muñoz et al. (2010) reported the importance of

the presence of *M. xanthus* cells in the crystallization of bio-struvite, irrespective of whether the cells were living or dead (entire or disrupted).

The intracellular $SI_{struvite}$ of the studied microorganisms indicated their potential to form intracellular bio-struvite crystals (Figure 3-5 b). *B. antiquum* and *I. loihiensis* were observed to have an intracellular $SI_{struvite}$ >0. This is in agreement with previous observations that *B. antiquum* and *I. loihiensis* uptake and accumulates a considerable amount of PO_4-P and Mg^{2+} within their cells (Table 3-3). These accumulated nutrients might combine with NH_4-N inside cells, for intracellular bio-struvite formation. Furthermore, TEM images showed that most *B. antiquum* cells contained several membrane-bound intracellular compartments enclosing electron-dense clustered granules (Figure 3-6 a–c). These cell structures are suggested to be lipid vesicles, due to a similar structure of previously reported lipid vesicles (Spiegel et al., 2013). Although a high-energy electron beam had been reported to destroy small/thin struvite (Omar, Gonzalez-Muñoz and Peñalver, 1998), and thus the occurrence of dispersive clustered materials (Figure 3-6 c), such intact membrane-bound compartments suggested that intracellular vesicles were where crystallization took place. Similar intact membrane-bound structures enclosing electron-dense clustered materials were observed inside *I. loihiensis* cell (Figure 3-6 d). This was supported by several studies because water-insoluble phosphates were observed in the cytoplasm of *B. antiquum* cells that were grown in medium rich in PO_4-P and Mg^{2+} (Smirnov et al., 2005). Others have reported the occurrence of morphologically homogenous struvite in the *P. tetraurelia* cell cytoplasm (Grover, Rope and Kaneshiro, 1997), and the formation of minerals enclosed by multi-layered ultrastructure within cells' cytoplasm (Bailey et al., 2007). Thus, the bio-struvite mineralization by *B. antiquum* and *I. loihiensis* cultures was suggested as a BCM process, where the bio-struvite is produced in intracellular functional structures (Grover, Rope and Kaneshiro, 1997). Yet it is not known whether its capability to produce intracellular phosphates minerals in nutrient-rich conditions can help them survive in stress or nutrient-poor conditions. No similar cell structure was seen in the other three microbial cultures during their stationary phase.

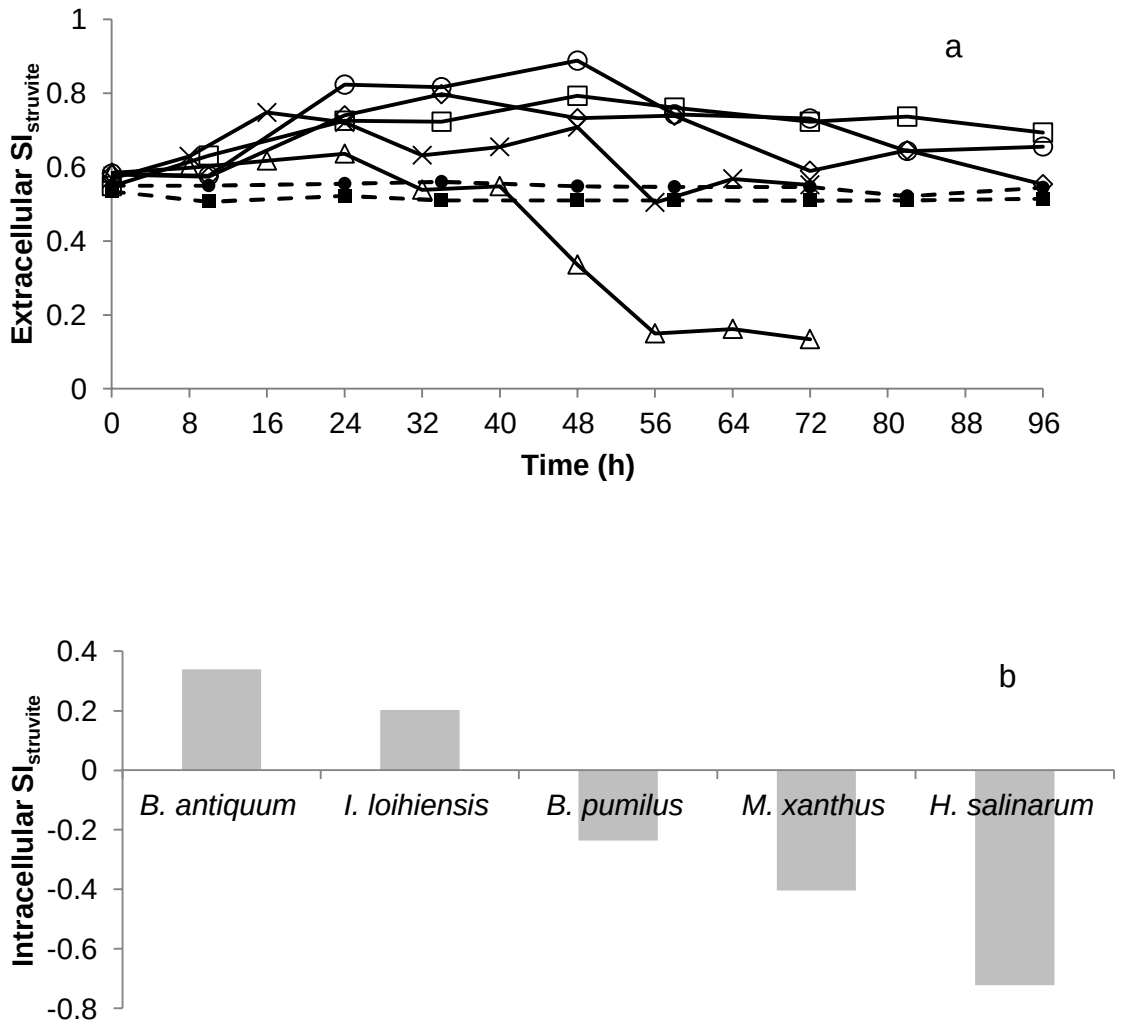

Figure 3-5 Variation of extracellular $SI_{struvite}$ (a), and microbial intracellular $SI_{struvite}$ (b) during the 72/96 h incubation time in microbial cultures of *H. salinarum* (×), *B. pumilus* (◊), *M. xanthus* (○), *B. antiquum* (Δ) and *I. loihiensis* (□) and without NaCl (●) and with 1% NaCl (■).

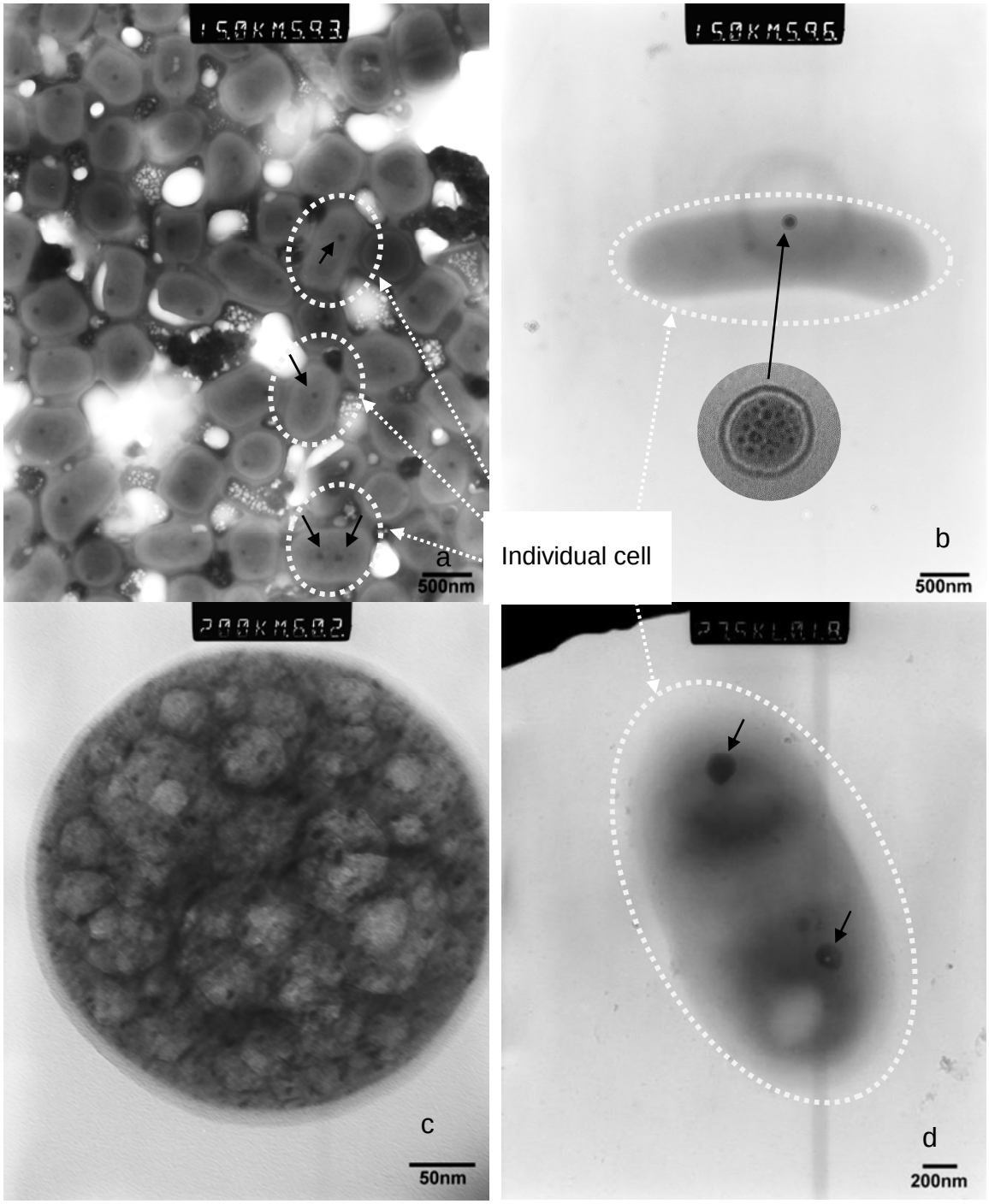

Figure 3-6 TEM pictures shows (a) an overview of *B. antiquum* culture (60 h), cells containing one or two vesicles (black arrows); (b) a vesicle-like structure (black arrows) inside *B. antiquum* cell, with intact membrane structure, and occupied with electron-dense clustered granules; (c) detail of the vesicle, whose internal structures were destroyed by a high-energy electron beam, resulting in the internal space being full of dispersive clustered materials and bubbles. (d) Electron-dense clustered materials (black arrows) inside *I. loihiensis* cell (60 h).

3.3.5 Bio-struvite crystal growth

Figure 3-7 shows that a rapid crystal growth occurred during the microbial exponential phase of growth (8–24 h), when D_{v50}, the particle median diameter for a volume distribution, increased from 0 to 85–145 µm, and the percentage of crystals above 100 µm increased from 0 to 44–71%. The rapid growth was followed by a constant level of size distribution that was maintained until the end of the incubation period, when large crystals above 100 µm finally represented 55–87% of total particles (Figure 3-7 b). No crystal was observed in the controls. The crystal growth also correlated to the variation of solution $SI_{struvite}$ (Figure 3-5 a), where the rapid increase of values occurred after 8–24 h incubation time, reached peak values within 48 h and maintained $SI_{struvite}$ >0 until the end of the incubation period. In particular, the crystal growth in *B. antiquum* culture was maintained at a constant level (Dv_{50}≈100 µm) after 40 h incubation, even with a reduction of solution $SI_{struvite}$ from 0.55 to 0.13 in *B. antiquum* culture (Figure 3-5 a).

Based on the final crystal size distribution (Table 3-4), the microorganisms could be identified into two groups: *H. salinarum, B. pumilus* and *M. xanthus* produced large crystal groups (Dv_{50} =170–215 µm) (Figure 3-8 a-c) and a gap size between Dv_{50} and Dv_{90} with a wide range of about 200 µm. In contrast, *B. antiquum* and *I. loihiensis* produced relatively small crystal groups (Dv_{50} =110–130 µm) (Figure 3-8 d-e) and narrow gap range (Dv_{90} - Dv_{50}) about 110 µm. Such crystals within a narrow size range of distribution suggest homogeneous size and better reproducibility (Table 3-4, Figure 3-8), which can be correlated to the BCM process, where the biomineral products are highly biologically controlled (Sinha et al., 2014).

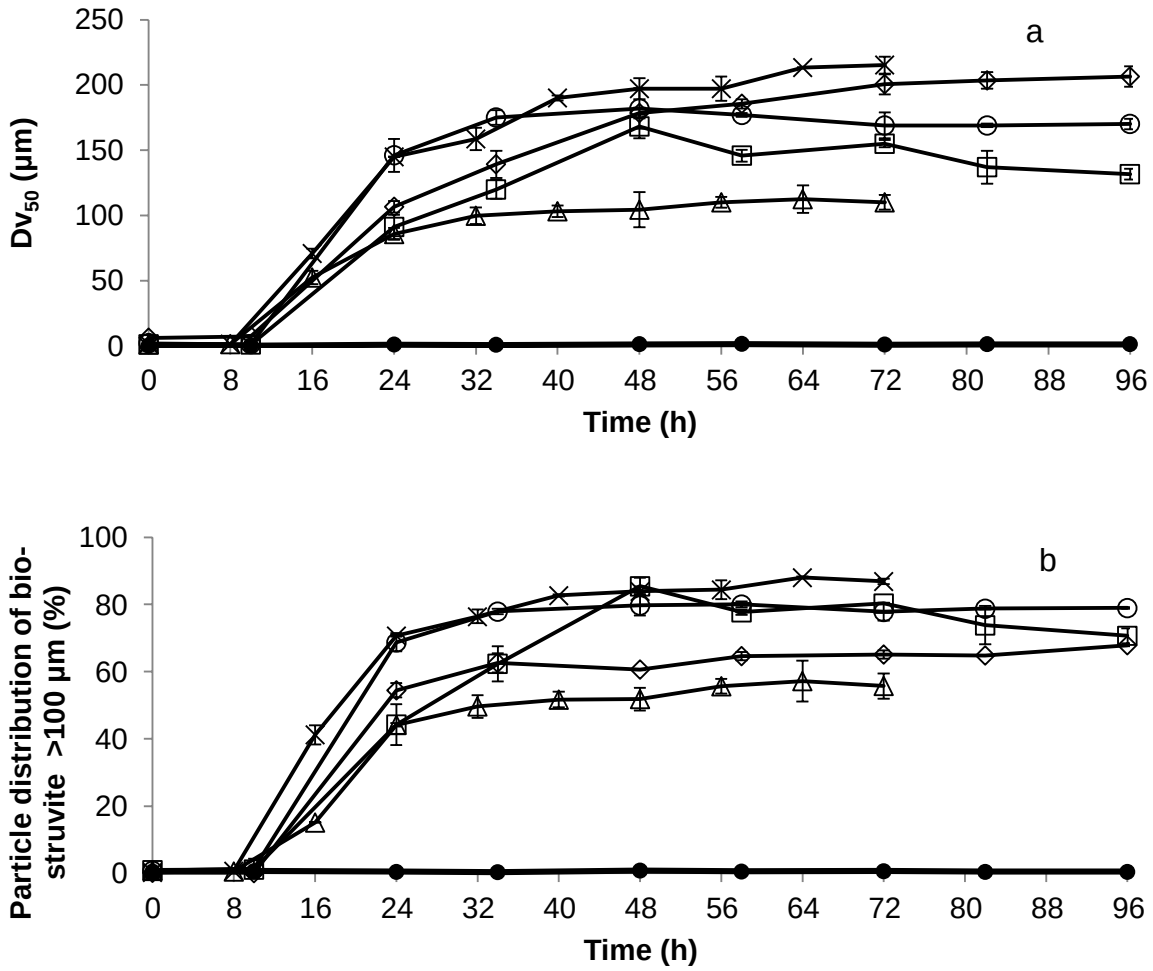

Figure 3-7 Variation of D_{v50} (a) and percentage of bio-struvite crystal >100 µm (b) in synthetic solution over time, in the presence of *H. salinarum* (×), *B. antiquum* (Δ), *B. pumilus* (◊), *M. xanthus* (○) and *I. loihiensis* (□) and in non-inoculated controls (●). Error bars indicate standard deviation of duplicates. D_{v50} is the value of the particle diameter at 50% in the cumulative distribution on the basis of volume.

Table 3-4 Dv_{50} and Dv_{90} of bio-struvite crystals by the end of the incubation period (average ± standard deviation of duplicates)

	H. salinarum	*B. antiquum*	*M. xanthus*	*B. pumilus*	*I. loihiensis*	Control
Dv_{50} (µm)	215±6	110±6	170±4	204±6	132±4	0
Dv_{90} (µm)	404±3	213±17	349±10	488±11	245±16	0

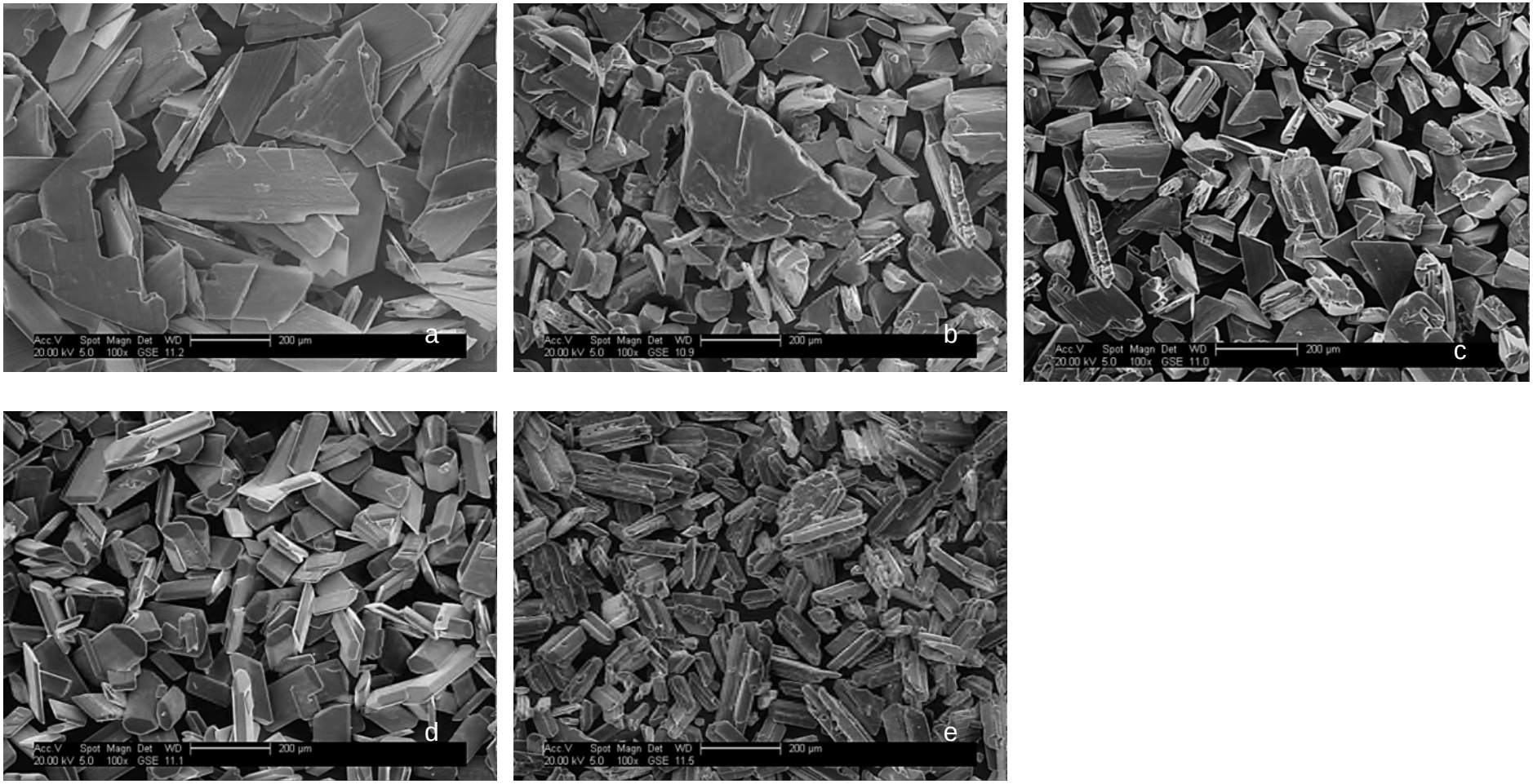

Figure 3-8 SEM photographs showing an overview of bio-struvite produced by (a) - *H. salinarum,* (b) - *B. pumilus,* (c) - *M. xanthus*, (d) - *B. antiquum* and (e) - *I. loihiensis* at the end of the incubation period. Bar scale – 200 µm.

3.3.6 Bio-struvite biomineralization mechanisms

The analysis of microbial growth and activities, crystal growth and morphology, $SI_{struvite}$ and TEM observations supports the identification of BCM from the BIM process amongst the microorganisms investigated (Table 3-5). *B. antiquum and I. loihiensis* could produce bio-struvite in synthetic solution via BCM process, whereas *H. salinarum, B. pumilus and M. xanthus* produce bio-struvite through BIM process (Table 3-5). In both conditions, the solution supersaturation for bio-struvite mineralization was briefly controlled by the microbial activity that resulted in an increase in NH_4-N concentration and pH (Sinha et al., 2014), and cells/cell clusters also contributed to the heterogeneous nucleation by electrostatic interaction (Arias, Cisternas and Rivas, 2017; Decho, 2000). BIM occurs in open environments where the composition of the solution highly influences biomineralization and as a consequence the crystals produced are heterogeneous in size and morphology (Mann, 2001). In contrast, isolated environment such as lipid vesicles ensure BCM specific conditions where the chemical composition of solution and location of bio-struvite was highly cellular controlled, and therefore the product was of higher reproducibility and homogeneity (Mann, 2001). For example, the bio-struvite production by *B. antiquum* was also observed in a different synthetic media, whereas *H. salinarum* did not produce struvite in this media, but induced $Mg_2PO_4OH•4H_2O$ crystals instead (Smirnov et al., 2005).

Table 3-5 Key features of bio-struvite mineralization by *H. salinarum, B. antiquum, B. pumilus, M. xanthus and I. loihiensis* in synthetic solution.

	Biologically induced mineralization	Biologically controlled mineralization
H. salinarum	• pH elevation • NH_4-N production • Crystal morphology heterogeneity • Crystal heterogeneous size: Dv_{90}–Dv_{50} =189.00 μm • Intracellular $SI_{struvite}$ = -0.72	
B. antiquum		• pH elevation • NH_4-N production • Crystal morphology homogeneity • Crystal size homogeneity: Dv_{90}–Dv_{50} =103.00 μm • Clustered materials enclosed in intracellular membrane-bound structures • Intracellular $SI_{struvite}$ = 0.34
B. pumilus	• pH elevation • NH_4-N production • Crystal morphology heterogeneity • Crusted cell/cell clusters • Crystal heterogeneous size: Dv_{90}–Dv_{50} = 284 μm • Intracellular $SI_{struvite}$ = -0.24	
I. loihiensis		• pH elevation • NH_4-N production • Crystal morphology homogeneity • Crystal size homogeneity: Dv_{90}–Dv_{50} =113 μm • Clustered materials enclosed in intracellular membrane-bound structures • Intracellular $SI_{struvite}$ = 0.20
M. xanthus	• pH elevation • NH_4-N production • Crystal morphology heterogeneity • Crystal heterogeneous size: Dv_{90}–Dv_{50} =179 μm • Intracellular $SI_{struvite}$ = -0.40	

3.3.7 Application of BCM for nutrient recovery by bio-struvite from municipal wastewater treatment

The total P in municipal wastewater typically varies between 5 and 20 mg/L, of which 1–5 mg/L is organic P and the rest is inorganic P (Ivanov et al., 2005). Both P resources were reported to have potential use for bio-struvite production (Simoes, 2017). Considerable amounts of NH_4-N can be produced during the degradation of nitrogenous material such as protein. Moreover, WWTP location (hard water area, coastal area and receiving industrial discharge) and applied process (e.g. clay material used as supports in anaerobic digester release and ion exchange) can contribute to Mg^{2+} source (Jardin and Pöpel, 2001). Despite the rich storage of these three nutrients in WWTP, the P recovery by abiotic struvite precipitation still requires an additional chemical dose/applied process (e.g. ion exchange) to adjust the pH and increase the PO_4-P (Huang, Yang and Li, 2014; Mijangos et al., 2004), as well as seeding that is widely applied to reduce the energy barrier for crystallization (Kempter et al., 2015), hence adding costs. This study reveals the microbial capability of the selected microorganisms to increase pH and reduce the energy barrier for crystallization to increase the potential of bio-struvite production in waste streams with low $SI_{struvite}$. That is, the application of bio-struvite can reduce the expense for the pH adjustment and PO_4-P elevation. Furthermore, although both BIM and BCM are capable of removing N and P from wastewater by bio-struvite, BIM cannot provide crystals products of species-specific physiochemical characterization (Mann, 2001). Because such a biomineralization process is sensitive to the environment and can be significantly influenced by the extreme complexity of wastewater, this may result in other kinds of phosphate minerals. BCM, however, formed in compartmentalized microenvironments and was highly regulated by cells. This study also proposed two bacteria (*B. antiquum* and *I. loihiensis*) involved in BCM bio-struvite formation, which has potential for recovering nutrients such as N and P from wastewater by bio-struvite of more controlled quality.

3.4 Conclusions

- The microorganisms investigated can biodegrade proteins to release NH_4-N and raise the pH to create supersaturated condition for bio-struvite to nucleate. The presence of microbial cells reduced the $SI_{struvite}$ for bio-struvite heterogeneous nucleation, which enables the bio-struvite to be produced at low PO_4-P. The occurrence of crusted cell/cell clusters in *B. pumilus* culture is related to epicellular mineralization.
- The investigated microorganisms predominantly produced bio-struvite crystals of either coffin-lid, long-bar or trapezoidal-platy shapes and they exerted influence on the crystal morphology.
- *H. salinarum, B. pumilus* and *M. xanthus* produced bio-struvite of heterogeneous size through the BIM process, as a result of poor cellular control during the biomineralization.
- *B. antiquum* and *I. loihiensis* produced bio-struvite through the BCM process, of homogeneous size and morphology and better reproducibility, as a result of high cellular control during biomineralization. The intracellular $SI_{struvite}$ was high, where membrane-bound compartments occupied with electron-dense granules/materials were observed in the cytoplasm. *B. antiquum* and *I. loihiensis* are proposed to have potential to recover nutrients from waste streams by bio-struvite of more controlled quality.

3.5 References

Ali, M.I. et al. (2005) ‘Thermodynamics and solution chemistry of struvite’, *Journal of the Indian Institute of Science*, 85(September), pp. 141–149.

Arias, D. et al. (2017) ‘Biomineralization mediated by ureolytic bacteria applied to water treatment: a review’, *Crystals*, 7(11), p. 345.

Bailey, J. V. et al. (2007) ‘Evidence of giant sulphur bacteria in Neoproterozoic phosphorites’, *Nature*, 445(7124), pp. 198–201.

Bhuiyan, M.I.H. et al. (2007) ‘A solubility and thermodynamic study of struvite’, *Environmental Technology*, 28(9), pp. 1015–1026.

Bhuiyan, M.I.H. et al. (2008a) ‘Thermal decomposition of struvite and its phase transition’, *Chemosphere*, 70(8), pp. 1347–1356.

Bhuiyan, M.I.H. et al. (2008b) ‘Phosphorus recovery from wastewater through struvite formation in fluidized bed reactors: A sustainable approach’, *Water*

Science and Technology, 57(2), pp. 175–181.

Braissant, O. et al. (2003) ‘Bacterially induced mineralization of calcium carbonate in terrestrial environments: the role of exopolysaccharides and amino acids’, *Journal of Sedimentary Research*, 73(3), pp. 485–490.

Coe, F.L. et al. (2005) ‘Kidney stone disease’, *Journal of Clinical Investigation*, 115(October), pp. 2598–2608.

Conley, D.J. et al. (2009) ‘Controlling eutrophication: nitrogen and phosphorus’, *Science*, 323, pp. 1014–1015.

Le Corre, K.S. et al. (2005) ‘Impact of calcium on struvite crystal size, shape and purity’, *Journal of Crystal Growth*, 283(3–4), pp. 514–522.

Decho, A.W. (2000) ‘Microbial biofilms in intertidal systems: an overview’, *Continental Shelf Research*, 20(10–11), pp. 1257–1273.

Doyle, J.D. and Parsons, S. a. (2002) ‘Struvite formation, control and recovery’, *Water Research*, 36(16), pp. 3925–3940.

Elser, J.J. (2012) ‘Phosphorus: a limiting nutrient for humanity?’, *Current Opinion in Biotechnology*, 23(6), pp. 833–838.

EURASYP (2014) *Natural yeast – the nutritious basis for yeast extract*., *EURASYP (European Association for Specialty Yeast Products)* Available at: http://www.yeastextract.info/news-and-downloads/news/135/natural-yeast-the-nutritious-basis-for-yeast-extract (Accessed: 1 February 2018).

EURASYP (2011) *Yeast extract*., *EURASYP (European Association for Specialty Yeast Products)* Available at: http://hefeextrakt.info/public/documents/yeast-products/yeast_extract.pdf (Accessed: 1 February 2018).

Frankel, R.B. and Bazylinski, D.A (2003) ‘Biologically induced mineralization by bacteria’, *Reviews in Mineralogy and Geochemistry*, 54(1), pp. 95–114.

Frost, R.L. et al. (2004) ‘Thermal decomposition of struvite: Implications for the decomposition of kidney stones’, *Journal of Thermal Analysis and Calorimetry*, 76(3), pp. 1025–1033.

Galbraith, S.C. and Schneider, P.A. (2010) ‘A review of struvite nucleation studies’, in *Nutrient Recovery from Wastewater Streams*. , pp. 69–78.

Gao, G. (2008) ‘Physiological and ecological characteristics of blue-green algae in Lake Taihu’, in Qin, B. (ed.) *Lake Taihu, China: dynamics and environmental change*. Springer Science & Business Media., pp. 197–227.

González-Muñoz, M.T. et al. (2008) ‘Ca-Mg kutnahorite and struvite production by *Idiomarina* strains at modern seawater salinities’, *Chemosphere*, 72(3), pp. 465–472.

González-Muñoz, M.T. et al. (2010) ‘Bacterial biomineralization: new insights from *Myxococcus*-induced mineral precipitation’, *Geological Society, London,*

Special Publications, 336(1), pp. 31–50.

Grover, J.E. et al. (1997) 'The occurrence of biogenic calcian struvite, (Mg,Ca)$NH_4PO_4.6H_2O$, as intracellular crystals in *Paramecium*', *Journal of Eukaryotic Microbiology*, 44(4), pp. 366–373.

Gustafsson, J.P. (2000) *Visual MINTEQ* 3.1. KTH, Sweden

Huang, H. et al. (2014) 'Recovery and removal of ammonia–nitrogen and phosphate from swine wastewater by internal recycling of struvite chlorination product', *Bioresource Technology*, 172, pp. 253–259.

Ivanov, V. et al. (2005) 'Phosphate removal from the returned liquor of municipal wastewater treatment plant using iron-reducing bacteria', *Journal of Applied Microbiology*, 98(5), pp. 1152–1161.

Jardin, N. and Pöpel, H.J. (2001) 'Refixation of phosphates released during bio-P sludge handling as struvite or aluminium phosphate', *Environmental Technology*, 22(11), pp. 1253–1262.

Jurtshuk, P. (1996) 'Bacterial Metabolism', in Samuel Baron (ed.) *Medical Microbiology*. 4th edn. Galveston (TX): University of Texas Medical Branch at Galveston.

Kataki, S. et al. (2016) 'Phosphorus recovery as struvite: recent concerns for use of seed, alternative Mg source, nitrogen conservation and fertilizer potential', *Resources, Conservation and Recycling*, 107, pp. 142–156.

Kempter, A. et al. (2015) 'Phosphate removal from waste water by a seeding approach using novel seeding material', *Desalination and Water Treatment*, 55(10), pp. 2638–2646.

Leng, Y. and Soares, A. (2018) 'Biochemical characterisation of bio-mineralising struvite producing microorganisms (in preparation)', *Chemosphere*

Li, H. et al. (2015) 'Biomimetic synthesis of struvite with biogenic morphology and implication for pathological biomineralization', *Nature Scientific Reports*, , pp. 1–8.

Logan, B.E. (2005) 'Cellular growth and reproduction', in *Structural and functional relationships in prokaryotes*. New York: Springer, pp. 292–347.

Logan, B.E. (2008) 'Kinetics and mass transfer', in *Microbial fuel cells*. John Wiley & Sons, Inc.

Macaskie, L.E. et al. (2000) 'Enzymically mediated bioprecipitation of uranium by a *Citrobacter* sp.: A concerted role for exocellular lipopolysaccharide and associated phosphatase in biomineral formation', *Microbiology*, 146(8), pp. 1855–1867.

Mann, S. (2001) *Biomineralization : principles and concepts in bioinorganic materials chemistry*. Oxford University Press.

Mijangos, F. et al. (2004) 'Synthesis of struvite by ion exchange isothermal

supersaturation technique', *Reactive and Functional Polymers*, 60 Elsevier, pp. 151–161. Available at: 10.1016/J.REACTFUNCTPOLYM.2004.02.019 (Accessed: 11 January 2018).

Mindat (2018) *Struvite*., *Mindat.org* Available at: https://www.mindat.org/min-3811.html (Accessed: 5 February 2018).

Nocker, A. et al. (2017) 'When are bacteria dead? A step towards interpreting flow cytometry profiles after chlorine disinfection and membrane integrity staining', *Environmental Technology*, 38(7), pp. 891–900.

Omar, N. Ben et al. (1998) 'Struvite crystallization on *Myxococcus* cells', *Chemosphere*, 36(3), pp. 475–481.

Omelon, S. et al. (2013) 'A review of phosphate mineral nucleation in biology and geobiology', *Calcified Tissue International*, 93(4), pp. 382–396.

Orange, F. et al. (2009) 'Experimental silicification of the extremophilic archaea *Pyrococcus abyssi* and *Methanocaldococcus jannaschii*: Applications in the search for evidence of life in early earth and extraterrestrial rocks', *Geobiology*, 7(4), pp. 403–418.

Parsons, S.A. and Smith, J.A. (2008) 'Phosphorus removal and recovery from municipal wastewaters', *Elements*, 4(2), pp. 109–112.

Prywer, J. and Torzewska, A. (2010) 'Biomineralization of struvite crystals by *Proteus mirabilis* from artificial urine and their mesoscopic structure', *Crystal Research and Technology*, 45(12), pp. 1283–1289.

Prywer, J. and Torzewska, A. (2009) 'Bacterially induced struvite growth from synthetic urine: experimental and theoretical characterization of crystal morphology', *Crystal Growth and Design*, 9(8), pp. 3538–3543.

Prywer, J. et al. (2012) 'Unique surface and internal structure of struvite crystals formed by *Proteus mirabilis*', *Urological research*, 40(6), pp. 699–707.

Ratke, L. and Voorhees, P.W. (2013) *Growth and coarsening: Ostwald ripening in material processing*. Springer Science & Business Media.

Ronteltap, M. et al. (2010) 'Struvite precipitation from urine - Influencing factors on particle size', *Water Research*, 44(6), pp. 2038–2046.

Sadowski, R.R. et al. (2014) 'Morphology of struvite crystals as an evidence of bacteria mediated growth', *Crystal Research and Technology*, 49(7), pp. 478–489.

Schultze-Lam, S. et al. (1996) 'Mineralization of bacterial surfaces', *Chemical Geology*, 132, pp. 171–181.

Da Silva, S. et al. (2000) 'Effect of culture conditions on the formation of struvite by *Myxococcus xanthus*', *Chemosphere*, 40(12), pp. 1289–1296.

Simoes, F. (2017) *A new route to recover phosphorus from waste water: biological struvite production School*. Cranfield University.

Simoes, F. et al. (2017) ‘Understanding the growth of the bio-struvite production *Brevibacterium antiquum* in sludge liquors’, *Environmental Technology*, Taylor & Francis, pp. 1–10.

Sinha, A. et al. (2014) ‘Microbial mineralization of struvite: a promising process to overcome phosphate sequestering crisis’, *Water Research*, 54, pp. 33–43.

Smirnov, A. et al. (2005) ‘Formation of insoluble magnesium phosphates during growth of the archaea *Halorubrum distributum* and *Halobacterium salinarium* and the bacterium *Brevibacterium antiquum*’, *FEMS Microbiology Ecology*, 52(1), pp. 129–137.

Soares, A. et al. (2014) ‘Bio-Struvite: A new route to recover phosphorus from wastewater’, *Clean - Soil, Air, Water*, 42(7), pp. 994–997.

Spiegel, C.N. et al. (2013) ‘Fine structure of the male reproductive system and reproductive behavior of *Lutzomyia longipalpis* sandflies (Diptera: Psychodidae: Phlebotominae)’, *PLoS ONE*, 8(9), p. e74898.

Stolp, H. (1988) *Microbial ecology: organisms, habitats, activities*. Cambridge University Press.

Tansel, B. et al. (2018) ‘Struvite formation and decomposition characteristics for ammonia and phosphorus recovery: A review of magnesium-ammonia-phosphate interactions’, *Chemosphere*, 194, pp. 504–514.

Weiner, S. and Dove, P.M. (2003) ‘An overview of biomineralization processes and the problem of the vital effect’, *Reviews in mineralogy and geochemistry*, 54(1), pp. 1–29.

Westall, F. (1999) ‘The nature of fossil bacteria: A guide to the search for extraterrestrial life’, *Journal of Geophysical Research*, 104451(25), pp. 437–16.

Ye, Z. et al. (2014) ‘Phosphorus recovery from wastewater by struvite crystallization: Property of aggregates’, *Journal of Environmental Sciences*, 26(5), pp. 991–1000.

Yee, N. et al. (2003) ‘The effect of cyanobacteria on silica precipitation at neutral pH: Implications for bacterial silicification in geothermal hot springs’, *Chemical Geology*, 199(1–2), pp. 83–90.

De Yoreo, J.J. et al. (2015) ‘Crystallization by particle attachment in synthetic, biogenic, and geologic environments’, *Science*, 349(6247), p. aaa6760.

4 Understanding the mechanisms of bio-struvite biomineralization in municipal wastewater

Authors: Y Leng, A Soares

Cranfield Water Science Institute, Vincent Building, Cranfield University, Bedfordshire, MK43 0AL, UK

Abstract

The mechanisms of struvite biomineralization were investigated for five microorganisms (*Bacillus pumilus, Brevibacterium antiquum, Myxococcus xanthus, Halobacterium salinarum* and *Idiomarina loihiensis*) in municipal wastewater. The microbial exponential phase of growth occurred within 12–48 h of incubation and the growth rates varied from 0.02 to 0.08 1/h. The different microorganisms removed 23–27 mg/L (66–79%) of phosphate from wastewater, which was recovered as biological struvite (i.e. bio-struvite) (identified by morphological, XRD and elemental analysis). The dominant morphology of the bio-struvite produced was of elongated trapezoidal-platy shape, and large crystal groups (Dv_{90} ≤450 µm) were produced. Bio-struvite crystals occurred with a relatively low extracellular supersaturation index (0.6–0.8). The bio-struvite formation in *B. pumilus M. xanthus, H. salinarum* culture linked to biologically induced mineralization. Whereas *B, antiquum* and *I. loihiensis* produced bio-struvite through a biologically controlled mineralization because the crystals presented homogeneity in morphology and size (D_{v90}–D_{v50}≈125 µm), and intracellular vesicle-like cell structures were observed enclosing electron-dense clustered granules/materials. Although wastewater affected the microbial growth and crystal morphology, it did not change the mechanisms involved in bio-struvite formation when compared with synthetic solution. Hence, phosphorus recovery though bio-struvite biomineralization has the potential to be applied to wastewater streams.

Keywords: phosphorus recovery; municipal wastewater; biological struvite

4.1 Introduction

The wide application of phosphorus (P) as a commercial fertilizer in crop production and as a food additive in the livestock industry over recent decades has raised concerns regarding its exhaustion in both quality and quantity (Gilbert, 2009). Meanwhile, excess P disposal into surface waters (river, lake, reservoir, etc.) has resulted in eutrophication and the loss of biodiversity that threatens the environment and ecosystems. P removal from waste streams and recovery by valuable products has become a priority in the wastewater industry, at the same time as the need for compliance with stringent effluent discharge limits (Huang, Yang and Li, 2014; UWWTD, 2013).

Struvite ($MgNH_4PO_4{\cdot}6H_2O$) recovery from wastewater streams has gained attention in recent decades. Struvite deposits as scaling within pipelines and dewatering equipment in wastewater treatment plants (WWTPs), particularly in sludge liquor lines of biological nutrient removal (BNR) processes (Doyle and Parsons, 2002). In these liquors, when the concentrations of orthophosphate (PO_4-P), ammonium (NH_4-N) and magnesium (Mg^{2+}) are high enough and when pH reaches proper ranges (e.g. 7-11) in high turbulent areas, the formation of struvite scaling takes place, blocking pipes and equipment spontaneously (Le Corre et al., 2005; Doyle and Parsons, 2002). However, struvite is rich in P and nitrogen (N), and has excellent slow-release property, therefore it has potential use as a good alternative to current commercial P and N fertilizer and at the same time can ease the dependence on the availability of phosphate rock reserves (Massey et al., 2009). Abiotic struvite precipitation has been reported to remove >90% of PO_4-P (Le Corre et al., 2009), but a minimum PO_4-P >100 mg/L is recommended for readily struvite crystallization (Rittmann et al., 2011). Compared with traditional chemical (or abiotic) struvite precipitation, a novel way of producing struvite is through biomineralization (i.e. bio-struvite), with advantages of high PO_4-P removal (93–95%), recovering P at low concentration (30.5 mg PO_4-P/L) to achieve high P quality effluents (1.5–2.1 mg PO_4-P/L), and no chemical additives to adjust pH (Soares et al., 2014). However, the mechanisms involved in bio-struvite formation in wastewater are still poorly understood.

Cell activity plays a key role in bio-struvite mineralization. Based on the degree of cell control, the biomineralization process is traditionally categorised into biologically induced (BIM) or controlled mineralization (BCM) processes (Dhami, Reddy and Mukherjee, 2012). One important feature that distinguishes them is that BCM occurs in compartmentalized compartments, where specialized regulation of mineral crystallization contributes to the formation of reproducible and species-specific crystallochemical biomineral products (Mann, 2001). The mechanisms involved in such biomineralization processes vary with microbial strains. Specific enzymes (e.g. urease) capable of breaking down nitrogenous organic matters have been described to be frequently associated with bio-struvite crystallization, by producing ammonia as a metabolic by-product to elevate pH and NH_4-N concentration (Li et al., 2015).

Nevertheless, most bio-struvite crystals have been reported to deposit adventitiously in open environment via the BIM process (Weiner and Dove, 2003). In particular, the cell outer layer was suggested to provide a nucleation and precipitation site for biominerals through negatively charged residues (e.g. polysaccharide) to interact with and accumulate cations (e.g. Mg^{2+}), which is referred to as epicellular mineralization (Mann, 2001). *Enterobacter sp.* have been reported to synthesize bio-struvite through BCM process due to the homogenous morphology, composition and mineralogy in crystals (Sinha et al., 2014). Bio-struvite observed in the cytoplasm of *B. antiquum* of cell (Smirnov et al., 2005), and in the intracellular lipid vesicles of *Paramecium tetraurelia* cell (Grover, Rope and Kaneshiro, 1997) also have been reported to be associated with BCM. Because these intracellular vesicles constitute a spatially enclosed environment that maintains a particular ionic composition and allows for increased concentrations of certain ions, thereby fine-tuning the biomineralization process (Mann, 2001). Furthermore, as in most BCM, the bio-struvite produced by *P. tetraurelia* was suggested to serve multi-functions including N excretion and nutrient storage (Grover, Rope and Kaneshiro, 1997).

This study aims to investigate the mechanisms of bio-struvite biomineralization by the selected microbial strains in municipal wastewater. These microbial strains were analysed for their ability to grow in wastewater, change wastewater

chemical composition and create supersaturated conditions. The crystals produced biologically were characterized for particle size distribution, crystal morphology and intracellular structures.

4.2 Materials and Methods

4.2.1 Microorganisms

The five microbial strains investigated in this study were purchased from commercial culture collections: *Halobacterium salinarum* (DSM 671, German Resource Centre for Biological Material, Germany), *Bacillus pumilus* (GB43, LGC Standards, Middlesex, UK), *Brevibacterium antiquum* (DSM 21545, German Resource Centre for Biological Material, Germany), *Myxococcus xanthus* (CECT 422, Spanish Type Culture Collection, University of Valencia, Paterna, Spain) and *Idiomarina loihiensis* (MAH1/CECT 5996, Spanish Type Culture Collection, University of Valencia, Paterna, Spain).

4.2.2 Wastewater

Municipal wastewater was collected from the outlet of primary lamella clarifiers of a municipal WWTP with a 2840-population equivalent (Cranfield, UK). The wastewater was filtered by a 10 μm nylon-mesh filter (Plastok, UK), followed by microfiber (equivalent to 0.7 μm), and finally filtered sterilised (0.22 μm PVDF membrane, EMD Millipore, UK). Because the concentrations of PO_4-P, NH_4-N and Mg^{2+} (constituent ions of struvite) in the wastewater were too low to create supersaturated condition for readily struvite crystallization, these nutrients were added to the wastewater (Table 4-1). Hence, 0.22 μm sterile filtered (Sartorius Stedim Biotech, Germany) concentrated solutions of magnesium sulphate heptahydrate (MgSO4:7H_2O), di-potassium hydrogen phosphate (K_2HPO_4), ammonium chloride (NH_4Cl) were supplemented together with bovine serum albumin (BSA) (0.5 g/L) as an organic carbon source (Leng and Soares, 2018a) for microbial growth. The modified municipal wastewater was used to investigate the microbial growth and struvite production in this study (Table 4-1).

Table 4-1 Chemical properties of the wastewater used in this study

	Wastewater collected after primary lamella clarifiers	Wastewater eligible for bio-struvite formation	References	Wastewater used in this study after addition of nutrients
pH	7.7±0.1	7.5–7.8	(Fang et al., 2016; Simoes et al., 2017)	7.7±0.1
SCOD (mg/L)	174±1	NP	NP	715±16
PO_4-P (mg/L)	5.4±0.5	30.5–41.0	(Simoes et al., 2017; Soares et al., 2014)	34.3±0.6
Mg^{2+} (mg/L)	8.6±0.3	38.9–74.0	(Simoes et al., 2017; Soares et al., 2014)	55.2±0.4
NH_4-N (mg/L)	33±2.6	336–629	(Sadowski, Prywer and Torzewska, 2014; Soares et al., 2014)	311.5 ±1.4
Ca^{2+} (mg/L)	36.0±1.6	NP	NP	36.6±0.4
K^{+} (mg/L)	22.0±1.9	NP	NP	93.1±1.1

NP – not provided

4.2.3 Microbial cultivation

Starter cultures were grown in 250 ml E-flasks containing 100 ml of a 4 g/L yeast extract solution (additional 1% w/v NaCl and 1 g/L Mg^{2+} were added to grow *I. loihiensis*), incubated on an orbital shaker (Stuart model SSL1, Fisher Scientific, UK) at agitation rate of 150 RPM at room temperature (21–24°C) for 96 h. For inoculation in the wastewater, the starter cultures were centrifuged (Sanyo MSE Falcon 6/300 centrifuge, 2400 RCF, 4 °C, 10 min) and washed with sterile 0.9% w/v NaCl solution. The pure microorganism pellets were re-suspended in the sterile wastewater and inoculated into 36 mL wastewater in

100 mL glass bottles (Pyrex, Fisher Scientific, UK). Additional 0.8% NaCl was added to the *I. loihiensis* culture to ensure its growth (González-Muñoz et al., 2008). The bottles were capped with foam stoppers and incubated on an orbital shaker (Stuart model SSL1, Fisher Scientific, UK) at 150 RPM at room temperature for 192 h. Samples were taken at regular intervals (12–48 h), through sacrificial bottles to minimize sampling errors due to the heterogeneity of the crystals produced, especially when completing the particle size distribution. All tests were completed in duplicate and controls were maintained under identical conditions but without inoculation.

4.2.4 Solution supersaturation

A computer application, Visual MINTEQ ver. 3.1 (Gustafsson, 2000), was used to quantify the solution supersaturation index of struvite ($SI_{struvite}$). This application is based on the thermodynamic equilibrium comprising Mg^{2+}, calcium (Ca^{2+}), PO_4-P, NH_4-N, hydrogen (H^+) and hydroxide (OH^-) with a struvite solubility product constant (K_{sp}) of $10^{-13.26}$ (Ohlinger, Young and Schroeder, 1998).

4.2.5 Abiotic and biological struvite preparation, isolation, purification and identification

Abiotic struvite was prepared in the same wastewater applied in section 4.2.3. Half a litre of solution of 0.05 M $MgSO_4 \cdot 7H_2O$ was mixed with 0.25 L solution containing 0.2 M $NH_4H_2PO_4$ and 0.001M K_2HPO_4 in a glass bottle (1L, Duran™, Fisher Scientific, UK). Both solutions were pre-adjusted to pH 9 by 1 M sodium hydroxide (Le Corre et al., 2005). The mixture was agitated at 150 RPM at room temperature for 24 h for abiotic struvite precipitation. To prepare enough bio-struvite for identification, 4 L sterile wastewater (eight 1-L glass bottles, each containing 0.5 L wastewater) was used to grow each microbial strain under the identical conditions to those described in section 4.2.3 for 192 h. At the end of the incubation time, the precipitates were separated from the liquid by filtration (10 µm nylon-mesh filter, Plastok, UK) and washed with deionized (DI) water twice, air-dried at 37°C for 4 h and finally weighed to determine the struvite production yield.

The morphology and chemical properties of the recovered precipitated were identified by a scanning electron microscope equipped with energy dispersive X-ray spectroscopy (SEM-EDX, XL 30 SFEG, Phillips, The Netherlands) and an X-ray powder diffractometer (XRD, D5000, Siemens/Bruker, Germany). Diffraction data were collected with a step size of 0.04 over the range $20° < 2\theta < 90°$, and were analyzed with the DIFFRAC.SUITE™ EVA software package (Bruker AXS GmbH, Germany). The chemical characterization of the precipitates, including PO_4-P, NH_4-N, Mg^{2+}, Ca^{2+} and K^+ was also investigated in crystal dissolution (1.25 g/L, prepared in extra pure water pre-adjusted to pH 2 by 1 M hydrogen chloride).

4.2.6 Analytical methods

The intact cell counts over the incubation period were estimated with flow cytometry (BD Accuri C6, BD Biosciences, US) analyses using the SYBR Green I (SG) - propidium iodide (PI) co-staining method (Nocker et al., 2017). The concentrations of PO_4-P and NH_4-N were analysed using a Smartchem (Smartchem200, AMS/Alliance Instruments, France) according to the manufacturer's instructions (Labmedics, Abingdon, UK); Mg^{2+} Ca^{2+} and K^+ were analysed by an atomic absorption spectroscope (AAS, Analyst 800, PerkinElmer, UK) equipped with flaming and electrothermal spectrometers; pH was determined with a digital pH-meter (Jenway 3540, Bibby Scientific, UK); soluble chemical oxygen demand (SCOD) was analysed by Spectroquant® cell test kits (Merck, VWR, UK). The crystal size was estimated by volume-based particle size distribution (D_v) analysis using a Mastersizer (Malvern 3000, Malvern Instruments Ltd, UK) with a Hydro EV dispersion unit (stirring speed of 1200 RPM). A high-resolution microscope (L-series upright compound microscope, Division of GT vision Ltd, UK) was applied for observation of crystal morphology and interactions between microorganisms and crystals. For examination of intracellular crystals, the microbial cells were harvested during the stationary growth phase (60 h) and diluted with DI water to achieve approx. 200–300 cells/µL. A drop of the diluted culture was transferred to a 400-mesh Formvar and carbon-coated copper grid, air-dried and examined by high-resolution transmission electron microscopy (TEM, CM 20, Philips, Japan).

4.3 Results and Discussion

4.3.1 Microorganism growth in municipal wastewater

The lag phase of microbial growth was observed during the first 12 h incubation, followed by exponential phase of growth until 48 h (Figure 4-1). The estimated growth rates (μ) for the different microorganisms varied between 0.02 and 0.08 1/h (Table 4-2). The intact cell counts of the tested microorganisms were then maintained at a constant level from 48 to 192 h incubation, indicating a stationary phase. The only exception was observed for *M. xanthus*, where a 60% decrease of intact cell counts occurred after 148 h of incubation (Figure 4-1). During the incubation period, the SCOD was reduced by 170–320 mg/L (>90% was reduced during the exponential phase of growth), leaving a considerable amount of SCOD (500–600 mg/L) in the solution (Table 4-2). Neither microbial growth nor SCOD reduction was observed in the non-inoculated controls.

The additional BSA (as a carbon source) may have contributed to the microbial growth to some extent, because a previous study reported low growth rates (μ ≤0.004 1/h) of four of the selected microorganisms in wastewater streams with no extra carbon source, although a different method (turbidity measurement) was used (Soares et al., 2014). Although most of the selected microorganisms can use BSA as a carbon source (Leng and Soares, 2018a), the microbial growth rates in wastewater were 60–90% lower than those in synthetic solution (μ=0.16–0.28 1/h) where yeast extract was used as a carbon source (Leng, Simoes and Soares, 2018). Compared with BSA, yeast extract not only contains protein but also vitamins (B1, B2, B6, niacin, folic acid, etc.) and minerals (K^+, Na^+, Mg^{2+}, Fe^{2+}, Zn^{2+}) as essential macro/micronutrients for microbial growth (EURASYP, 2014). The shortage of such nutrients might have limited the microbial growth in wastewater, but further investigations are required to determine which factors limited microbial growth.

In this study, *B. antiquum* presented the highest growth rate (μ=0.08 1/h) and shortest lag phase compared with the other four microorganisms (Table 4-2, Figure 4-1). This growth rate is the same order of magnitude than previously

reported (μ=0.06 1/h) in wastewater using acetate as the major carbon source (equivalent to 1000 mg/L chemical oxygen demand) (Simoes et al., 2017). In contrast to *B. antiquum*, *I. loihiensis* presented a relative lower growth rate (μ=0.02 1/h) in wastewater (Table 4-2). The growth of *I. loihiensis* requires NaCl (0.7–20% w/v) and could be favoured in municipal wastewater with salinities of 2 % w/v NaCl (González-Muñoz et al., 2008).

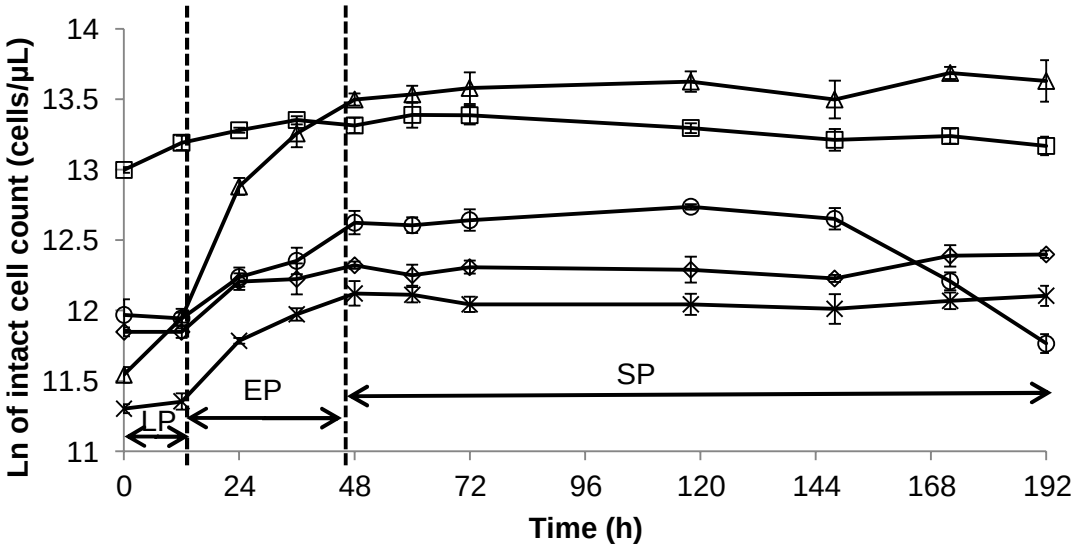

Figure 4-1 Natural logarithm of intact cell counts of *H. salinarum* (×), *B. antiquum* (Δ), *B. pumilus* (◊), *M. xanthus* (○) and *I. loihiensis* (□) in wastewater over 192 h incubation time. Error bars represent standard deviation obtained from duplicate tests. (LP- lag phase, EP- exponential phase, SP- stationary phase of growth)

Table 4-2 Growth rates of pure microbial strains and SCOD removal in wastewater (average ± standard deviation of duplicates)

	H. salinarum	*B. pumilus*	*B. antiquum*	*M. xanthus*	*I. loihiensis*
Growth rate (1/h)	0.04	0.03	0.08	0.03	0.02
SCOD removal	148±4 mg/L 21%	237±7 mg/L 33%	316±4 mg/L 44%	241±4 mg/L 34%	172±4 mg/L 24%

4.3.2 Crystal identification and morphology

All the microorganisms tested produced crystals in wastewater (Figure 4-2 a–e), and the dominant biologically produced crystals had the same morphology of elongated trapezoidal-platy shape as previously reported struvite (Kemacheevakul et al., 2015; Munch and Barr, 2001). Furthermore, the XRD results showed that the biologically produced crystals had similar peak profiles to the standard struvite (pattern COD 9007674). Thus, the crystals biologically recovered from wastewater were clearly identified as struvite. A detailed analysis of the crystal morphology face expressions showed that [011] and [111] were the dominant faces, and the *I. loihiensis* lacked [00$\bar{1}$] faces expression (Table 4-3). The specific morphology of trapezoidal-platy shaped bio-struvite is mainly due to crystals' slow growth rates that were evenly distributed among the various crystal planes (Abbona and Boistelle, 1979). On the other hand, abiotic struvite was found to be mainly X-shaped branched or comprising dendritic crystals (Figure 4-2 f). Such morphology was previously reported to frequently occur at pH ≥9 (Ye et al., 2014).

The struvite has been reported to have an crystal structure asymmetric along the c-axis, owing to its internal atomic arrangement (Prywer and Torzewska, 2009). Microorganisms have been reported to exert influence on struvite morphology by molecular electrostatic interactions between molecular structures of the crystal surface (e.g. [011] face terminated by NH_4^+, [00$\bar{1}$] face with high density of Mg^{2+}) and negatively charged microbial cell wall and extracellular polymers (e.g. polysaccharide of *Proteus mirabilis*) (Prywer and Torzewska, 2009). The secretion of phosphate groups by phosphatase activity has also been reported to contribute to the electronegative charged density of the cell outer layer (Macaskie et al., 2000). In this study, the bio-struvite crystal growth was observed to elongate along the a-axis and asymmetric along the c-axis (Figure 4-2 d). Moreover, the [011] face was significantly more enhanced than the other faces, as the crystal grew, suggesting that during bio-struvite crystal growth in wastewater, more microbial cells bonded to the [011] face other than [00$\bar{1}$] or [111] faces. In the case of *I. loihiensis* bio-struvite, the small

[00$\bar{1}$] faces resulted in extremely thin trapezoidal-platy shaped crystals (Figure 4-2 e). Such selective interactions between microbial cells and the molecular structure of the crystal surface lead to the elongated trapezoidal-platy shaped morphology.

Parallel grouping and various types of twinning were observed during the stationary phase of microbial growth, including parallel grouping, contact twining (Figure 4-2 e), penetrate twining (Figure 4-2 b) and cyclic twining (Figure 4-2 d), with contact twining along [00$\bar{1}$] faces being the most common twining types. Contact twining and penetrate twining of bio-struvite were reported to be dependent on high pH (e.g. pH 9–9.5) (Prywer and Torzewska, 2010). In this study, however, the twinning occurred at relatively low pH of 8.2 to 8.4. Both parallel grouping and twinning encouraged the formation of large crystals and morphology evolution (Li et al., 2015). The truncated apices were observed at both small and large bio-struvite crystals (Figure 4-2 a-b), for all microbial cultures in this study. The appearance of truncated apices was a signal that the struvite crystals had lost their rectangular symmetry (Sadowski, Prywer and Torzewska, 2014).

The chemical properties of bio-struvite were further examined by element analysis (Table 4-3). The chemical characteristics of the bio-struvite and abiotic struvite produced from the same wastewater were compared. Both types of struvite presented similar chemical characteristics. The crystals' dissolution contained PO_4-P (11.9-12.7%), NH_4-N (5.2-5.8%) and Mg^{2+} (9.3-9.8%) in equal molar concentration ([Mg^{2+}]:[PO_4-P]:[NH_4-N] =1:1:1) (Table 4-3), which showed a same nutrients composition as previously reported bio-struvite recovered from synthetic media (Leng, Simoes and Soares, 2018). Nevertheless, the SEM-EDX showed the stoichiometric ratio [Mg]:[P]:[O] on the crystal's surface was 1:1:4, and the N was under limit of detection. Significant loss of N and O on the crystal surface structure was observed, in comparison to the theoretical stoichiometric ratio [Mg]:[P]:[N]:[O] (1:1:1:10). Struvite was reported to be thermally unstable in air ≥40 °C, a temperature at which it may start losing bound water (H_2O) followed by ammonia (NH_3) molecules (Frost, Weier and Erickson, 2004). In this

study, the air-drying method applied before SEM-EDX analysis may have caused volatilization of N (as NH_3) and O (as H_2O) within the struvite crystalline framework, particularly on the crystal surface.

Both of the bio-struvite and abiotic struvite recovered from wastewater contained K^+ (0.2–0.8 mg/g) and Ca^{2+} (0.1–0.8 mg/g) (Table 4-3). Bio-struvite presented a relatively lower content of Ca^{2+} (≤0.2 mg/g) and higher K^+ (≥0.6 mg/g) (Table 4-3). The purity of struvite produced in wastewater was affected by Ca^{2+} and K^+, due to their relatively high concentrations in wastewater (measured at Ca^{2+} of 36.6 mg/L and K^+ of 93.1 mg/L, Table 4-1). In particular, the molar ratio $[Mg^{2+}]$:$[Ca^{2+}]$ in wastewater used for struvite production in this study was about 2.5:1, which may result in precipitation of a considerable amount of amorphous calcium phosphates (Ca-P) on the abiotic struvite, introducing impurity into crystal, as previously observed (Le Corre et al., 2005). On the other hand, the detected relatively high K^+ content in bio-struvite may relate to the uptake and accumulation of K^+, as essential macronutrient, within microbial cells (Britto and Kronzucker, 2008), whereby more K^+ could be released to the crystal surface when the cells bond to the crystal surface via specific molecular interactions (Sadowski, Prywer and Torzewska, 2014).

Table 4-3 Predominant crystal faces and element analysis of crystal dissolution of bio-struvite and abiotic struvite recovered from wastewater (average ± standard deviation of duplicates)

Predominant crystal faces						
	H. salinarum	*B. pumilus*	*B. antiquum*	*M. xanthus*	*I. loihiensis*	Abiotic struvite
[011]	X	X	X	X	X	X
[111]	X	X	X	X	X	X
$[00\bar{1}]$	X	X	X	X		X
Element analysis						
	H. salinarum	*B. pumilus*	*B. antiquum*	*M. xanthus*	*I. loihiensis*	Abiotic struvite
PO_4-P (mg/g)*	121.7±2.0	121.9±3.9	122.6±3.3	118.1±2.8	121.9±3.3	127.2±3.6
NH_4-N (mg/g)*	57.1±0.3	56.2±1.1	57.6±0.2	53.9±0.8	55.6±0.3	52.4±0.3
Mg^{2+} (mg/g)*	97.1±0.7	96.2±0.3	97.7±0.9	93.1±0.6	94.6±0.6	96.0±1.2
Ca^{2+} (mg/g)*	0.2±0.0	0.2±0.0	0.2±0.0	0.2±0.1	0.1±0.0	0.8±0.0
K^+ (mg/g)*	0.7± 0.0	0.7±0.0	0.8±0.0	0.6±0.0	0.6±0.0	0.2±0.0

* – mg/g struvite recovered from wastewater

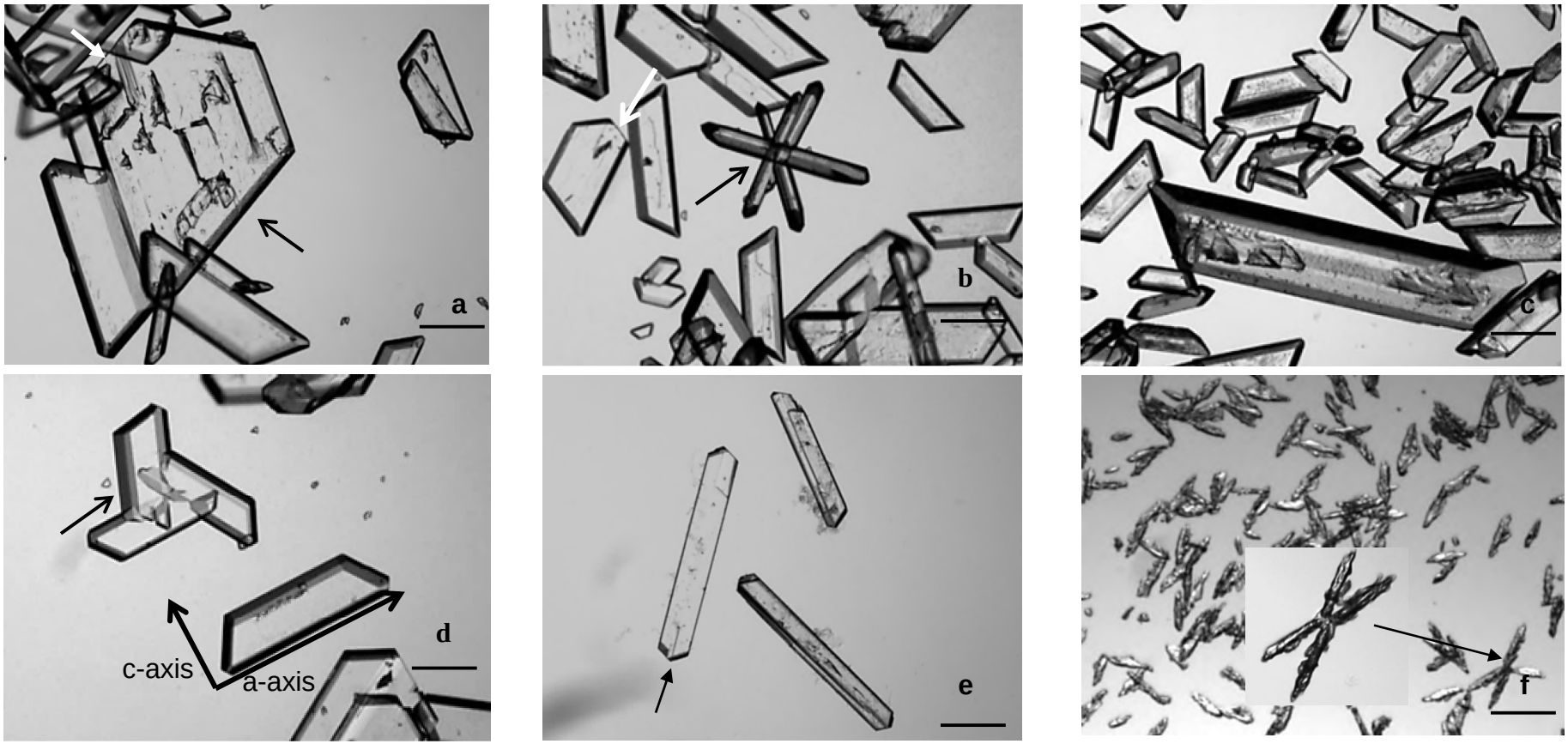

Figure 4-2 Bio-struvite crystals produced during stationary phase of growth (118 h) by (a) - *H. salinarum*, parallel grouping (black arrow), truncated apex (white arrow); (b) - *B. pumilus*, penetrate twining (black arrow), truncated apex (white arrow); (c) - *M. xanthus*; (d) - *B. antiquum*, cyclic twining (black arrow); (e) - *I. loihiensis*, contact twinning (black arrow). (f) - abiotic struvite, X-shaped (black arrow). Bar scale – 88.32 µm.

4.3.3 Bio-struvite production in wastewater and solution supersaturation

H. salinarum showed the highest production of bio-struvite in wastewater (154 mg bio-struvite/L wastewater), followed by *B. antiquum* (130 mg bio-struvite/L wastewater), *B. pumilus* (125 mg bio-struvite/L wastewater), *I. loihiensis* (119 mg bio-struvite/L wastewater) and *M. xanthus* (93 mg bio-struvite/L wastewater) (Table 4-4). The bio-struvite yields in this study were comparable to previously reported bio-struvite production (196±25, 198±42, 135±12 mg/L for *B. pumilus, H. salinarum,* and *B. antiquum*, respectively) in sludge dewatering liquors containing similar initial Mg^{2+} and PO_4-P and pH but with a 2.1–2.7 fold initial NH_4-N (Simoes, 2017). A relatively high final concentration of Mg^{2+} (32–38 mg/L) was observed in wastewater (Figure 4-3b), when compared with that in synthetic solution (2–11 mg/L) (Leng, Simoes and Soares, 2018). Thus, Mg^{2+} was not anticipated to limit the bio-struvite production.

The removal of nutrients from wastewater was 23–27 mg/L (66–79%) for PO_4-P and 17–21 mg/L (30–42%) for Mg^{2+} by the end of the incubation period (Table 4-4). The molar ratio of removed [PO_4-P]:[Mg^{2+}] in this study was about 1:1, corresponding to the chemical composition of struvite (Table 4-3). A significant drop of PO_4-P (62–73%) was observed within the exponential phase (0-48 h) (Figure 4-3 a). The PO_4-P and Mg^{2+} recovered by bio-struvite crystals (>10 µm) was 36-56% and 16-29%, respectively (Table 4-4). The pH increased rapidly during the first 24–36 h of incubation from 7.6–7.7 to 8.1–8.3, respectively, and maintained a relatively constant level (pH 8.2–8.4) until the end of the incubation period (Figure 4-3 c). The NH_4-N concentration increased over time (Figure 4-3 d) by 30–57 mg/L (Table 4-3). Previous studies have indicated that bio-struvite production results from a pH increase (due to NH_4-N release during metabolic breakdown of nitrogenous organic matters (e.g. proteins) and the integration of NH_4-N with PO_4-P and Mg^{2+} present in the environment (Sinha et al., 2014). In this study, correlations between microbial growth, NH_4-N, pH, PO_4-P and Mg^{2+} could be observed. In contrast to the increase of NH_4-N and pH, the concentrations of Mg^{2+} and PO_4-P in the wastewater dropped as a result of

struvite crystallization (Figure 4-3 a-d). However, the capability of bio-struvite to remove and recover P from wastewater streams in this study might be underestimated. Municipal wastewater typically contains 5–20 mg/l total P, of which 1–5 mg/L is organic P and the rest is inorganic P (Ivanov et al., 2005). Only inorganic P can be directly applied for abiotic struvite precipitation. Bio-struvite, however, was reported to be capable of using organic and condensed P, besides PO_4-P, with organic and condensed P contributing to 48% of the P recovered by bio-struvite (Simoes, 2017).

The solution $SI_{struvite}$ with respect to the struvite phase increased from 0.4–0.5 and peaked at 0.7–0.8 during the exponential phase of growth (24-48 h); the solution $SI_{struvite}$ then steadily decreased to 0.4–0.5 by the end of the 192-h incubation period (Figure 4-3 e). The bio-struvite $SI_{struvite}$ in wastewater presented the same overall trend and similar peak values of $SI_{struvite}$ as in synthetic solutions (Leng, Simoes and Soares, 2018), and a relatively high NH_4-N in solutions (>300 mg/L) contributed to maintain a final $SI_{struvite}$ >0. Such a $SI_{struvite}$ curve enables the biomineralization process and removed 23–27 mg/L of PO_4-P from wastewater (Table 4-4). Bio-struvite crystals were observed to occur during 12-24 h incubation in the inoculated bottles, corresponding to $SI_{struvite}$ of 0.6 to 0.8 (Figure 4-3 e). The overall $SI_{struvite}$ of *I. loihiensis* culture was observed relative low ($SI_{struvite}$ =0.4-0.7), which might be accountable to the production of thin platy crystals (Figure 4-2 e), because the crystal morphology is positively correlated with SI (Abbona and Boistelle, 1979). Furthermore, when comparing the $SI_{struvite}$ of the inoculated wastewater with that of abiotic struvite solution, it was observed the $SI_{struvite}$ required for bio-struvite crystallization is much lower ($SI_{struvite}$ =0.6-0.8) than previously reported a minimum $SI_{struvite}$ of 1.2 for spontaneously precipitation of abiotic struvite (Galbraith and Schneider, 2010) and a $SI_{struvite}$ range of 2 to 6 identified for PO_4-P removal >80% (Bhuiyan, Mavinic and Koch, 2008b).

A reduction of Ca^{2+} (2–8 mg/L) in the inoculated wastewater was observed (Figure 4-3 f), and the solution SI of calcium hydroxyapatite (HAP) was of 11 to 14, for potential formation of HAP. The presence of Ca^{2+} was reported to hinder

the bio-struvite production due to the priority of mineral precipitation (Rivadeneyra et al., 2006a). However, in this study, it is noted that the molar ratio of removed [Mg^{2+}]:[Ca^{2+}] by *B. antiquum* (18) was higher than the others (6–10), indicating that *B. antiquum* produced a substance containing more Mg^{2+} and less Ca^{2+}.

Table 4-4 Bio-struvite production and changes of PO_4-P, NH_4-N, Mg^{2+} Ca^{2+} concentrations and pH in the presence of microbial strains and in the non-inoculated control at the end of 192 h incubation (average ± standard deviation of duplicates)

	H. salinarum	*B. antiquum*	*M. xanthus*	*B. pumilus*	*I. loihiensis*	Non-inculcated control
Bio-struvite production (mg bio-struvite*/L wastewater treated)	154±5	130±4	93±5	125±6	119±3	0
pH increase	0.6±0.0	0.7±0.0	0.6±0.0	0.6±0.0	0.6±0.0	<0.1
NH_4-N production	41±1 mg/L	57±1 mg/L	49±0 mg/L	47±1mg/L	30±3 mg/L	<1 mg/L
PO_4-P removal	26±0mg/L 76%	27±0mg/L 79%	24±1mg/L 71%	26±0mg/L 75%	23±1mg/L 66%	<1 mg/L 0%
Mg^{2+} removal	21±1mg/L 38%	19±0mg/L 42%	17±1mg/L 31%	21±0mg/L 38%	17±0mg/L 30%	<1 mg/L 0%
PO_4-P recovered as bio-struvite*	19 mg/L 56%	16 mg/L 47%	12 mg/L 36%	16mg/L 46%	15 mg/L 43%	0 0%
Mg^{2+} recovered as bio-struvite*	15 mg/L 27%	13 mg/L 29%	9 mg/L 16%	12 mg/L 22%	12 mg/L 21%	0 0%

* – Bio-struvite crystals >10 µm

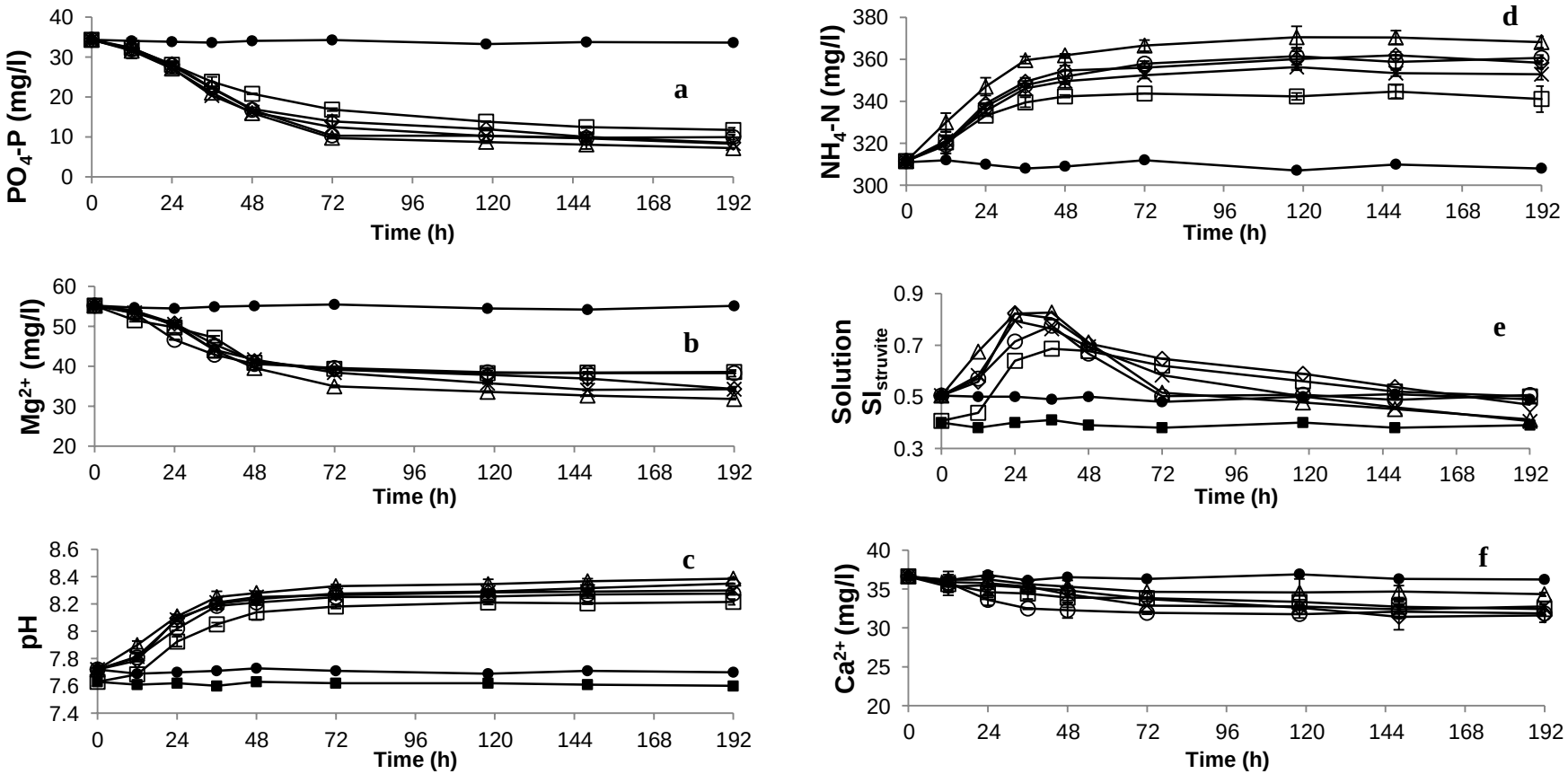

Figure 4-3 Changes in PO_4-P(a), Mg^{2+}(b), pH (c), NH_4-N (d), solution $SI_{struvite}$ (e) and Ca^{2+} (f) in wastewater during cultivation of *H. salinarum* (×), *B. antiquum* (Δ), *B. pumilus* (◊), *M. xanthus* (○), *I. loihiensis* (□) and non-inoculated controls (● – wastewater, ■ – wastewater with additional 0.8% NaCl) with time (error bars represent standard deviation obtained from duplicates).

4.3.4 Bio-struvite growth

The particle size distribution of bio-struvite showed an overall increasing trend with time: rapid crystal growth occurred within the first 72 h of incubation, followed by constant levels of the crystal size distribution that was maintained until the end of the incubation period (Figure 4-4). By the end of incubation period, the large crystal groups (>100 μm) accounted for 41–46% of the total particles (Table 4-5). The final D_{v50} and D_{v90} were 85–178 μm and 212–451 μm, respectively (Table 4-5), which was comparable to the average size of typical spontaneous chemical precipitated struvite (up to 136 μm) in hydrolysed urine ($SI_{struvite}$ =2.11) (Ronteltap et al., 2010). An overview of the size and morphology of bio-struvite and abiotic struvite is presented in Figure 4-5. Compared with bio-struvite, the abiotic struvite was relatively small with an average size of around 30 μm (Figure 4-5f).

It was observed that *B. antiquum* and *I. loihiensis* bio-struvite had a narrow gap range between D_{v50} and D_{v90}, of 123 and 127 μm, respectively; whereas *H. salinarum*, *B. pumilus* and *M. xanthu*s bio-struvite were of relatively wide gap ranges of particle size (D_{v90} - D_{v50} =257-273 μm) (Table 4-5). Moreover, the bio-struvite produced by *B. antiquum* and *I. loihiensis* were of more reproducibility regarding size and morphology (Figure 4-5 d–e), whereas the other three microbial strains produced bio-struvite with high heterogeneity (Figure 4-5 a–c). The narrow size distribution, homogeneity of morphology and composition are among the important features of the BCM process, and the formation of heterogeneous minerals is a signature of BIM (Weiner and Dove, 2003), whereby the magnetotactic bacteria was distinguished from iron-reducing bacteria in magnetite synthesis (Frankel and Bazylinski, 2003), and the bio-struvite formation by *Enterobacter sp*. and *P. tetraurelia* was identified as BCM process (Grover, Rope and Kaneshiro, 1997; Sinha et al., 2014). In this study, *B. antiquum* and *I. loihiensis* are suggested as bacteria capable to produce BCM bio-struvite due to homogeneity of crystal morphology and size.

When comparing the crystal growth of bio-struvite in wastewater with a synthetic solution, it was observed that the final crystal size distribution was similar, but the percentage of large crystal group (>100 μm) was reduced by 12-41%, and the reaction time required to reach constant level of crystal size

distribution was extended by 24–48 h in wastewater (Leng, Simoes and Soares, 2018). Particularly, the moderately halophilic *I. loihiensis* growing in 0.8% % w/v NaCl was observed to produce large bio-struvite crystals (D_{v90} >200 µm). Large long-bar shaped *I. loihiensis* bio-struvite (approx. 120 µm) was also observed in solution at even higher salinity (seawater) (González-Muñoz et al., 2008). A variety of halophiles have been reported to produce minerals in salt water (2.5–20% w/v NaCl), but the mineral particle size decreased as salinity increased (Rivadeneyra et al., 2006a).

Regarding the supersaturation degree for struvite crystallization, high solution $SI_{struvite}$ (e.g. $SI_{struvite}$ >1.7) was observed positive for struvite homogenous nucleation but negative for the crystal growth, and this dilemma was traditionally addressed by seeding with powder struvite or sand at low $SI_{struvite}$ solution (e.g. $SI_{struvite}$ =0.55) for heterogeneous precipitation and reduced reaction period (Le Corre et al., 2009; Mehta and Batstone, 2013). However, via biomineralization, the microbial cells have the potential to act as bio-seeds for mineral precipitation (e.g. iron, manganese) (Wang and Müller, 2009). Ben Omar et al. (1995) reported the importance of physical presence of cells (or cell debris) that may act as heterogeneous nuclei for struvite crystallization. In this study, the presence of microbial cells is proposed to reduce the energy barrier required for bio-struvite mineralization in wastewater. The solution $SI_{struvite}$ during 12-24 h incubation ($SI_{struvite}$ =0.6–0.8) (Figure 4-3 e) was too low to form a nucleation point spontaneously, but the presence of microbial cells helped reduce the energy barrier for struvite nucleation. The nucleation was followed by crystal growth within an appropriate $SI_{struvite}$ range from 0.4 to 0.8 (Figure 4-3 e). Furthermore, provided that the crystal nucleus depends on microbial cells, the number of bio-struvite crystals might be relative to microbial growth.

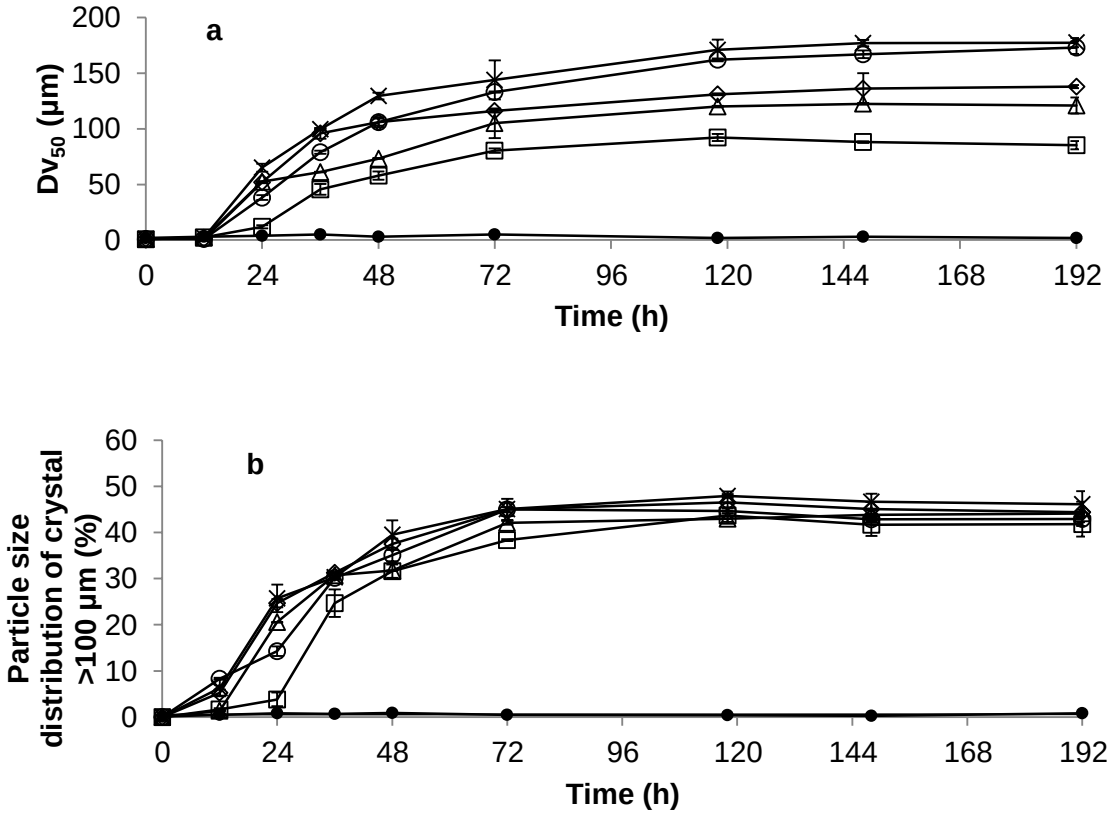

Figure 4-4 Variation of D_{v50} (a) and percentage of crystal size >100 µm (b) in the presence of *H. salinarum* (×), *B. antiquum* (Δ), *B. pumilus* (◊), *M. xanthus* (○) and *I. loihiensis* (□) in wastewater and non-inoculated controls (●) with time (error bars represent standard deviation obtained from duplicates). D_{v50} is the value of the particle diameter at 50% in the cumulative distribution on the basis of volume.

Table 4-5 D_{v50} and D_{v90} of bio-struvite crystals and in non-inoculated control in municipal wastewater at the end of 192 h incubation (average ± standard deviation of duplicates)

	H. salinarum	*B. antiquum*	*M. xanthus*	*B. pumilus*	*I. loihiensis*	Control
D_{v50} (µm)	178±4	131±7	163±6	138±1	85±4	2
D_{v90} (µm)	451±27	254±2	420±7	402±8	212±5	5

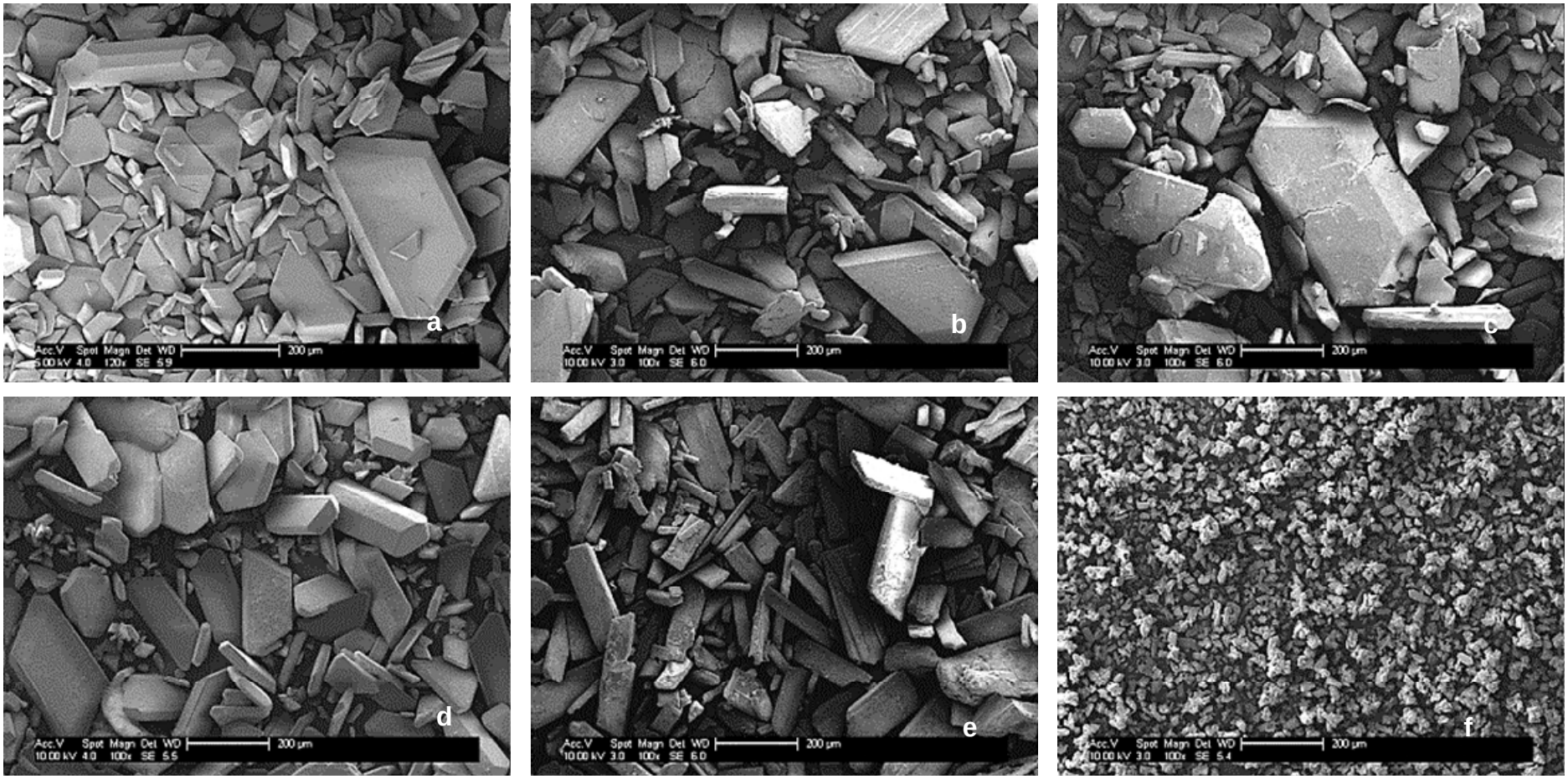

Figure 4-5 Overview of isolated purified bio-struvite crystals recovered from municipal wastewater inoculated with (a) - *H. salinarum*, (b) - *B. pumilus*, (c) - *M. xanthus*, (d) - *B. antiquum*, (e) - *I. loihiensis* by the end of 192 h, and (f) - abiotic struvite. Scale bar – 200 µm.

4.3.5 Bio-struvite biomineralization mechanisms in wastewater

When comparing the key features of bio-struvite mineralization in wastewater with those in synthetic solutions (Leng, Simoes and Soares, 2018), it is observed that the mechanisms involved in such biomineralization have not changed in municipal wastewater (Table 4-6). The microbial growth produced NH_4-N and increased the pH to create supersaturated condition for bio-struvite crystallization; the BCM (*B. antiquum* and *I. loihiensis*) was distinguished from BIM bio-struvite (*H. salinarum*, *B. pumilus* and *M. xanthus*) by homogeneity of crystals (e.g. size, morphology) and signature cell structures (e.g. intracellular vesicles enclosing electron-dense clustered materials).

Intracellular spherical structures within the membrane were observed within *B. antiquum* and *I. loihiensis* cells in wastewater by TEM, and some of them were identified containing electron-dense granules/materials (Figure 4-6 a–b). These cell structures are suggested to be lipid vesicles, due to a similar structure to previously reported lipid vesicles (Spiegel et al., 2013), and the dense granules inside the vesicle-like structures were morphologically similar to the intracellular bio-struvite crystals in *P. tetraurelia* cells (Grover, Rope and Kaneshiro, 1997). Intracellular vesicles are an important feature of the BCM process (Bazylinski and Frankel, 2003). The magnetosome formation by magnetotactic bacteria is one of the most characterized BCM processes. The bacteria form vesicles within cells, transport iron from the cytoplasm into the vesicles, and integrate ferrous with ferric to produce magnetite (Bazylinski and Frankel, 2003). Besides controlling the rates of ionic diffusion and pumping, the vesicles also exert influence on crystal size and morphology by placing a physical boundary or via selective interaction between specific membrane proteins and magnetite crystals (Arakaki, Webb and Matsunaga, 2003; Mann, 2001). The formation of *B. antiquum* and *I. loihiensis* bio-struvite in wastewater is here suggested to be a BCM process. The occurrence of bio-struvite crystals within the cytoplasm was also observed in *B. antiquum* cells (Smirnov et al., 2005). Furthermore, such intercellular structures may have a functional purpose (e.g. storage). Grover, Rope and Kaneshiro (1997) proposed that *P. tetraurelia* produced vesicles rich in lipid, to extract metals from solution, increase ion concentrations

inside vesicles, and produce intracellular bio-struvite for nitrogen excretion or storage.

Crusted two-cell and tetrad cell clusters were observed in *B. pumilus* culture in wastewater (Figure 4-6 c), and these crusted cell structures have potential to form aggregates. Similar cell structures were observed in *Thiomargarita* embryo infestation (Bailey et al., 2007) and microbial silicification (Yee et al., 2003). The crusted cell structures are proposed as a result of extensive epicellular mineralization in wastewater. An iron-rich capsule and granules structure were frequently reported materials to partially to completely encrust the bacterial cells, along with siliceous spheroidal crystallite spheroids embedded within iron-rich capsular material or spheres (Konhauser and Riding, 2012). In this study, the Gram-positive *B. pumilus* characterized by an anionic thick outer layer (~ 25 nm wide peptidoglycan framework) have potential to form a thick and robust mineral crust around its cell (Schultze-Lam et al., 1996; Westall, 1999). However, as a typical BIM process, the epicellular mineralization occurred in an open environment, and the process and mineral products highly depend on the environment (Mann, 2001).

In this study, the microorganisms made use of wastewater enriched with BSA as a carbon source to grow, indicating that the microbes can adapt to wastewater. This study revealed the capability of the microorganisms to produce bio-struvite of high quality and large size in wastewater of low PO_4-P and low $SI_{struvite}$, without chemical dosing for pH adjustment. Furthermore, the occurrence of BCM bio-struvite in wastewater revealed the potential application of *B. antiquum* and *I. loihiensis* for nutrient recovery from wastewater by bio-struvite of more controlled quality. Chemical precipitation is currently the most common way to produce struvite in wastewater streams, but the efficiency is highly reliant on pH and nutrient concentrations (Mehta et al., 2015). The application of bio-struvite in municipal wastewater can remove P and N without additional cost for pH adjustment and PO_4-P elevation, along with COD reduction as an additional benefit. To control the chemical composition of the compartmentalized micro-environment, the BCM processes generally highly rely on the positive pumping of specific ions (Mann, 2001). Thus, the two bacteria

(*B. antiquum* and *I. loihiensis*) proposed to be involved in BCM bio-struvite formation have the potential to remove/recover nutrients from raw municipal wastewater with low PO_4-P concentration (e.g. 4–15 mg/L) (Henze and Comeau, 2008) and produce bio-struvite of more controlled quality.

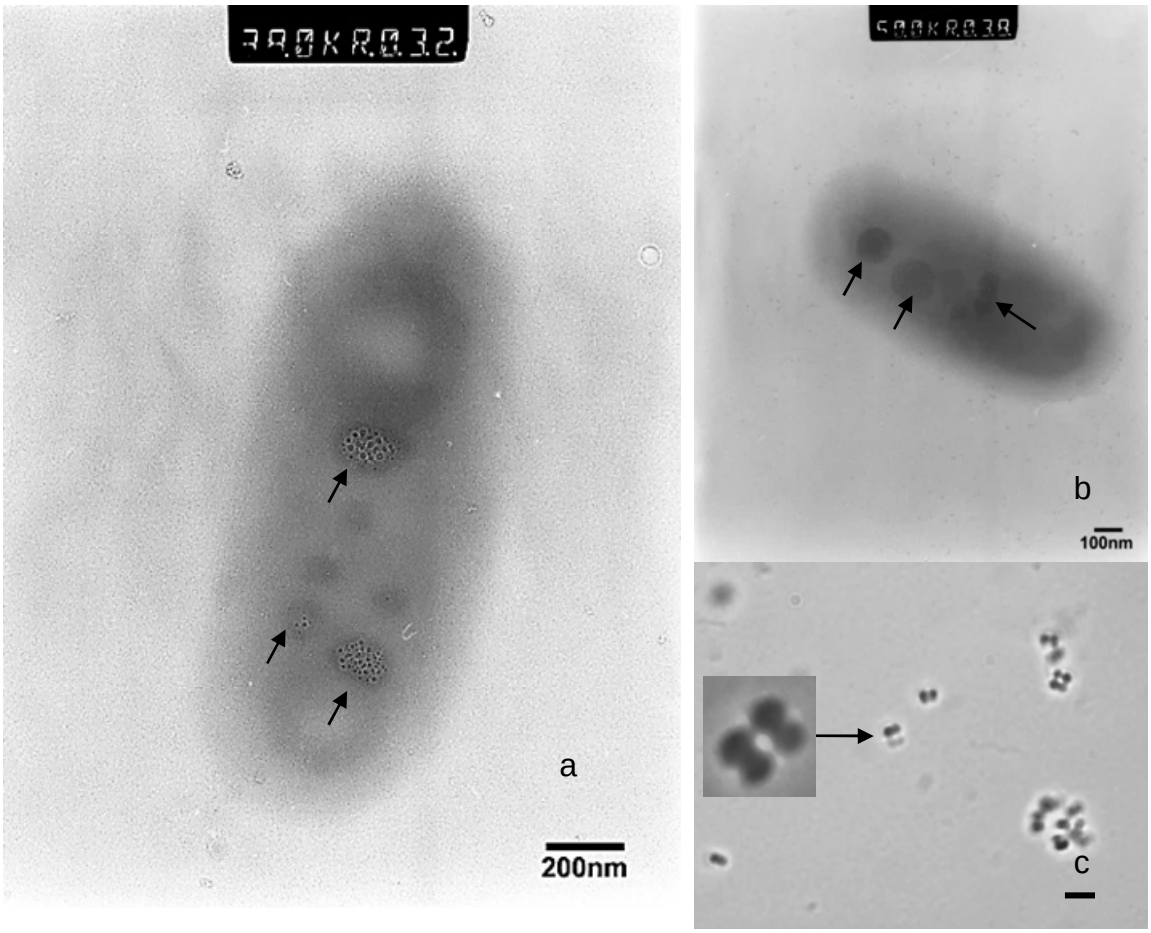

Figure 4-6 TEM photo shows membrane-enclosed electron-dense granules/materials (arrows) inside (a) - *B. antiquum* cell and (b) - *I. loihiensis* cells in wastewater (60h). (c) Light microscope photograph showing crusted cell structures (arrows) in *B. pumilus* culture (24 h).

Table 4-6 Key features of bio-struvite mineralization by *H. salinarum, B. antiquum, B. pumilus, M. xanthus and I. loihiensis* in wastewater.

	Evidence supporting biologically induced mineralization	Evidence supporting biologically controlled mineralization
H. salinarum	• pH elevation • NH_4-N production • Crystal morphology heterogeneity • Crystal size heterogeneity: D_{v90}–D_{v50}=273 μm	
B. pumilus	• pH elevation • NH_4-N production • Crystal morphology heterogeneity • Crystal size heterogeneity: D_{v90}–D_{v50}=257 μm • Crusted cell structure	
M. xanthus	• pH elevation • NH_4-N production • Crystal morphology heterogeneity • Crystal size heterogeneity: D_{v90}–D_{v50}=264 μm	
B. antiquum		• pH elevation • NH_4-N production • Crystal morphology homogeneity • Crystal size homogeneity: D_{v90}–D_{v50}=123 μm • Intracellular vesicle-like structures
I. loihiensis		• pH elevation • NH_4-N production • Crystal morphology homogeneity • Crystal size homogeneity: D_{v90}–D_{v50}=127 μm • Intracellular vesicle-like structures

4.4 Conclusions

- The selected microbial strains presented growth rates of 0.02–0.08 1/h in municipal wastewater (with additional carbon source) and contributed to bio-struvite production by NH_4-N production, increasing pH and reducing the energy barrier for crystallization.

- Bio-struvite yield, PO_4-P removal and PO_4-P recovery varied with microorganisms, and ranged from 93–154 mg bio-struvite/L wastewater, 23–26 mg/L and 12–19 mg/L, respectively. Formation of bio-struvite occurred in wastewater when the $SI_{struvite}$ achieved 0.6- 0.8. Large crystal groups ($D_{V90=}$210–450 μm) were observed. However, compared with synthetic solution, the proportion of large crystal groups (>100 μm) in wastewater was reduced by 12-41%, and the reaction time required to reach constant level of crystal size distribution was extended to 48-72 h.
- The recovered bio-struvite contained Mg^{2+}, PO_4-P and NH_4-N in equal molar concentrations. The microorganisms exerted control during the crystal growth, leading to elongated trapezoidal-platy shaped bio-struvite crystals with an enhanced [011] faces.
- *H. salinarum*, *B. pumilus* and *M. xanthus* being identified as using a BIM process. Crusted cell structures were observed in *B. pumilus* cultures, which may be associated with epicellular mineralization.
- The formation of *B. antiquum* and *I. loihiensis* bio-struvite in wastewater was identified as a BCM process. Intracellular vesicle-like structures were observed occupied with electron-dense granules/materials, and the bio-struvite was observed to be homogeneous in terms of morphology and size. Thus, the way in which microbial cells induce/control bio-struvite formation was not changed in wastewater, and *B. antiquum* and *I. loihiensis* have increased potential to recover P from wastewater using bio-struvite of controlled quality.

4.5 References

Abbona, F. and Boistelle, R. (1979) ‘Growth morphology and crystal habit of struvite crystals ($MgNH_4PO_4 \cdot 6H_2O$)’, *Journal of Crystal Growth*, 46(3), pp. 339–354.

Arakaki, A. et al. (2003) ‘A novel protein tightly bound to bacterial magnetic particles in *Magnetospirillum magneticum* strain AMB-1’, *Journal of Biological Chemistry*, 278(10), pp. 8745–8750.

Bailey, J. V. et al. (2007) ‘Evidence of giant sulphur bacteria in Neoproterozoic phosphorites’, *Nature*, 445(7124), pp. 198–201.

Bazylinski, D.A. and Frankel, R.B. (2003) ‘Biologically controlled mineralization

in prokaryotes', *Reviews in Mineralogy and Geochemistry*, 54(1), pp. 217–247.

Bhuiyan, M.I.H. et al. (2008) 'Phosphorus recovery from wastewater through struvite formation in fluidized bed reactors: A sustainable approach', *Water Science and Technology*, 57(2), pp. 175–181.

Britto, D.T. and Kronzucker, H.J. (2008) 'Cellular mechanisms of potassium transport in plants', *Physiologia Plantarum*, 133(4), pp. 637–650.

Le Corre, K.S. et al. (2005) 'Impact of calcium on struvite crystal size, shape and purity', *Journal of Crystal Growth*, 283(3–4), pp. 514–522.

Le Corre, K.S. et al. (2009) 'Phosphorus recovery from wastewater by struvite crystallization: a review', *Critical Reviews in Environmental Science and Technology*, 39(6), pp. 433–477.

Dhami, N.K. et al. (2012) 'Biofilm and microbial applications in biomineralized concrete', in *Advanced Topics in Biomineralization*. InTech, pp. 137–164.

Doyle, J.D. and Parsons, S. a. (2002) 'Struvite formation, control and recovery', *Water Research*, 36(16), pp. 3925–3940.

EURASYP (2014) *Natural yeast – the nutritious basis for yeast extract*., *EURASYP (European Association for Specialty Yeast Products)* Available at: http://www.yeastextract.info/news-and-downloads/news/135/natural-yeast-the-nutritious-basis-for-yeast-extract (Accessed: 1 February 2018).

Fang, C. et al. (2016) 'Phosphate enhance recovery from wastewater by mechanism analysis and optimization of struvite settleability in fluidized bed reactor', *Scientific Reports*, 6, pp. 1–10.

Frankel, R.B. and Bazylinski, D. a (2003) 'Biologically induced mineralization by bacteria', *Reviews in Mineralogy and Geochemistry*, 54(1), pp. 95–114.

Frost, R.L. et al. (2004) 'Thermal decomposition of struvite: Implications for the decomposition of kidney stones', *Journal of Thermal Analysis and Calorimetry*, 76(3), pp. 1025–1033.

Galbraith, S.C. and Schneider, P.. (2010) 'A review of struvite nucleation studies', in *Nutrient Recovery from Wastewater Streams*. , pp. 69–78.

Gilbert, N. (2009) 'The disappearing nutrient', *Nature*, 461(7265), pp. 716–718.

González-Muñoz, M.T. et al. (2008) 'Ca-Mg kutnahorite and struvite production by *Idiomarina* strains at modern seawater salinities', *Chemosphere*, 72(3), pp. 465–472.

Grover, J.E. et al. (1997) 'The occurrence of biogenic calcian struvite, $(Mg,Ca)NH_4PO_4.6H_2O$, as intracellular crystals in *Paramecium*', *Journal of Eukaryotic Microbiology*, 44(4), pp. 366–373.

Gustafsson, J.P. (2000) *Visual MINTEQ* 3.1. KTH, Sweden

Henze, M. and Comeau, Y. (2008) 'Wastewater characterization', in *Biological wastewater treatment: principles modelling and design*. IWA publishing, pp. 33–

52.

Huang, H. et al. (2014) ‘Recovery and removal of ammonia–nitrogen and phosphate from swine wastewater by internal recycling of struvite chlorination product’, *Bioresource Technology*, 172, pp. 253–259.

Ivanov, V. et al. (2005) ‘Phosphate removal from the returned liquor of municipal wastewater treatment plant using iron-reducing bacteria’, *Journal of Applied Microbiology*, 98(5), pp. 1152–1161.

Kemacheevakul, P. et al. (2015) ‘Effect of magnesium dose on amount of pharmaceuticals in struvite recovered from urine’, *Water Science and Technology*, 72(7), pp. 1102–1110.

Konhauser, K. and Riding, R. (2012) ‘Bacterial biomineralization’, in H., A. et al. (eds.) *Fundamentals of Geobiology*. Blackwell Publishing Ltd, pp. 105–130.

Leng, Y. et al. (2018) ‘Understanding the mechanisms of bio-struvite biomineralization (in preparation)’, *Bioresource Technology*

Leng, Y. and Soares, A. (2018) ‘Biochemical characterisation of bio-mineralising struvite producing microorganisms (in preparation)’, *Chemosphere*

Li, H. et al. (2015) ‘Biomimetic synthesis of struvite with biogenic morphology and implication for pathological biomineralization’, *Nature Scientific Reports*, , pp. 1–8.

Macaskie, L.E. et al. (2000) ‘Enzymically mediated bioprecipitation of uranium by a *Citrobacter* sp.: A concerted role for exocellular lipopolysaccharide and associated phosphatase in biomineral formation’, *Microbiology*, 146(8), pp. 1855–1867.

Mann, S. (2001) *Biomineralization : principles and concepts in bioinorganic materials chemistry*. Oxford University Press.

Massey, M.S. et al. (2009) ‘Effectiveness of recovered magnesium phosphates as fertilizers in neutral and slightly alkaline soils’, *Agronomy Journal*, 101(2), pp. 323–329.

Mehta, C.M. and Batstone, D.J. (2013) ‘Nucleation and growth kinetics of struvite crystallization’, *Water Research*, 47(8) Elsevier Ltd, pp. 2890–2900.

Mehta, C.M. et al. (2015) ‘Technologies to recover nutrients from waste streams: a critical review’, *Critical Reviews in Environmental Science and Technology*, 45(4), pp. 385–427.

Munch, E. V. and Barr, K. (2001) ‘Controlled struvite crystallisation for removing phosphorus from anaerobic digester sidestreams’, *Water Research*, 35(1), pp. 151–159.

Nocker, A. et al. (2017) ‘When are bacteria dead? A step towards interpreting flow cytometry profiles after chlorine disinfection and membrane integrity staining’, *Environmental Technology*, 38(7), pp. 891–900.

Ohlinger, K.N. et al. (1998) ‘Predicting struvite formation in digestion’, *Water Research*, 32(12), pp. 3607–3614.

Ben Omar, N. et al. (1995) ‘*Myxococcus xanthus*’ killed cells as inducers of struvite crystallization. Its possible role in the biomineralization processes’, *Chemosphere*, 30(12), pp. 2387–2396.

Prywer, J. and Torzewska, A. (2009) ‘Bacterially induced struvite growth from synthetic urine: experimental and theoretical characterization of crystal morphology’, *Crystal Growth and Design*, 9(8), pp. 3538–3543.

Prywer, J. and Torzewska, A. (2010) ‘Biomineralization of struvite crystals by *Proteus mirabilis* from artificial urine and their mesoscopic structure’, *Crystal Research and Technology*, 45(12), pp. 1283–1289.

Rittmann, B.E. et al. (2011) ‘Capturing the lost phosphorus’, *Chemosphere*, 84(6), pp. 846–853.

Rivadeneyra, M.A. et al. (2006) ‘Precipitation of minerals by 22 species of moderately halophilic bacteria in artificial marine salts media: Influence of salt concentration’, *Folia Microbiologica*, 51(5), pp. 445–453.

Ronteltap, M. et al. (2010) ‘Struvite precipitation from urine - Influencing factors on particle size’, *Water Research*, 44(6), pp. 2038–2046.

Sadowski, R.R. et al. (2014) ‘Morphology of struvite crystals as an evidence of bacteria mediated growth’, *Crystal Research and Technology*, 49(7), pp. 478–489.

Schultze-Lam, S. et al. (1996) ‘Mineralization of bacterial surfaces’, *Chemical Geology*, 132, pp. 171–181.

Simoes, F. (2017) *A new route to recover phosphorus from waste water: biological struvite production School*. Cranfield University.

Simoes, F. et al. (2017) ‘Understanding the growth of the bio-struvite production *Brevibacterium antiquum* in sludge liquors’, *Environmental Technology*, Taylor & Francis, pp. 1–10.

Sinha, A. et al. (2014) ‘Microbial mineralization of struvite: a promising process to overcome phosphate sequestering crisis’, *Water Research*, 54, pp. 33–43.

Smirnov, A. et al. (2005) ‘Formation of insoluble magnesium phosphates during growth of the archaea *Halorubrum distributum* and *Halobacterium salinarium* and the bacterium *Brevibacterium antiquum*’, *FEMS Microbiology Ecology*, 52(1), pp. 129–137.

Soares, A. et al. (2014) ‘Bio-Struvite: A new route to recover phosphorus from wastewater’, *Clean - Soil, Air, Water*, 42(7), pp. 994–997.

Spiegel, C.N. et al. (2013) ‘Fine structure of the male reproductive system and reproductive behavior of *Lutzomyia longipalpis* sandflies (Diptera: Psychodidae: Phlebotominae)’, *PLoS ONE*, 8(9), p. e74898.

UWWTD (2013) *Phosphorous Standard for Wastewater Treatment Works*.

Wang, X. and Müller, W.E.G. (2009) ‘Marine biominerals: perspectives and challenges for polymetallic nodules and crusts’, *Trends in Biotechnology*, 27(6), pp. 375–383.

Weiner, S. and Dove, P.M. (2003) ‘An overview of biomineralization processes and the problem of the vital effect’, *Reviews in mineralogy and geochemistry*, 54(1), pp. 1–29.

Westall, F. (1999) ‘The nature of fossil bacteria: A guide to the search for extraterrestrial life’, *Journal of Geophysical Research*, 104451(25), pp. 437–16.

Ye, Z. et al. (2014) ‘Phosphorus recovery from wastewater by struvite crystallization: Property of aggregates’, *Journal of Environmental Sciences*, 26(5), pp. 991–1000.

Yee, N. et al. (2003) ‘The effect of cyanobacteria on silica precipitation at neutral pH: Implications for bacterial silicification in geothermal hot springs’, *Chemical Geology*, 199(1–2), pp. 83–90.

5 Properties of bio-struvite and abiotic struvite and boundary conditions for crystallization

Authors: Y Leng, A Soares

Cranfield Water Science Institute, Vincent Building, Cranfield University, Bedfordshire, MK43 0AL, UK

Abstract

Halobacterium salinarum, *Bacillus pumilus*, *Brevibacterium antiquum*, *Myxococcus xanthus* and *Idiomarina loihiensis* were capable of growing in wastewater to remove phosphorus within ortho-phosphate ranging from 5.4 to 62.4 mg/L in wastewater. Biological struvite (bio-struvite) (identified by morphological, XRD and elemental analysis) production in wastewater was observed starting from 19.7 mg ortho-phosphate/L, compared with ≥62.4 mg ortho-phosphate/L and pH adjustment, required for abiotic struvite precipitation. The initial nutrient concentrations presented a high positive correlation with ortho-phosphate removal efficiency, bio-struvite production and crystal size distribution. *B. antiquum* distinguished itself from the other four microbial stains by relatively stable ortho-phosphate removal (67-97%) independent of the initial nutrients concentration. Furthermore *B. antiquum* removed ortho-phosphate from initial concentrations of 5.4 mg/L to ≤1 mg/L. The bio-struvite recovered presented high purity and contained low heavy metal contents, which enable the bio-struvite to meet proposed regulations for inorganic fertilizer. Phosphorus recovery as bio-struvite presented several key advantages: phosphorus recovery from concentrations ≥19.7 mg ortho-phosphate/L, no need to adjust pH, reduced initial supersaturation index for struvite nucleation and purity similar or better than abiotic struvite. Hence phosphorus recovery through bio-struvite presents interesting benefits and opportunities to be applied to wastewater treatment plants.

Keywords: biological struvite, phosphorus removal, heavy metal, purity

5.1 Introduction

Excess amounts of phosphorus (P) entering surface water can result in eutrophication and loss of biodiversity that threaten the aquatic environment. Legislation regarding P discharges (e.g. European Urban Wastewater Treatment Directive, Water Framework Directive) are becoming more stringent and improvement of wastewater treatment plants (WWTPs) to remove P is imperative in many countries (Hendriks and Langeveld, 2017). On the other hand, P is an essential element to living organisms, and fertilizers containing P are widely used in the agriculture industry. The price of commercial P fertilizer has kept on increasing due to the world-widely shortage reserve of phosphate rock, the main mineral resource for current inorganic P fertilizer production (Egle et al., 2016).

Struvite (magnesium ammonium phosphate hexahydrate-$MgNH_4PO_4.6H_2O$) has gained considerable attention in the wastewater industry due to its capability to remove and recover P from wastewater streams (Doyle and Parsons, 2002). Furthermore, owing to its high content of P and nitrogen (N), low degree of impurities and excellent slow-release property (Massey et al., 2009), struvite has been recognized as a good alternative to P-rich fertilizers. Struvite crystallizes when molar ratio of [PO_4-P]:[Mg^{2+}]:[NH_4-N] is around 1:1:1 and nutrient concentration exceeds the product solubility. It has been proposed that P recovery via struvite is only economically viable at P concentrations >50 mg/L, when promoted by pH adjustment and seeding (Cornel and Schaum, 2009; Le Corre et al., 2009). Efficient P removal of up to 96% by struvite precipitation have been achieved at pH 9.5, with molar ratio [PO_4-P]:[Mg^{2+}]:[NH_4-N] of 1.3:4:1 and by applying seeding to promote nucleation (Shih et al., 2017). Other reports indicate that struvite precipitation occurs at molar ratios 1:1.3 in relation to [PO_4-P]:[Mg^{2+}] and molar ratio of at least 1:1 for [PO_4-P]:[NH_4-N] (Cieślik and Konieczka, 2017). Yet the potential P recovery from WWTPs via struvite was quantified at a maximum of 30%, in relation to the P available in the raw wastewater (Egle, Rechberger and Zessner, 2015). A minimum of 100 mg PO_4-P/L was reported to be required for readily spontaneous precipitation struvite crystallization (Rittmann et al., 2011), which

is 10 times higher than typical values of raw municipal wastewater (Henze and Comeau, 2008).

Soares et al. (2014) reported P recovery by struvite biomineralization (i.e. bio-struvite) in municipal wastewater, where *Brevibacterium antiquum* and *Bacillus pumilus* not only removed PO_4-P to final 1.5-2.1 mg/L but also recovered P as bio-struvite (28.6 mg P in bio-struvite/L wastewater by *B. antiquum*). In sludge dewatering liquors, Simoes et al. (2017) reported the bio-struvite production up to 21.5 mg P as bio-struvite/L of liquors, by pure cultures of *B. antiquum*. However, the benefits of bio-struvite application to WWTP in comparison with abiotic struvite, and the quality (e.g. purity, heavy metal contents) of bio-struvite recovered from wastewater are still poor documented.

This study aims to understand benefits of bio-struvite application on WWTPs by investigating the limiting nutrient concentrations required for P removal and recovery by bio-struvite and abiotic struvite in municipal wastewater. The purity and heavy metal content of the recovered bio-struvite and abiotic struvite was also investigated.

5.2 Materials and Methods

5.2.1 Microorganisms

The five microbial strains investigated in this study were purchased from commercial culture collections: *Halobacterium salinarum* (DSM 671, German Resource Centre for Biological Material, Germany), *Bacillus pumilus* (GB43, LGC Standards, Middlesex, UK), *Brevibacterium antiquum* (DSM 21545, German Resource Centre for Biological Material, Germany), *Myxococcus xanthus* (CECT 422, Spanish Type Culture Collection, University of Valencia, Paterna, Spain) and *Idiomarina loihiensis* (MAH1/CECT 5996, Spanish Type Culture Collection, University of Valencia, Paterna, Spain).

5.2.2 Municipal wastewater

Municipal wastewater was collected from outlet of primary lamella clarifiers of a municipal WWTP with 2840 population equivalent (PE) (Cranfield, UK). The

wastewater was filtered by a 10 μm nylon-mesh filter (Plastok, UK), followed by microfiber (equivalent to 0.7 μm), and finally filtered sterilised (0.22 μm PVDF membrane, EMD Millipore, UK). The microbial capability to remove PO_4-P and produce struvite was examined at different concentrations of PO_4-P (5.4-62.4 mg/L, 4-levels) and NH_4-N (35-332 mg/L, 3-levels) in the sterile wastewater (Table 1). Filter sterilised (0.22 μm) concentrated solutions of magnesium sulphate heptahydrate ($MgSO_4 \cdot 7H_2O$), di-potassium hydrogen phosphate (K_2HPO_4), ammonium sulphate ($(NH_4)_2SO_4$) were supplemented together with bovine serum albumin (BSA) for organic carbon source (Leng and Soares, 2018a) for microbial growth (tests ①-⑫) (Table 5-1).

Table 5-1 Characteristics of the raw wastewater collected from a municipal WWTP and the wastewater with different concentrations of NH_4-N and PO_4-P (average ± standard deviation of duplicates) used to investigated struvite precipitation

		Molar ratio [P]:[Mg]:[N]	PO_4-P (mg/L)	NH_4-N (mg/L)	pH	Mg^{2+} (mg/L)	Ca^{2+} (mg/L)	K^+ (mg/L)	SCOD (mg/L)
Raw wastewater		1:2:14	5.4±0.3	35.0±0.6	7.76±0.05	8.2±0.5	39.0±0.6	21.0±0.2	150 ±5
Wastewater with different concentrations of PO_4-P and NH_4-N tested	①	1:13:14	5.4	35	7.86-8.00	56	39	93	750*
	②	1:4:4	19.7						
	③	1:2:2	33.9						
	④	1:1:1	62.4						
	⑤	1:13:74	5.4	180	7.83-7.89				
	⑥	1:4:20	19.7						
	⑦	1:2:12	33.9						
	⑧	1:1:6	62.4						
	⑨	1:13:136	5.4	332	7.76-7.80				
	⑩	1:4:37	19.7						
	⑪	1:2:22	33.9						
	⑫	1:1:12	62.4						

* containing 0.5 g/L BSA, equivalent to 600 mg/L SCOD

5.2.3 Microbial cultivation

Starter cultures were grown in 250 ml E-flasks containing 100 mL yeast extract solution of 4 g/L (additional 1% w/v NaCl and 1 g/L Mg^{2+} to grow *I. loihiensis*), incubated on an orbital shaker (Stuart model SSL1, Fisher Scientific, UK) at 150

RPM at room temperature (21-24°C) for 96 h. For inoculation in wastewater, the starter cultures were centrifuged (Sanyo MSE Falcon 6/300 centrifuge, 2400 RCF, 4 °C, 10 min) and washed with sterile 0.9% w/v NaCl solution. The pure microorganism pellets were re-suspended in sterile wastewater and inoculated in 40 mL wastewater in 100 mL glass bottles (Pyrex, Fisher Scientific, UK), Additional 0.8% w/v NaCl was added to *I. loihiensis* culture to ensure its growth (González-Muñoz et al., 2008). The bottles were capped with foam stoppers and incubated on the orbital shaker at 150 RPM at room temperature for 196 h. The samples were taken at the start and at the end of incubation time. All tests were completed in duplicate and controls were maintained under identical conditions but without inoculation.

5.2.4 Analytical methods

The intact cell counts in microbial culture were estimated with a flow cytometer (BD Accuri C6, BD Biosciences, US) analyses using SYBR Green I (SG) - propodium iodide (PI) co-staining method (Nocker et al., 2017). The flow cytometer was also used to distinguish inorganic nanoparticles from cells by SG staining. Assuming there is no free deoxyribonucleic or ribonucleic acid in microbial cultures, the inorganic nanoparticles counts were estimated by using total nanoparticle counts minus total cell counts. Several chemical parameters were monitored. The concentrations of PO_4-P and NH_4-N were analysed using a Smartchem (Smartchem200, AMS/Alliance Instruments, France) according to the manufacturer's instruction (Labmedics, Abingdon, UK). Magnesium and Ca^{2+} were analysed by atomic absorption spectroscopy (AAS, Analyst 800, PerkinElmer, UK) equipped with flaming and electrothermal spectrometers; aluminium (Al), potassium (K) and heavy metals including chromium (Cr), iron (Fe), nickel (Ni), copper (Cu), arsenic (As), cadmium (Cd), lead (Pb) and mercury (Hg) were analysed by inductively coupled plasma mass spectrometry system (ICP-MS, NexION 350, PerkinElmer, UK). The pH was determined by digital pH-meter (Jenway 3540, Bibby Scientific, UK). Soluble chemical oxygen demand (SCOD) was analysed by Spectroquant® cell test kit (Merck, VWR, UK). To avoid loss of microbial cells and fine particles (<10 µm) in filtration, that may affect the analysis of particle size distribution, a qualitative assessment

(QA) of the crystal production was applied ahead of the crystal size analysis. The qualitative assessment of crystal production for each test (Table 5-1) (40 mL wastewater) was completed by transferring the wastewater and crystals to a 500 mL glass beaker, stirring the wastewater clockwise to allow crystals settled at the bottom centre of the beaker and pictures were taken. This was followed by volume-based particle size distribution (D_v) analysis using a Mastersizer (Malvern 3000, Malvern Instruments Ltd, UK) with a Hydro EV dispersion unit (stirring speed of 1200 RPM).

A computer application, Visual MINTEQ ver. 3.1 (Gustafsson, 2000), was used to quantify the supersaturation index of struvite ($SI_{struvite}$). This application is based on the thermodynamic equilibrium consists of Mg^{2+}, calcium (Ca^{2+}), PO_4-P, NH_4-N, hydrogen (H^+) and hydroxide (OH^-) with a solubility product constant (K_{sp}) of $10^{-13.26}$ (Le Corre et al., 2009).

5.2.5 Abiotic and biological struvite preparation, isolation, purification and identification

Abiotic struvite was prepared in sterile wastewater: 100mL solution containing 0.2 M $NH_4H_2PO_4$ and 0.001 M K_2HPO_4 was added to 200 mL solution of 0.05 M $MgSO_47H_2O$; both solutions were pre-adjusted to pH 9 by 1 M sodium hydroxide (NaOH) and mixed in a glass bottle (1L, Duran™, Fisher Scientific, UK) (Le Corre et al., 2005). The mixture was agitated at 150 RPM at room temperature for 24 h for abiotic struvite precipitation.

To prepare enough bio-struvite for identification, additional 4 L sterile wastewater was applied for each microbial strain under the identical condition (the same as described in section 5.2.3) for 196 h incubation.

At the end of incubation period, biological and chemical precipitants were separated from the liquid by filtration (10 µm nylon-mesh filter, Plastok, UK) and washed with deionized (DI) water twice, passed for air-dry at 37°C for 4h and finally weighed to determine the production yield.

The morphology properties of the purified dry precipitants were characterised by scanning electron microscope equipped with energy dispersive X-ray

spectroscopyand (SEM-EDS, XL 30 SFEG, Phillips, The Netherlands), and X-ray powder diffractometer (XRD, D5000, Siemens/Bruker, Germany). Diffraction data were collected with a step size of 0.04 over the range 20° < 2θ < 90°, and was analysed by DIFFRAC.SUITE™ EVA software package (Bruker AXS GmbH, Germany) to compare with the standard struvite curve (pattern COD 9007674) . The chemical characterisation of the precipitants including PO_4-P, NH_4-N, Mg^{2+}, Ca^{2+}, K^+ , Al^{3+} and heavy metals (Cr, Fe, Ni, Cu, As, Cd, Pb and Hg) was investigated by SEM equipped with energy dispersive X-ray spectroscopy or crystal dissolution of 1.25 g/L (prepared in extra pure water pre-adjusted to pH 2 by 1 M hydrogen chloride).

5.2.6 Statistical analysis

The statistically significant difference in terms of P removal efficiency, crystal production and crystal size distribution (by Dv_{50} - the particle median diameter for a volume distribution) was investigated by two-tailed T-test (significance level $\alpha = 0.05$) in relation to the different microbial strains, concentrations of initial NH_4-N and PO_4-P. Statistical tests were considered significant at $p < 0.05$ (Schünemann et al., 2008). The 95% confidence intervals (CIs) were also examined to estimate the range of mean values of P removal efficiency, crystal production and Dv_{50}. The statistical correlation was applied to distinguish the significant relationship between eight variables, including initial parameters (pH, NH_4-N and PO_4-P, molar ratio of initial [PO_4-P] to [NH_4-N], solution $SI_{struvite}$) and PO_4-P removal efficiency, crystal production and Dv_{50}, where the critical significance levels (R) was applied: $0.6 \leq R < 0.8$ was considered strong correlation and $R \geq 0.8$ was considered very strong correlation (Tenenbaum, 2005). All the statistical analysis was performed using Microsoft Excel 2010 (Microsoft, Redmond, Washington, USA).

5.3 Results and Discussion

5.3.1 Microbial growth and crystal identification

The microbial intact cell count increased by 1-2 fold at the end of 196h incubation period, in each of the twelve tests with different concentrations of

PO_4-P and NH_4-N (Figure 5-1). As the initial NH_4-N increasing from 35 to 332 mg/L, the final intact cell count of *B. antiquum* and *B. pumilus* increased by 9 and 28%, respectively (Figure 5-1). Such positive effect of NH_4-N (510 - 839 mg/L) on *B. antiquum* growth was reported in sludge dewatering liquors where acetate and oleic acid were used as major carbon source (Simoes et al., 2017). The microbial growth was correlated with SCOD reduction, which varied with the microbial species: 54- 57% for *B. antiquum*, 46-50% for *B. pumilus*, 37-43% for *M. xanthus*, 27-31% for *H. salinarum* and 26-28% for *I. loihiensis*. Neither intact microbial cell nor SCOD removal was observed in non-inoculated control.

By the end of incubation period, all the microorganisms produced struvite in municipal wastewater (Figure 5-2 a-e), as identified by XRD, SEM-EDX and element analysis of crystal solution. No abiotic struvite was observed in non-inoculated control. The XRD results demonstrated that the crystals biologically recovered from wastewater had similar peak profiles to the standard struvite (pattern COD 9007674), and thus they were of the same orthorhombic crystal structure as struvite. Furthermore, the SEM-EDX and crystal solution showed the stoichiometric ratio [Mg]:[P]:[N]:[O] of the crystals was 1:1:1:4, corresponding to the chemical formula of struvite in dehydrated phase ($MgNH_4PO_4$). The loss of oxygen (by molecular water) within crystalline framework and loss of N (by ammonia) of crystal surface was observed in both bio-struvite and abiotic struvite (Figure 5-2 f) in this study. This was likely due to the thermal decomposition even at low temperature (Frost, Weier and Erickson, 2004).

Both struvite crystals were observed to have a porous surface (Figure 5-2 g-h), which was similar as the previously reported surface structures of abiotic struvite (Kofina and Koutsoukos, 2005) and bio-struvite (Prywer, Torzewska and Płociński, 2012). The porous surface originated from oriented aggregation and embedding of crystalline subunits into the crystalline framework, and in case of bio-struvite, was associated with bacterial adhesion and biofilm development (Prywer, Torzewska and Płociński, 2012). The comparison of the particles matrix on the crystal surface in this study showed slight difference in terms of the porosity and building units: wide gap between small units (high porosity)

was observed on the bio-struvite crystal surface. The particle size of the small building units for bio-struvite was relatively larger (1.5-2 µm x 1-1.5 µm) (Figure 5-2 g-g') than the abiotic struvite (0.8 µm x 0.4 µm) (Figure 5-2 h).

High quantity of Ca^{2+} of 1.67 - 8.24 weight percent (wt%) was detected by SEM-EDX on the abiotic struvite surface, whereas the Ca^{2+} on bio-struvite crystal surface was found less than 0.5 wt%. The Ca^{2+} was reported to affect the morphology and purity of abiotic struvite by competitively combining with PO_4-P at pH ≥9 to aggregate on the struvite surface (Le Corre et al., 2005). Barrere et al. (2004) reported the deposition calcium phosphate (Ca-P) nanoparticles on titanium implants to form a mineral coat which was with a similar structure as the mineral layer observed in this study (Figure 5-2 h). Thus the thin mineral layer on the abiotic struvite is proposed as Ca-P coating, which was not observed on the bio-struvite surface.

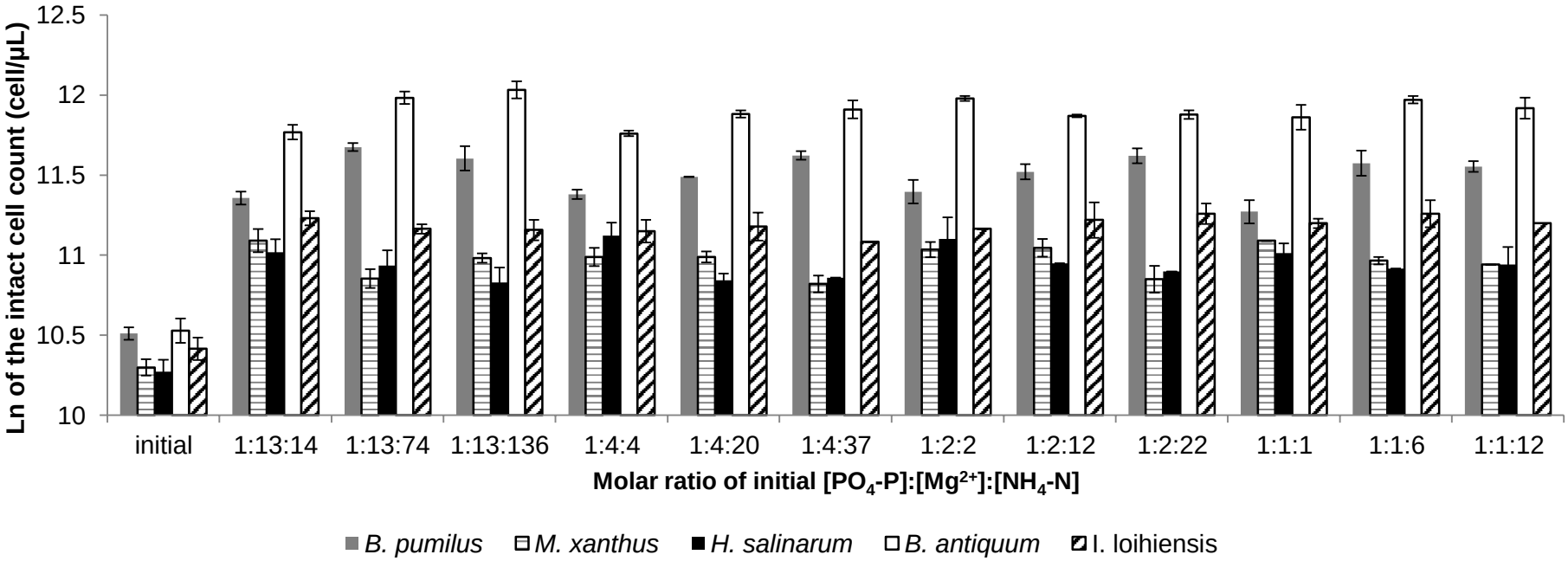

Figure 5-1 Natural logarithm of intact cell counts of the *H. salinarum*, *B. antiquum*, *B. pumilus*, *M. xanthus* and *I. loihiensis* in municipal wastewater at initial and by the end of 196h incubation at different molar ratio of initial nutrient concentrations within PO_4-P range of 5.4 to 62.4 mg/L in wastewater. Error bars represent standard deviation obtained from duplicates.

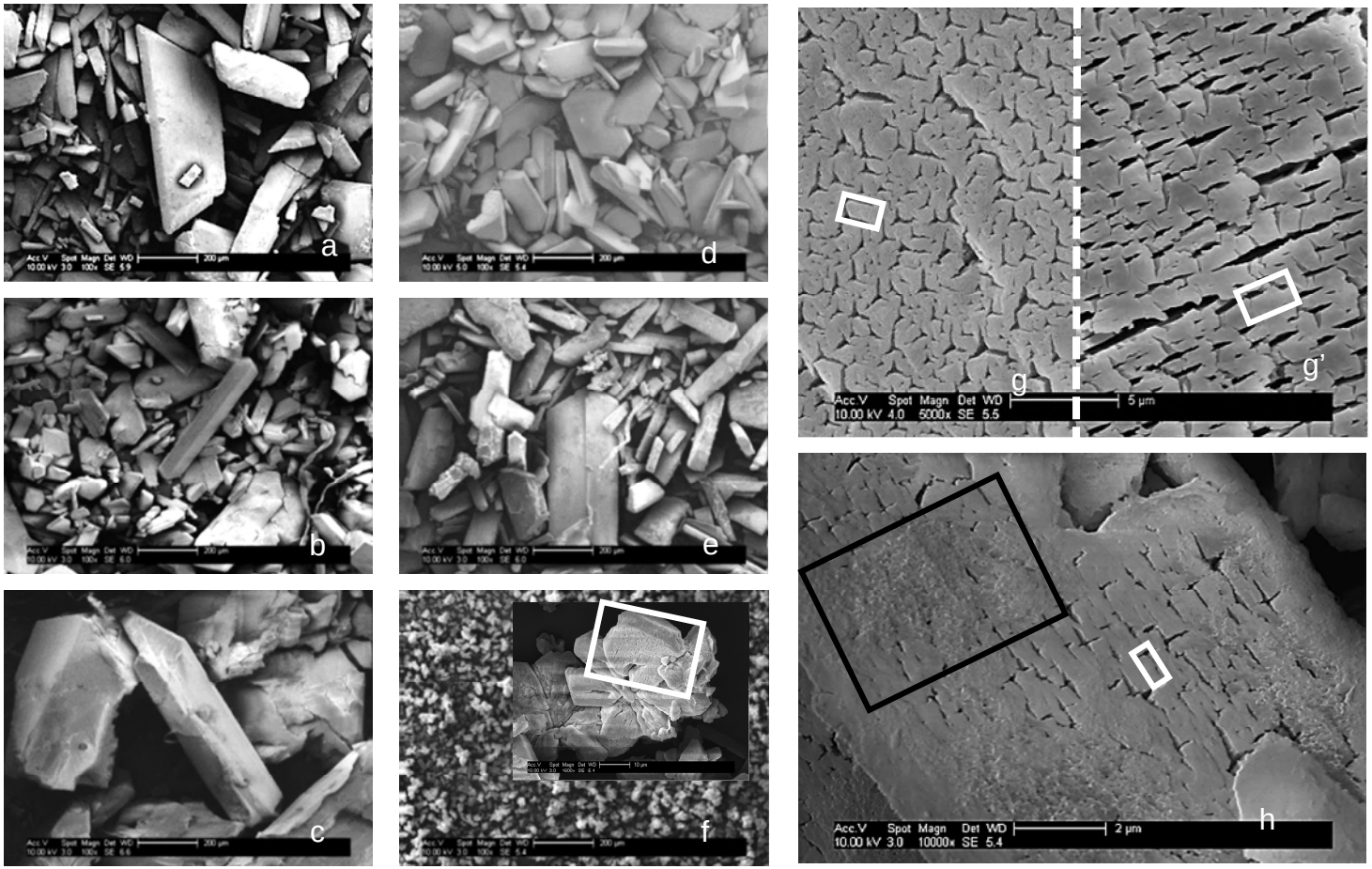

Figure 5-2 SEM photo of the isolated bio-struvite crystals recovered from (a) *H. salinarums*, (b) *B. pumilus*, (c) *M. xanthus*, (d) *B. antiquum*, (e) *I. loihiensis* cultures in wastewater (196h); (f) overview of abiotic struvite (scale bar - 200 µm) and single crystal (white square, scale bar - 10 µm). Crystal surface of bio-struvite produced by *B. antiquum* (g), *M. xanthus* (g') (scale bar - 5 µm) and abiotic struvite (scale bar - 2 µm) (h), white squares indicate the single building unit of struvite aggregated to the crystal surface and black square indicate the nano-calcium phosphate layer.

5.3.2 Phosphate removal, crystal production and size distribution

The capability of microorganisms to remove PO_4-P from wastewater varied with the microbial strains: 67- 97% for *B. antiquum*, 51-89% for *B. pumilus*, 18-89% for *M. xanthus*, 11-89% for *H. salinarum* and 16-82% for *I. loihiensis* (Figure 5-3 a). The initial concentrations of PO_4-P and NH_4-N correlated with the PO_4-P removal efficiency (Figure 5-3 a). Within initial PO_4-P range of 19.7 to 62.4 mg/L, the P removal efficiency was increased by 18% (*B. antiquum*), 22% (*H. salinarum*), 24% (*M. xanthus*), 29% (*B. pumilus*) and 67% (*I. loihiensis*) as the NH_4-N concentration increased (Figure 5-3 a). Within NH_4-N range of 180 to 332 mg/L, as the PO_4-P increased from 5.4 to 62.4 mg/L, the P removal efficiency by *B. pumilus, I. loihiensis, M. xanthus* and *H. salinarum* increased by 24%, 37%, 59% and 69% respectively (Figure 5-3 a). For *B. antiquum*, the highest PO_4-P removal efficiency (87-97%) occurred at 5.4 mg PO_4-P/L, and achieved final ≤1 mg PO_4-P/L (Figure 5-3 a), which met the EU standard for P discharge either below 2 mg/L (WWTPs of 10000-100000 PE) or 1 mg/L (WWTPs >100000 PE) (UWWTD, 2013).

The microbial strains were observed to produce bio-struvite crystal in wastewater containing initial PO_4-P of 19.7 to 62.4 mg/L (Figure 5-3 c). In particularly, at initial PO_4-P of 19.7 mg/L and NH_4-N of 35 mg/L, only *B. antiquum* and *B. pumilus* produced bio-struvite, corresponding to initial $SI_{struvite}$ of -0.43 (Figure 5-3 c). For all inoculated wastewater, the final concentration Mg^{2+} was observed above 15 mg/L, thus the Mg^{2+} did not limit bio-struvite crystal production. A considerable amount of Ca^{2+} (19-21 mg/L) was removed from wastewater with initial [PO_4-P]:[NH_4-N]:[Mg^{2+}]:[Ca^{2+}] of 2:2:2:1, and final pH of 8.4 to 8.5. This was corresponding to the occurrence of an abundant of inorganic particles in microbial cultures (inorganic particles/total particles of 13-76%) and observation of amorphous nanoparticles. Thus it was suggested that Ca^{2+} had potential to combine with PO_4-P to form Ca-P nanoparticles in wastewater. The presence of Ca^{2+} was reported to have negative impact on struvite purity within pH range of 7 to 10.5, where the struvite content decreased from around 70 to 30% as pH increased from 8.0 to 9.0 (Hao et al., 2013).

It was noted that at initial PO_4-P of 5.4 mg/L, even without visible bio-struvite crystal production (Figure 5-3 c), PO_4-P was removed by 4.7-5.2 mg/L from the *B. antiquum* culture, and by 0.6-3.5 mg/L from the other microbial cultures (Figure 5-3 a). Assuming that PO_4-P was the only P resource in wastewater, and accounted for 3% of microbial cell by dry weight (DW) (e.g. synthesis of membrane structure, adenosine triphosphate) (Stolp, 1988). The single cell DW were assumed 1.6-2.8 × 10^{-10} mg (Logan, 2005, 2008). The PO_4-P mass balance was determined by Equation 5-1:

$$P_{\text{removed from wastewater}} = P_{\text{cell construction}} + P_{\text{uptake}} \quad \textbf{(Equation 5-1)}$$

Thus the PO_4-P uptake by each single microbial cell was equivalent to 31-45 % PO_4-P DW of *B. antiquum,* 34-49 % PO_4-P DW of *B. pumilus*, 35-54 % PO_4-P DW of *I. loihiensis*, 14-73 % PO_4-P DW of *H. salinarums* and 36-59 % PO_4-P DW of *M. xanthus,* respectively. The capability of these microorganisms to accumulate PO_4-P from wastewater in this study, was comparable to the luxury P uptake by polyphosphate-bacteria with typical 7-10% P DW (occasionally 20-30% P DW) in enhanced biological phosphorus removal (EBPR) (Gerardi, 2011; Malamis, Katsou and Fatone, 2015; Urdalen, 2013). However, the polyphosphate (poly-P) accumulating organisms (PAOs) incorporate and release considerable amount of P as intracellular poly-P in biomass (Malamis, Katsou and Fatone, 2015). In this study, the mechanisms involved in P removal were related to the biomineralization, considering the observed simultaneous removal of PO_4-P (0.6-5.2 mg/L), Ca^{2+} (0.6-3.9 mg/L) and Mg^{2+} (1.3-4.0 mg/L).

The Dv_{50} correlated positively with the initial nutrient concentration, as shown in Figure 5-3 b. Initial PO_4-P ≥19.7 mg/L and NH_4-N ≥180 mg/L were essential to obtain large bio-struvite crystal groups (Dv_{50} ≥100 μm) (Figure 5-3 b).

After 196h incubation, neither PO_4-P removal nor crystal production was observed in non-inoculated control. The pH of controls was then raised to around 8.5 by 1 M NaOH. After 72h incubation, tiny crystals (Figure 5-3 c) with orthorhombic crystal structure as struvite were observed in wastewater containing PO_4-P of 62.4 mg/L and NH_4-N of 332 mg/L, with PO_4-P removal of 38 mg/L (61%), abiotic struvite production of 2.5 QA and Dv_{50} of 78 μm (Figure

5-3 a-c). The estimated initial $SI_{struvite}$ for abiotic struvite precipitation in this study was 1.52, higher than that for bio-struvite production of (-0.43) to 0.84 in this study (Figure 5-3 c), and the previously reported initial $SI_{struvite}$ <0.6 in synthetic solution (Leng, Simoes and Soares, 2018) and ≤0.5 in wastewater (Leng and Soares, 2018b).

When compared the bio-struvite biomineralization with abiotic struvite precipitation in this study, the former recovered struvite in larger crystal groups, at lower initial PO_4-P and without chemical dose for pH adjustment (Figure 5-3). These bio-struvite production was associated with the specific metabolic pathways and organic cellular substance/structures involved in bio-struvite biomineralization, whereby microorganisms reduced energy barrier for heterogeneous nucleation of bio-struvite and promoted its crystallization process (Arias, Cisternas and Rivas, 2017).

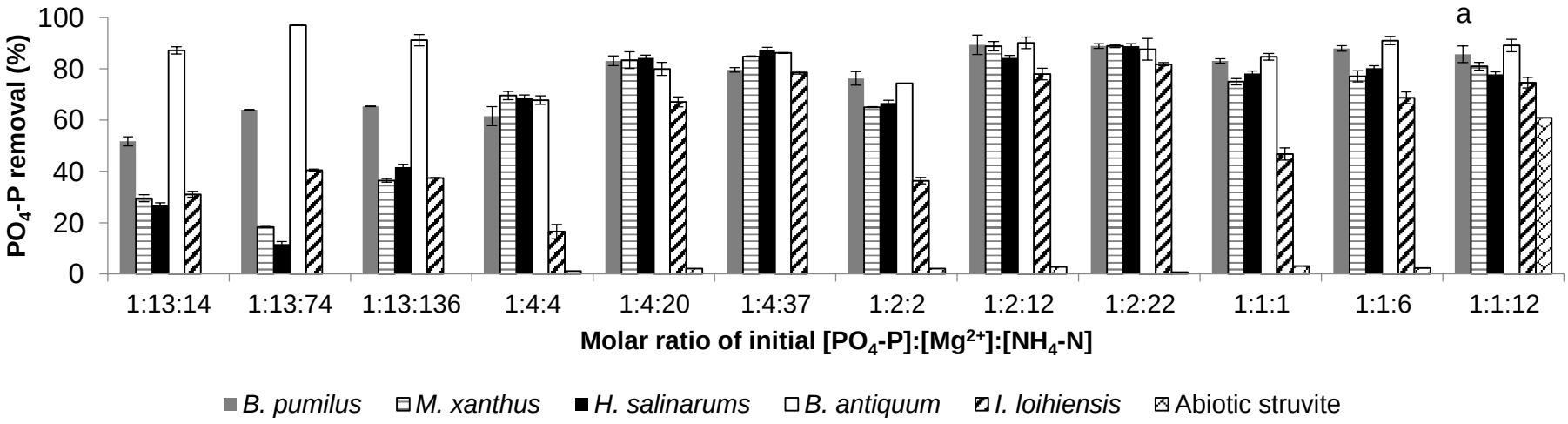
a
100
80
60
40
20
0
PO4-P removal (%)
1:13:14
1:13:74
1:13:136
1:4:4
1:4:20
1:4:37
1:2:2
1:2:12
1:2:22
1:1:1
1:1:6
1:1:12
Molar ratio of initial [PO4-P]:[Mg2+]:[NH4-N]
B. pumilus
M. xanthus
H. salinarums
B. antiquum
I. loihiensis
Abiotic struvite

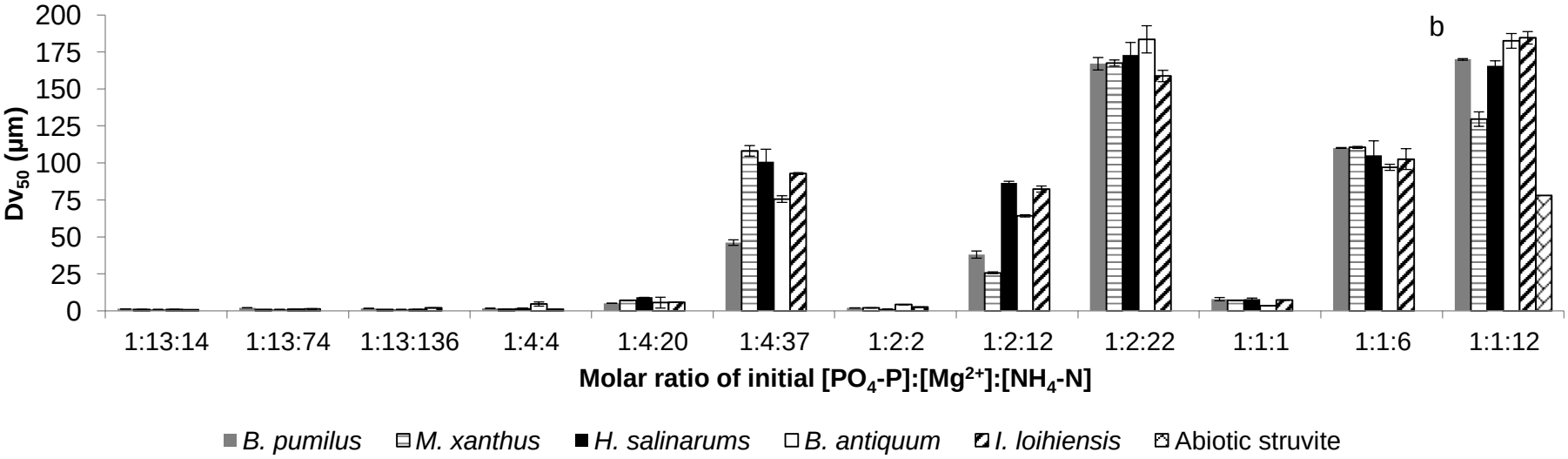
b
200
175
150
125
100
75
50
25
0
Dv50 (µm)
1:13:14
1:13:74
1:13:136
1:4:4
1:4:20
1:4:37
1:2:2
1:2:12
1:2:22
1:1:1
1:1:6
1:1:12
Molar ratio of initial [PO4-P]:[Mg2+]:[NH4-N]
B. pumilus
M. xanthus
H. salinarums
B. antiquum
I. loihiensis
Abiotic struvite

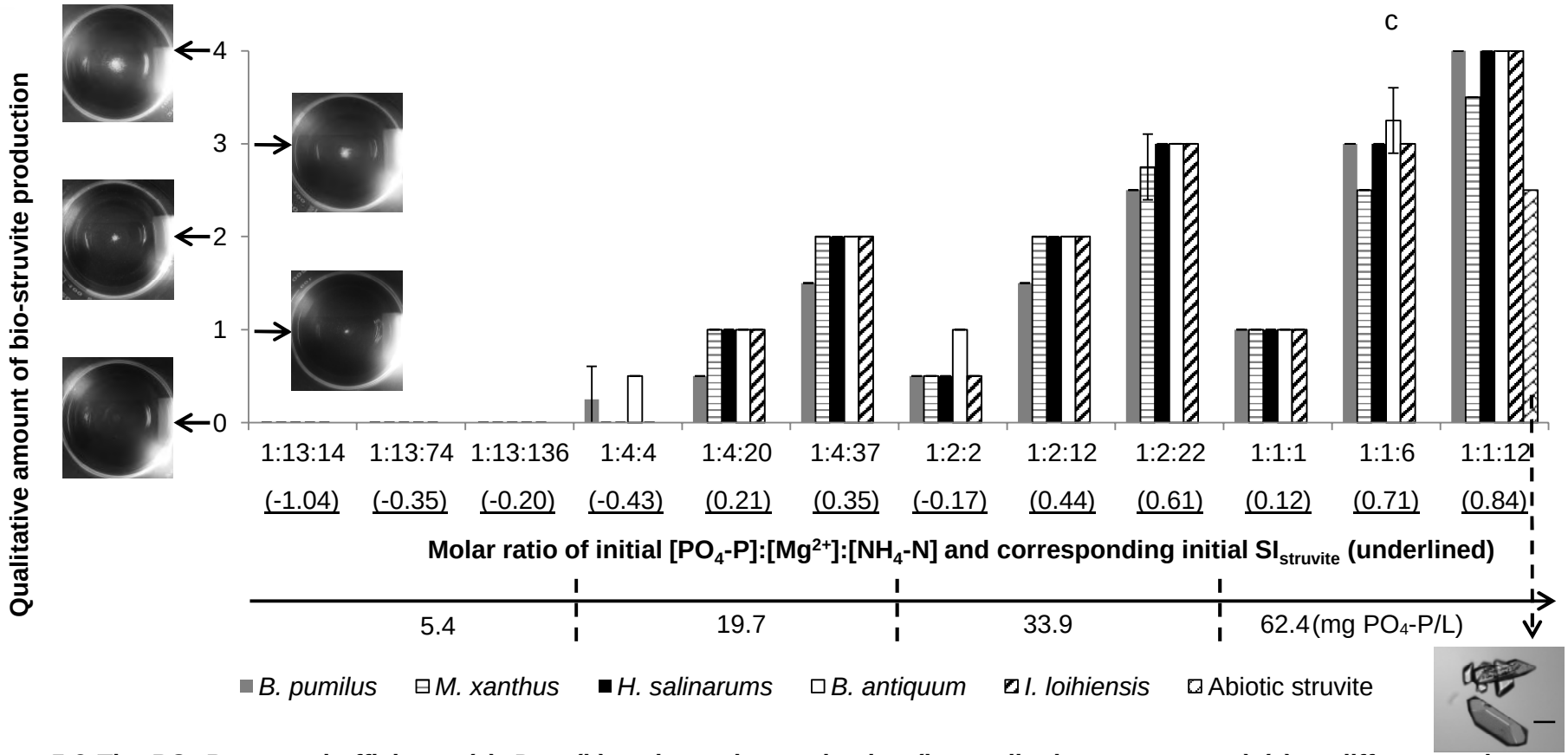

Figure 5-3 The PO_4-P removal efficiency (a), Dv_{50} (b) and struvite production (by qualitative assessment) (c) at different molar ratio of initial nutrient concentrations and the corresponding $SI_{struvite}$ values (underlined) within PO_4-P range of 5.4 to 62.4 mg/L in wastewater. The five microorganisms shared same initial $SI_{struvite}$ values (underlined) for each molar ratio of initial nutrient concentrations. Error bars represent standard deviation obtained from duplicates. Dv_{50} represented the particle median diameter for a volume distribution. Abiotic struvite formed at pH of 8.5 (photo with scale bar – 10.19 µm).

5.3.3 Statistical significance and correlation

B. antiquum was observed to distinguish itself from the other four microbial strains regarding P removal efficiency in wastewater (Table 5-2). There was no significant difference among the five tested microorganisms regarding Dv_{50} and crystal production, but a significant difference between the inoculated and the non-inoculated controls was observed (Table 5-2). With respect to different initial PO_4-P concentrations, there was significant difference regarding P removal efficiency when initial PO_4-P increased from 5.4 and 19.7 mg/L, and regarding Dv_{50} and crystal production when initial PO_4-P increased from 5.4 to 19.7 and to 33.9 mg/L (Table 5-2). Moreover, Dv_{50} varied significantly as the initial NH_4-N increased from 35 to 180 and to 332 mg/L, but the changes of initial NH_4-N concentrations did not significantly correlated with the P removal efficiency and bio-struvite production (Table 5-2). Therefore, within the investigated range, the initial NH_4-N concentration presented a positive correlation with Dv_{50}. On the other side, the significant initial PO_4-P concentration that impacted P removal efficiency was 19.7 mg/L, and an initial PO_4-P concentration of 33.9 mg/L impacted bio-struvite production and size distribution. Initial nutrient concentrations above the significant values did not significantly increase the P removal efficiency, bio-struvite production and crystal size distribution.

The 95% confidence intervals (CIs) of P removal efficiency (80-91%) by *B. antiquum* showed a relatively high PO_4-P removal within narrow range, when compared that of the other four microorganisms (68-84% of *B. pumilus,* 51-82% of *M. xanthus*, 50-83% of *H. salinarums* and 41-69% of *I. loihiensis*) (Table 5-2). This indicates a relative stable high P removal efficiency by *B. antiquum* within the investigated nutrient concentrations. The 95% CIs of Dv_{50} at initial 332 mg NH_4-N/L, 33.9 mg PO_4-P/L and 62.4 mg PO_4-P/L were of 72-141, 36-118 and 55-133 μm, respectively (Table 5-2). This indicated potential formation of large bio-struvite crystal groups (Dv_{50}>100 μm) for readily settlement in wastewater at initial NH_4-N of 332 mg/L combined with initial PO_4-P ≥33.9 mg/L. The highest

95% CIs of crystal production occurred at initial 62.4 mg PO_4-P/L, followed by initial 33.9 mg PO_4-P/L and 332 mg NH_4-N/L (Table 5-2).

Initial PO_4-P, NH_4-N and $SI_{struvite}$ were identified to have significant positive correlations with P removal efficiency, bio-struvite production and Dv_{50} (Table 5-3). Compared with the initial PO_4-P and NH_4-N, the $SI_{struvite}$ was observed to have significant correlations with Dv_{50} and bio-struvite production (Table 5-3). The P removal efficiency by *B. antiquum* was less dependence on these three initial parameters than the other four microorganisms, whereas the P removal efficiency by *B. pumilus* highly depended on the initial $SI_{struvite}$ (Table 5-3). Significant positive correlations were also observed among P removal efficiency, Dv_{50} and bio-struvite production, especially between Dv_{50} and bio-struvite production (Table 5-3). This indicated a potential of high P removal efficiency integrated with P recovery by bio-struvite of more production and larger size, as shown in a 3D scatter plot (Figure 5-4), where all the large 3D spheres (crystal production, QA≥3) were filled with colour representing high Dv_{50} (≥80 μm), and appeared with P removal efficiency more than 75%.

Table 5-2 Statistical significance (T-test) and 95% confidence intervals with respect to P removal, Dv_{50} and crystal production at different concentrations of initial NH_4-N and PO_4-P in the five selected microbial cultures

			p value			95% confidence intervals (CI)		
			P removal efficiency	Dv_{50}	Crystal production	P removal efficiency	Dv_{50} (μm)	Crystal production(QA)
Microbial strains	*B. pumilus*	*M. xanthus*	0.233	0.980	0.937	68-84%	4-88	0.4-2.1
		H. salinarum	0.244	0.761	0.795			
		B. antiquum	0.048	0.834	0.681			
		I. loihiensis	0.010	0.754	0.970			
		control	0.000	0.033	0.008			
	M. xanthus	*H. salinarum*	0.991	0.776	0.849	51-82%	7-87	0.5-2.1
		B. antiquum	0.024	0.850	0.729			
		I. loihiensis	0.234	0.768	0.969			
		control	0.000	0.026	0.005			
	H. salinarum	*B. antiquum*	0.028	0.930	0.884	50-83%	11-98	0.5-2.3
		I. loihiensis	0.250	0.986	0.828			
		control	0.000	0.018	0.006			
	B. antiquum	*I. loihiensis*	0.001	0.917	0.715	80-91%	7-96	0.6-2.3
		control	0.000	0.026	0.004			
	I. loihiensis	control	0.000	0.022	0.009	41-69%	10-100	0.4-2.1
Initial PO_4-P	5.4 mg/L	19.7 mg/L	0.007	0.014	0.000	34-63%	1	0
	19.7 mg/L	33.9 mg/L	0.336	0.046	0.024	63-83%	8-54	0.6-1.4
	33.9 mg/L	62.4 mg/L	0.952	0.532	0.073	71-87%	36-118	1.2-2.3
	62.4 mg/L					73-85%	55-133	1.8-3.3
Initial NH_4-N	35 mg/L	180 mg/L	0.068	0.001	0.068	50-70%	2-4	0.2-0.6
	180 mg/L	332 mg/L	0.606	0.003	0.085	62-84%	22-64	0.9-1.9
	332 mg/L					68-85%	72-141	1.5-2.8

Table 5-3 Significant correlations between the initial parameters and P removal, Dv_{50} and crystal production (R ≥0.6) in ● *B. pumilus*, ▲ *M. xanthus*, ♦ *H. salinarum*, ■ *B. antiquum*, ★ *I. loihiensis* cultures

	P removal efficiency		Dv_{50} (μm)		Crystal production (QA)	
	R ≥0.8	0.6 ≤R <0.8	R ≥0.8	0.6 ≤R <0.8	R ≥0.8	0.6 ≤R <0.8
Initial NH_4-N (mg/L)		▲ ♦ ★		● ▲ ♦ ■ ★		♦
Initial PO_4-P (mg/L)		●		■		● ▲ ■ ★
Initial $SI_{struvite}$	●	▲ ♦ ★	▲ ♦ ■ ★	●	● ▲ ♦ ■ ★	
Dv_{50} (μm)		● ★				
Crystal production (QA)	★	● ▲ ♦	● ▲ ♦ ■ ★			

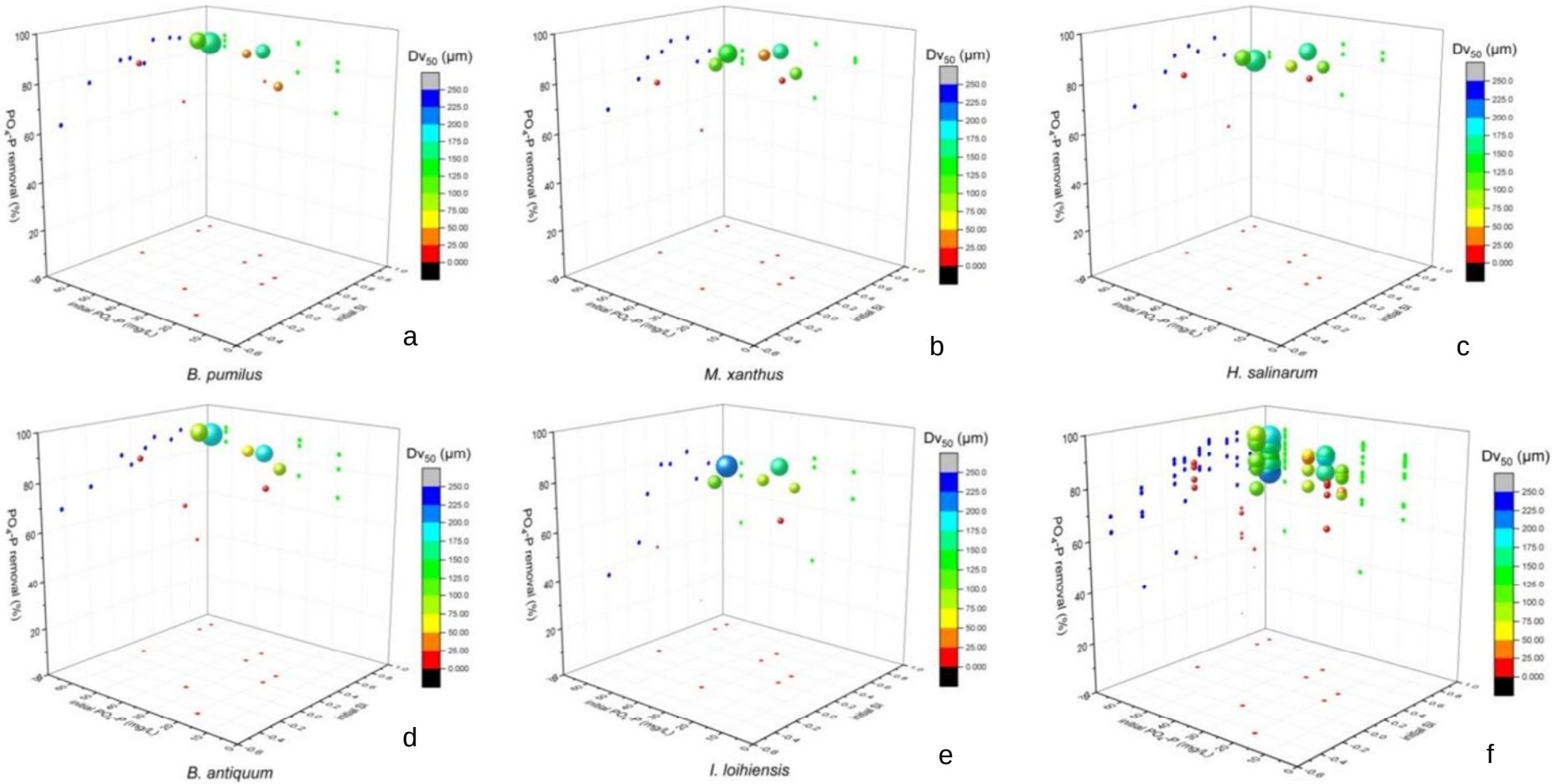

Figure 5-4 The 3D scatter plot with colorbar and data projections on all three axis planes showed the P removal, Dv_{50} (sphere color) and crystal production (sphere size, QA>0) at different initial PO_4-P concentration and $SI_{struvite}$ in (a) - *B. pumilus*, (b) - *M. xanthus*, (c) - *H. salinarum*, (d) - *B. antiquum,* and (e) - *I. loihiensis* cultures. (f) Data integration for the microorganisms tested.

5.3.4 Purity and heavy metal content

No significant difference was observed regarding the purity between bio-struvite recovered from wastewater with PO_4-P of 33.9 mg/L and abiotic struvite recovered from PO_4-P >2000 mg/L (Table 5-5). Both products were observed to have the same purity as theoretical struvite ($MgNH_4PO_4.6H_2O$). Bio-struvite contained nutrients equivalent to 11.8-12.3% P, 5.4-5.8% N and 15.5-16.2% MgO, and the abiotic struvite contained nutrients equivalent to 12.6% P, 5.7% N and 16.4% MgO (Table 5-5). The purity of both bio-struvite and abiotic struvite was within the proposed acceptable purity range of struvite for fertilizer usage, with requirement of nutrients' content equivalent to 10.0-13.9% P, 4.6-6.3% N and 13.1-18.1% MgO (ESPP, 2015). Both P and N content met the EU minimum requirement as inorganic fertiliser, thus the bio-struvite has potential use as P and N fertilizer alternative. Bio-struvite was also observed contain K (0.6-0.8 g/kg) and Ca (0.1-0.2 g/kg) that were recognized as essential macronutrients for organism growth (Table 5-5). Although the K content in bio-struvite was relatively higher than abiotic struvite (0.2 g/kg), it was still far below than the EU regulated level of K in inorganic fertiliser (FWG, 2014).

The raw wastewater contained various heavy/toxic metals (Table 5-4). However, the amount of heavy metal Cr, Ni, Cu, As, Cd, Pb and Hg in both bio-struvite and abiotic struvite met the EU maximum limitation (ESPP, 2015; FOMA, 2014; FWG, 2014). Compared with the abiotic struvite, the bio-struvite contained lower amounts of Ca, Al, Fe, Cr, Ni and Pb, but relatively higher amount of Cu, As, Cd and Hg (Table 5-5). In particular, bio-struvite produced by *M. xanthus* and *I. loihiensis* was observed contained higher Al (24.8-26.3 mg/kg), Fe (3.25-4.18 mg/kg), Cr (0.23-0.26 mg/kg), Ni (0.11-0.14 mg/kg) and Pb (0.36-0.38 mg/kg) than the other there microbial strains (Table 5-5). The highest Cd content (0.66 mg/kg) was found in the *B. pumilus* bio-struvite, compared with the other four bio-struvite (0-0.26 mg/kg), and the abiotic struvite (<1 µg/kg) (Table 5-5).

When comparing the bio-struvite produced from sewage sludge ash (SSA), which was also proposed as a P-fertilizer alternative recovered from WWTP, it was observed that the SSA contained higher toxic/heavy metal contents but lower P content (9.4% P) (Herzel et al., 2016). Thus the bio-struvite is of better quality regarding P and heavy metal content. Furthermore, the bio-struvite recovered from primary settled municipal wastewater in this study was found of similar purity as previously reported bio-struvite (11.9% P) which was recovered from sludge dewatering liquors, but lower of heavy metal contents, especially the Hg, As and Ni (Simoes, 2017). The impurity of bio-struvite may due to the influence of the heavy metal-concentrated environment. Braissant et al. (2007) reported the potential of EPS to bind heavy metal ions (e.g. Cd, Cu, Pd, Hg, Fe, Cr, Ni). Such microbial biomineralization may lead to precipitation of mineral containing inorganic pollutants under proper conditions (Benzerara et al., 2011). Moreover, microorganism may possess resistance or tolerance to specific heavy metal (e.g. Cd) by accumulating and concentrating them within cells (Voica et al., 2016). These microbial cells have potential to release the heavy metal to the mineral surface during the biomineralization, via molecular interaction between cell and the crystal surface (Prywer and Torzewska, 2009).

Table 5-4 Quantification of the heavy/toxic metal in raw municipal wastewater

Al	Fe	Cr	Ni	Cu	As	Cd	Pb	Hg
19.30± 0.42 ug/L	79.90± 0.28 ug/L	1.05± 0.04 ug/L	2.28± 0.02 ug/L	12.45± 0.07 ug/L	1.00± 0.01 ug/L	0.15± 0.00 ug/L	0.15± 0.00 ug/L	0.05± 0.00 ug/L

Table 5-5 Quantification of macronutrients and heavy/toxic metal in bio-struvite and abiotic struvite (average ± standard deviation of triplicates)

		B. antiquum	*B. pumilus*	*H. salinarum*	*M. xanthus*	*I. loihiensis*	Abiotic struvite	Theoretical struvite [a]	EU permissible levels
Macronutrient	PO_4-P (g/kg)	122.6±3.3 (12.3% P)	121.9± 3.9 (12.2 % P)	121.7±1.9 (12.2% P)	118.1±2.8 (11.9% P)	121.9±3.3 (12.2% P)	127.2±3.6 (12.7% P)	12.6% P	1% (total P_2O_5) [bd]
	NH_4-N (g/kg)	57.7±0.2 (5.8% N)	56.2±1.1 (5.6% N)	57.1±0.4 (5.7% N)	53.94±0.8 (5.4% N)	55.6±0.3 (5.6% N)	52.42±0.3 (5.2% N)	5.7% N	2% (total N) [bd]
	Mg (g/kg)	97.7±0.9 (16.2% MgO)	96.2±0.3 (16.0% MgO)	97.1±0.7 (16.2% MgO)	93.1±0.6 (15.5% MgO)	94.6±0.6 (15.8% MgO)	96.0±1.2 (16.0% MgO)	16.4% MgO	NYD
	K (g/kg)	0.8± 0.0	0.7±0.0	0.7±0.0	0.7 ±0.0	0.6± 0.0	0.2±0.0	0	1.5% (water-soluble K_2O) [bd]
	Ca (g/kg)	0.2± 0.0	0.2±0.0	0.2±0.0	0.2±0.1	0.1±0.0	0.8±0.0	0	NYD
Heavy/toxic metal	Al (mg/kg)	18.5±0.7	12.0±0.4	22.9±0.8	24.8±0.5	26.3±0.3	31.2±0.9	0	NYD
	Fe (mg/kg)	2.65±0.23	2.19±0.62	<LOD	3.25±0.45	4.18±0.07	8.69±0.38	0	NYD
	Cr (mg/kg)	0.17±0.02	0.23±0.03	0.15±0.01	0.26±0.02	0.23±0.01	0.38±0.00	0	2 mg/kg [cd]
	Ni (mg/kg)	0.11±0.00	0.08±0.04	0.07±0.01	0.11±0.03	0.14±0.01	1.19±0.10	0	120 mg/kg [cd]
	Cu (mg/kg)	0.33±0.19	0.53±0.18	0.18±0.02	1.57±0.26	1.24±0.03	0.42±0.03	0	200 mg/kg [ce]
	As(mg/kg)	0.38±0.01	0.30±0.02	0.32±0.01	0.27±0.04	0.39±0.04	0.07±0.02	0	60 mg/kg [cd]
	Cd (mg/kg)	0.06±0.05	0.66±0.01	<LOD	0.04±0.02	0.26±0.02	0.00±0.00	0	60 mg/kg (if P_2O_5>5%) [cd]
	Pb (mg/kg)	0.18±0.03	0.32±0.04	0.11±0.01	0.38±0.16	0.36±0.02	0.40±0.02	0	150 mg/kg [cd]
	Hg (mg/kg)	0.03±0.01	0.11±0.05	0.03±0.01	0.03±0.00	0.02±0.01	0.00±0.00	0	2 mg/kg [cd]

LOD - limit of detection; NYD – not yet defined

[a] - Theoretical struvite with chemical formula: $MgNH_4PO_4.6H_2O$; [b]- Minimum nutrient content in solid inorganic fertilisers; [c]- maximum heavy metal content in inorganic fertilisers; [d] - EU Fertilisers Working Group 2014 (FOMA, 2014; FWG, 2014) ; [e] - EU Fertiliser Regulation revision proposal 2014 (ESPP, 2015)

5.3.5 Implication for wastewater industry

Most of the previously reported struvite process has been applied to waste streams rich of PO_4-P and NH_4-N, such as side streams and liquors from anaerobic digestion (Rahman et al., 2014). Le Corre (2006) suggested several preferred wastewater sources for struvite precipitation at WWTP, mostly sludge dewatering liquors, and highly dependent on the performance of sludge digestion to generate enough nutrient constituents.

In this study, P removal and P recovery by bio-struvite were observed at relatively low PO_4-P of 5.4 and 19.7 mg/L, respectively. Thus compared with abiotic struvite precipitation, bio-struvite biomineralization could be applied to wastewater streams with a much lower and wider range of PO_4-P concentrations. The eligible wastewater sources at WWTP for bio-struvite biomineralization could range from raw municipal wastewater (4-15 mg PO_4-P/L and NH_4-N >35 mg/L) to settled wastewater (7.5 mg PO_4-P/L) and to return centrate (50-200 mg PO_4-P/L) (Henze and Comeau, 2008; Ivanov et al., 2005; Soares et al., 2014). However, aeration and nitrogenous organic compounds are also required to provide enough dissolved oxygen and carbon sources for microbial growth and specific metabolic pathways (Leng and Soares, 2018a). In particular, due to the capability of *B. antiquum* to reduce PO_4-P from 5.4 mg/L to <1 mg/L found in this study, this bacteria may have potential use to achieve high PO_4-P effluent quality. The application of microbial stains for P removal and recovery may vary with wastewater characteristics. In some WWTPs as the one described by Jaffer et al. (2002) for example, all the wastewater streams presented conditions suitable for microbial growth of the tested microbial strains (Leng and Soares, 2018a), *B. antiquum* and *B. pumilus* can be applied for PO_4-P removal from raw wastewater and settled wastewater (PO_4-P of 5.7 to 14.2 mg/L, NH_4-N of 16.1 to 23.9 mg/L, Mg^{2+} of 8 to 8.9 mg/L), and additional Mg^{2+} source might be required. In sludge dewatering liquors (PFT liquor, centrifuge liquor) containing 33.2 to 94.9 mg PO_4-P/L, 129-615 mg NH_4-N/L and 13-44 mg Mg^{2+}/L, all the five tested can be applied for P recovery by bio-

struvite. In particular, the centrifuge liquor was higher in pH, PO_4-P, NH_4-N and Mg^{2+}, and lower in Ca^{2+}, thus it is anticipated with better performance than PFT liquor regarding crystallization process and struvite purity (Rahman et al., 2014).

5.4 Conclusions

- The selected microorganisms were capable to produce bio-struvite in wastewater containing PO_4-P ≥19.7 mg/L.
- *B. antiquum* distinguish itself from the other four microbial strains by relatively stable P removal efficiency as the initial nutrient concentrations changing, and reduced PO_4-P from 5.4 to less than 1 mg/L.
- The initial NH_4-N, PO_4-P and $SI_{struvite}$ had positive relationship with P removal efficiency, crystal production and size distribution. The initial NH_4-N concentration had significantly positive effect on bio-struvite crystal size distribution. A significant initial PO_4-P concentration for P removal efficiency (63-83%) was 19.7 mg/L, and for bio-struvite production and Dv_{50} was 33.9 mg/L.
- Bio-struvite recovered from wastewater was of high purity and presented extremely low heavy metal content. It met the inorganic fertilisers regulation proposed by Fertilisers Working Group, which enable its potential use as a good alternative of P and N fertilizer.
- Compared with the abiotic struvite precipitation, PO_4-P recovery through bio-struvite presents interesting benefits and opportunities to be applied to wastewater treatment plants.

5.5 References

Arias, D. et al. (2017) ‘Biomineralization mediated by ureolytic bacteria applied to water treatment: a review’, *Crystals*, 7(11), p. 345.

Barrere, F. et al. (2004) ‘Nano-scale study of the nucleation and growth of calcium phosphate coating on titanium implants’, *Biomaterials*, 25(14), pp. 2901–2910.

Benzerara, K. et al. (2011) ‘Significance, mechanisms and environmental implications of microbial biomineralization’, *Comptes Rendus Geoscience*, 343(2–3), pp. 160–167.

Braissant, O. et al. (2007) ‘Exopolymeric substances of sulfate-reducing bacteria: Interactions with calcium at alkaline pH and implication for formation of carbonate minerals’, *Geobiology*, 5(4), pp. 401–411.

Cieślik, B. and Konieczka, P. (2017) ‘A review of phosphorus recovery methods at various steps of wastewater treatment and sewage sludge management. The concept of “no solid waste generation” and analytical methods’, *Journal of Cleaner Production*, 142, pp. 1728–1740.

Cornel, P. and Schaum, C. (2009) ‘Phosphorus recovery from wastewater: needs, technologies and costs’, *Water Science and Technology*, 59(6), pp. 1069–1076.

Le Corre, K.S. (2006) *Understanding Struvite Crystallization and Recovery*. Cranfield University.

Le Corre, K.S. et al. (2005) ‘Impact of calcium on struvite crystal size, shape and purity’, *Journal of Crystal Growth*, 283(3–4), pp. 514–522.

Le Corre, K.S. et al. (2009) ‘Phosphorus recovery from wastewater by struvite crystallization: a review’, *Critical Reviews in Environmental Science and Technology*, 39(6), pp. 433–477.

Doyle, J.D. and Parsons, S.A. (2002) ‘Struvite formation, control and recovery’, *Water Research*, 36(16), pp. 3925–3940.

Egle, L. et al. (2016) ‘Phosphorus recovery from municipal wastewater: an integrated comparative technological, environmental and economic assessment of P recovery technologies’, *Science of the Total Environment*, 571, pp. 522–542.

Egle, L. et al. (2015) ‘Overview and description of technologies for recovering phosphorus from municipal wastewater’, *Resources, Conservation and Recycling*, 105, pp. 325–346.

ESPP (2015) *Proposed E.U., fertiliser regulation criteria for recovered struvite*. Available at: https://phosphorusplatform.eu/images/download/ESPP struvite FR criteria proposal sent 24-4-15.pdf (Accessed: 1 February 2018).

FOMA (2014) *Comments heavy metals limits on fertilising materials*. Available at: http://ec.europa.eu/transparency/regexpert/index.cfm?do=groupDetail.groupDetailDoc&id=13108&no=5 (Accessed: 1 February 2018).

Frost, R.L. et al. (2004) ‘Thermal decomposition of struvite: Implications for the decomposition of kidney stones’, *Journal of Thermal Analysis and Calorimetry*, 76(3), pp. 1025–1033.

FWG (2014) *Essential safety and quality requirements for fertilising materials Fertilisers Working Group meeting General principles : safety*. Available at: http://ec.europa.eu/transparency/regexpert/index.cfm?do=groupDetail.groupDetailDoc&id=12426&no=7 (Accessed: 1 February 2018).

Gerardi, M.H. (2011) ‘Biological nutrient removal’, in *Troubleshooting the sequencing batch reactor*. John Wiley & Sons, pp. 143–150.

González-Muñoz, M.T. et al. (2008) ‘Ca-Mg kutnahorite and struvite production by *Idiomarina* strains at modern seawater salinities’, *Chemosphere*, 72(3), pp. 465–472.

Gustafsson, J.P. (2000) *Visual MINTEQ* 3.1. KTH, Sweden

Hao, X. et al. (2013) ‘Looking beyond struvite for P-recovery’, *Environmental Science and Technology*, 47(10), pp. 4965–4966.

Hendriks, A.T.W.M. and Langeveld, J.G. (2017) ‘Rethinking wastewater treatment plant effluent standards: nutrient reduction or nutrient control?’, *Environmental Science and Technology*, 51(9), pp. 4735–4737.

Henze, M. and Comeau, Y. (2008) ‘Wastewater characterization’, in *Biological wastewater treatment: principles modelling and design*. IWA publishing, pp. 33–52.

Herzel, H. et al. (2016) ‘Sewage sludge ash - A promising secondary phosphorus source for fertilizer production’, *Science of the Total Environment*, 542, pp. 1136–1143.

Ivanov, V. et al. (2005) ‘Phosphate removal from the returned liquor of municipal wastewater treatment plant using iron-reducing bacteria’, *Journal of Applied Microbiology*, 98(5), pp. 1152–1161.

Jaffer, Y. et al. (2002) ‘Potential phosphorus recovery by struvite formation’, *Water Research*, 36(7), pp. 1834–1842.

Kofina, A.N. and Koutsoukos, P.G. (2005) ‘Spontaneous precipitation of struvite from synthetic wastewater solutions’, *Crystal Growth and Design*, 5(2), pp. 489–496.

Leng, Y. et al. (2018) ‘Understanding the mechanisms of bio-struvite biomineralization (in preparation)’, *Bioresource Technology*

Leng, Y. and Soares, A. (2018a) ‘Biochemical characterisation of bio-mineralising struvite producing microorganisms (in preparation)’, *Chemosphere*

Leng, Y. and Soares, A. (2018b) ‘Understanding the mechanisms of bio-struvite formation in municipal wastewater (in preparation)’, *Bioresource Technology*

Logan, B.E. (2005) ‘Cellular growth and reproduction’, in *Structural and functional relationships in prokaryotes*. New York: Springer, pp. 292–347.

Logan, B.E. (2008) ‘Kinetics and mass transfer’, in *Microbial fuel cells*. John Wiley & Sons, Inc.

Malamis, S. et al. (2015) ‘Integration of energy efficient processes in carbon and nutrient removal from sewage’, in Stamatelatou, K. and Tsagarakis, K. P. (eds.) *Sewage Treatment Plants: Economic Evaluation of Innovative Technologies for*

Energy Efficiency. IWA Publishing, pp. 74–81.

Massey, M.S. et al. (2009) 'Effectiveness of recovered magnesium phosphates as fertilizers in neutral and slightly alkaline soils', *Agronomy Journal*, 101(2), pp. 323–329.

Nocker, A. et al. (2017) 'When are bacteria dead? A step towards interpreting flow cytometry profiles after chlorine disinfection and membrane integrity staining', *Environmental Technology*, 38(7), pp. 891–900.

Prywer, J. and Torzewska, A. (2009) 'Bacterially induced struvite growth from synthetic urine: experimental and theoretical characterization of crystal morphology', *Crystal Growth and Design*, 9(8), pp. 3538–3543.

Prywer, J. et al. (2012) 'Unique surface and internal structure of struvite crystals formed by *Proteus mirabilis*', *Urological research*, 40(6), pp. 699–707.

Rahman, M.M. et al. (2014) 'Production of slow release crystal fertilizer from wastewaters through struvite crystallization - A review', *Arabian Journal of Chemistry*, 7(1), pp. 139–155.

Rittmann, B.E. et al. (2011) 'Capturing the lost phosphorus', *Chemosphere*, 84(6), pp. 846–853.

Schünemann, H.J. et al. (2008) 'Interpreting results and drawing conclusions', in Higgins, J. P. and Green, S. (eds.) *Cochrane Handbook for Systematic Reviews of Interventions: Cochrane Book Series*. John Wiley & Sons, pp. 1–24.

Shih, Y.J. et al. (2017) 'Recovery of phosphorus from synthetic wastewaters by struvite crystallization in a fluidized-bed reactor: effects of pH, phosphate concentration and coexisting ions', *Chemosphere*, 173, pp. 466–473.

Simoes, F. (2017) *A new route to recover phosphorus from waste water: biological struvite production School*. Cranfield University.

Simoes, F. et al. (2017) 'Understanding the growth of the bio-struvite production *Brevibacterium antiquum* in sludge liquors', *Environmental Technology*, Taylor & Francis, pp. 1–10.

Soares, A. et al. (2014) 'Bio-Struvite: A new route to recover phosphorus from wastewater', *Clean - Soil, Air, Water*, 42(7), pp. 994–997.

Stolp, H. (1988) *Microbial ecology: organisms, habitats, activities*. Cambridge University Press.

Tenenbaum, D. (2005) *From univariate to multivariate analysis Univariate analysis*., *Spring, Unc-ch* Available at: https://www.unc.edu/courses/2005spring/geog/090/001/2005-GEOG090-correlation.pdf (Accessed: 1 February 2018).

Urdalen, I. (2013) *Phosphorus recovery from municipal wastewater*. Trondheim.

UWWTD (2013) *Phosphorous Standard for Wastewater Treatment Works*.

Voica, D.M. et al. (2016) ‘Heavy metal resistance in halophilic bacteria and archaea’, *FEMS Microbiology Letters*, 363(14), pp. 1–9.

6 Discussion

The aim of this PhD thesis was to describe the inorganic-organic interactions between bio-struvite crystals and each of the five selected microbial strains, to identify the mechanisms involved in biomineralization process and to reveal benefits and possible application of bio-struvite in wastewater industry.

6.1 Microbial capability to produced bio-struvite in synthetic solution and wastewater

Results of Chapter 2, 3 and 4 showed that all the tested microorganisms were capable to produce bio-struvite in synthetic solution (Figure 2-2, Figure 2-3, Figure 3-3, Figure 3-8) and in municipal wastewater (Figure 4-2, Figure 4-5), as identified by XRD and element analysis. The experimental XRD data were compared to referenced patterns (COD 9007674) to identify the same orthorhombic crystal structure of bio-struvite as standard struvite. The element composition of bio-struvite was obtained by surface elemental analyzing (P, O, N and Mg) using SEM-EDX and measurement of constituent ion concentrations (PO_4-P, NH_4-N, Mg^{2+}) after dissolving the crystals recovered. The bio-struvite recovered from synthetic solution and wastewater contained 12.2-12.8% P and 11.8-12.2% P, respectively, and both of them were of equal stoichiometric ratio [Mg]:[P]:[N], indicating a dehydrated phase of $MgNH_4PO_4$.

Results of Chapter 2 showed that *B. pumilus*, *M. xanthus H. salinarum B. antiquum* and *I. loihiensis* were capable to make use of nitrogenous compounds (e.g. urea, protein/amino acids) as a carbon source. The presence of protein/amino acids in synthetic solution and wastewater (Chapter 3 and 4) supported microbial growth. Dissolved oxygen was also observed as vital factor in bio-struvite biomineralization. Although microbial growth of *B. pumilus* (μ=0.35 1/h) and *M. xanthus* (μ=0.24 1/h) was observed under anaerobic condition, and *I. loihiensis* (μ =0.12 1/h) was observed to grow under anoxic condition, no bio-struvite occurred in oxygen limited cultures. Only under aerobic conditions, the growth of *B. pumilus* (μ =0.37 1/h), *M. xanthus* (μ =0.43 1/h) and *I. loihiensis* (μ =0.15 1/h) was associated with bio-struvite production,

at 1700, 1746 and 1521 mg bio-struvite/L media, respectively. Unlike these three microbial stains, *H. salinarum* and *B. antiquum* only grew under aerobic condition, with growth rates of 0.18 1/h and 0.14 1/h, respectively, and produced bio-struvite at 1692 and 1550 mg bio-struvite/L media, respectively. Different DO levels lead to different metabolic pathways and thus products (e.g. ammonia) (Smolke, 2009). Results of Chapter 2 suggested only specific metabolic pathway, under aerobic condition was linked to the microbial metabolism that lead to bio-struvite mineralization. This is the first time that oxygen was identified as a critical parameter on biomineralization and bio-struvite production.

The morphology of bio-struvite (Chapter 2, 3, 4 and 5) was typically coffin-lid, long bar and trapezoidal-platy shaped (Figure 3-8, Figure 4-5), with enhanced [011], [111] and [00$\bar{1}$] faces. Such morphology are among the most typical previously reported morphology of struvite (Tansel, Lunn and Monje, 2018). Moreover, the structure of the bio-struvite recovered from wastewater (Figure 4-5) was as similar to the struvite surface in published literature (Kemacheevakul et al., 2015). No crystals were observed in non-inoculated controls in all experiments, which further supported the hypothesis that microbial cells played key role in bio-struvite biomineralization.

6.2 Bio-struvite production through biological induced biomineralization process

Results described in Chapter 3 and 4 demonstrated that three microorganisms - *B. pumilus*, *M. xanthus* and *H. salinarum* - produced bio-struvite through a biological induced biomineralization (BIM) process in synthetic solution and wastewater. All of them made use of protein/amino acids as a carbon source, as described in Chapter 2. *B. pumilus* growth in synthetic solution (μ =0.28 1/h) and wastewater (μ =0.03 1/h) raised the matrix pH to 8.56 and 8.35, released NH_4-N (69 mg/L in synthetic solution and 47 mg/L in wastewater), and produced bio-struvite (Dv_{50} of 204 and 138 μm, gap between Dv_{90} and Dv_{50} of 284 and 264 μm, in synthetic solution and wastewater respectively). *M. xanthus* growth

in synthetic solution (μ =0.19 1/h) and wastewater (μ =0.03 1/h) raised the matrix pH to 8.45 and 8.28, released NH_4-N (71 mg/L in synthetic solution and 49 mg/L in wastewater), and produced bio-struvite (Dv_{50} of 170 and 163 μm, gap between Dv_{90} and Dv_{50} of 179 and 257 μm, in synthetic solution and wastewater respectively). *H. salinarum* growth in synthetic solution (μ =0.23 1/h) and wastewater (μ =0.04 1/h) raised the matrix pH to 8.33 and 8.30, released NH_4-N (71 mg/L in synthetic solution and 41 mg/L in wastewater), and produced bio-struvite (Dv_{50} of 215 and 178 μm, gap between Dv_{90} and Dv_{50} of 189 and 273 μm, in synthetic solution and wastewater respectively).

Thus the microorganisms contributed to bio-struvite formation in a positive way, generally through biodegrading nitrogenous organic compounds that released NH_4-N and created alkaline solutions. The NH_4-N combined with the PO_4-P and Mg^{2+} in the solution and created supersaturation with respect to struvite phase ($SI_{struvite}$). This process is very common in bio-struvite biomineralization and was reported in published studies (González-Muñoz et al., 2010; Sinha et al., 2014). However, the bio-struvite biomineralization process was highly dependent on the metabolic products, solution pH and the concentration of constituent ions present in the solution. The produced bio-struvite had high heterogeneity in crystal size, and no intracellular vesicles were visible, thus the mechanism involved was identified as BIM process.

In particular, results of Chapter 2, 3 and 4 showed crusted *B. pumilus* cell/cell cluster (Figure 2-2 g, Figure 3-2 h-i, Figure 4-6 c), which was similar as previously reported mineralized microbial cells (Bailey et al., 2007), were observed during exponential and stationary phase. Such specific cell structure was suggested associated with a passive way of biomineralization, where the presence of cell membrane and extracellular polymeric substances (EPS) bind cations (e.g. Mg^{2+}) to promote heterogeneous nucleation (González-Muñoz et al., 2010). The negatively charged cell out layer of *B. pumilus* is likely to have accumulated Mg^{2+} to induce the bio-struvite particles along cell surface, and these which firmed attached to cell membrane to encrust cell/cell cluster.

6.3 Bio-struvite production through biological controlled biomineralization process

Results of Chapter 3 and 4 showed that *B. antiquum* and *I. loihiensis* contained intracellular vesicle-like structures, which enclosed electron-dense granules/materials, in both synthetic solution and in wastewater (Figure 3-6, Figure 4-6 a-b), which was recognized as a signature feature of biological controlled mineralization (BCM) process. Previous studies have shown that these vesicle-like structures served as compartmentalized microenvironments where the Mg^{2+}, PO_4-P and NH_4-N ions accumulated for crystal biomineralization (Grover, Rope and Kaneshiro, 1997; Mann, 2001; Smirnov et al., 2005).

Results of Chapter 2 showed that *B. antiquum* and *I. loihiensis* made use of nitrogenous compounds as a carbon source, which was similar as the other three microorganisms. Results of Chapter 3 and 4 showed that *B. antiquum* growth in synthetic solution (μ =0.21 1/h) and wastewater (μ =0.08 1/h) raised the matrix pH to 8.68 and 8.39, released NH_4-N (105 mg/L in synthetic solution and 57 mg/L in wastewater), and produced bio-struvite (Dv_{50} of 110 and 131 μm, gap between Dv_{90} and Dv_{50} of 103 and 123 μm, in synthetic solution and wastewater respectively). *I. loihiensis* growth in synthetic solution (μ =0.16 1/h) and wastewater (μ =0.02 1/h) raised the matrix pH to 8.43 and 8.22, released NH_4-N (105 mg/L in synthetic solution and 30 mg/L in wastewater), and produced bio-struvite (Dv_{50} of 132 and 85 μm, gap between Dv_{90} and Dv_{50} of 113 and 127 μm, in synthetic solution and wastewater respectively).

Compared with the other three microorganisms*, B. antiquum* and *I. loihiensis* produced bio-struvite of relatively small size, but with high homogeneity in crystal size and morphology. The morphology of bio-struvite crystals were modified from coffin-lid shape (*B. antiquum*) and long bar shape (*I. loihiensis*) in synthetic solution to trapezoidal-platy shape in wastewater, indicating the impact of wastewater on crystal morphology.

6.4 Benefits and possible application of bio-struvite in wastewater industry

Results of Chapter 3 and 4 indicated bio-struvite nucleation occurred when the solution $SI_{struvite}$ achieved 0.6 to 0.8 (Figure 3-5 a, Figure 4-3 e), which is lower than previously reported $SI_{struvite}$ for spontaneous precipitation of abiotic struvite (e.g. $SI_{struvite}$ = 1.13-3.33) (Ariyanto, Sen and Ang, 2014; Le Corre et al., 2009; Galbraith and Schneider, 2010). Homogeneous nucleation of abiotic struvite has been report to occur only in the supersaturated zone, followed by crystal growth ideally in metastable zone (Ulrich and Stelzer, 2011). The energy barrier for struvite crystallization could be reduced by seeding (e.g. sand, struvite powder) to promote heterogeneous nucleation/crystal growth in metastable zone (Cornel and Schaum, 2009; Liu et al., 2013). In the bio-struvite biomineralization process, the role of seeds was substituted with organic substance (e.g. cell outer layer, intracellular vesicles, EPS), and the anionic nature of these substances further promoted the heterogeneous nucleation via mechanisms described in Chapter 3 and 4. Thus compared with conventional abiotic struvite precipitation, bio-struvite biomineralization has the advantage to nucleate within a much reduced range of $SI_{struvite}$ (metastable zone), which was also beneficial for the subsequent crystal growth. Furthermore, unlike abiotic struvite precipitation where the pH adjustment is frequently necessary, by chemical dose (e.g. sodium hydroxide) (Le Corre et al., 2009), the tested microorganisms were capable to increase pH, as demonstrated Chapter 3 and 4, through aerobic metabolism of nitrogenous compounds to create alkaline condition (pH 8.4-8.7 in synthetic solution, pH 8.2-8.4 in wastewater), and at the same time remove organic carbon (measured as SCOD), which was recognized as other benefit.

The results of Chapter 5 showed the tested microorganisms were capable to produce bio-struvite in wastewater with PO_4-P concentration of ≥19.7 mg/L (Figure 5-3 c). This concentration was lower than the previously reported an economically rewarding minimum PO_4-P of 50 mg/L for P recovery (Cornel and Schaum, 2009). Furthermore, within the investigated PO_4-P range (5.4-62.4

mg/L), the significant initial PO_4-P concentration for P removal efficiency was 19.7 mg/L, and for bio-struvite production and Dv_{50} was 33.9 mg/L, respectively (Table 5-2). No significant difference of bio-struvite production was observed when initial PO_4-P concentration increased from 33.9 to 62.4 mg/L, i.e., above the significant concentration (Figure 5-3 c). Whereas the initial NH_4-N only presented significant positive effect on Dv_{50}, but could not significantly influence the P removal efficiency and bio-struvite production (Table 5-2). These results suggest that a wide P range concentrations can be used for bio-struvite biomineralization, enhancing the flexibility of the process for application in WWTP. In waste streams rich of NH_4-N (e.g. digester supernatant, return centrate), efficient bio-struvite crystal separation from liquid may occur by simple settling. In particular, the P removal efficiency by *B. antiquum* was high and relatively stable (67-97%), within the investigated range, and not significantly dependent on initial parameters (i.e. PO_4-P, NH_4-N, $SI_{struvite}$) (Figure 5-3 a, Table 5-3). Even at PO_4-P of 5.4 mg/L, *B. antiquum* removed 87-97% of PO_4-P from wastewater, and achieved final PO_4-P <1 mg/L (Figure 5-3 a). This correlates highly with results of Chapter 3 and 4, and re-enforce the interpretation that *B. antiquum* formed bio-struvite through BCM, where it absorbed and accumulated PO_4-P and Mg^{2+} inside specific cell structures to form intracellular bio-struvite. Furthermore, Simoes (2017) reported the microbial capability of *B. antiquum* to use organic and condensed P fractions to produce bio-struvite. It is suggested that *B. antiquum* has the potential to remove inorganic and organic P from raw municipal wastewater typically containing total P of 6-25 mg/L (Henze and Comeau, 2008).

The application of P recovery through bio-struvite at WWTPs needs to take the microorganisms biochemical properties into consideration (Smolke, 2009). Results of Chapter 2 showed that the tested microbial strains grew at temperatures within mesophilic range (22 to 34 °C), neutral pH to mild alkaline (7-8) and could use proteins as carbon source, but lacked the ability to directly use of carbohydrates. *I. loihiensis* preferred NaCl of 3.5% w/v, and the other microorganisms preferred NaCl of 0.5-1% w/v or even lower. The presence of

calcium (27.8 mg/L) had a positive impact on *I. loihiensis* growth, but negative to *M. xanthus* growth. Furthermore, *B. pumilus B. antiquum H. salinarum* and *M. xanthus* were observed capable to produce urease, thus P recovery through bio-struvite might have potential use in urine (pH about 6). The wastewater streams (e.g. raw settled liquors) that could be used for P recovery through bio-struvite in WWTPs would vary with microbial strains, according to the characteristic of wastewater streams. In any case, forced aeration and organic nitrogenous source is likely to be needed to meet the requirements for microbial growth and specific metabolic pathways that lead to bio-struvite production.

6.5 Potential usage of bio-struvite recovered from wastewater

The potential use of abiotic struvite as a fertilizer has been widely reported. However, the properties of bio-struvite have not been previously investigated in detail. Results in Chapter 5 showed that the nutrient content in bio-struvite recovered from wastewater was 11.9-12.3% P, 5.4-5.8% N and 15.5-16.2% MgO (Table 5-5), which was within a proposed acceptable purity range of struvite as fertilizer (ESPP, 2015) and met the EU permissible levels for N and P in inorganic fertilizer (FOMA, 2014; FWG, 2014). Besides, bio-struvite also contained small quantity of K^+ (0.6-0.8 g/kg) and Ca^{2+} (0.1-0.2 g/kg) that may benefit the plant growing. Furthermore, due to low solubility of abiotic struvite in water, the nutrients are released to soil at slow rate, which protect allows a commercially profitable application of single high dose without damage to plant growing (De-Bashan and Bashan, 2004). The heavy metal content (Cr, Ni, Cu, As, Cd, Pb and Hg) in bio-struvite was o much lower than the EU limit (Table 5-5) (ESPP, 2015; FOMA, 2014; FWG, 2014). Thus regarding to the nutrients and heavy metal content, the recovered bio-struvite has the potential to be applied as a slow release fertilizer, but further examination with respect to the organic contaminants (e.g. pharmaceuticals), pathogens and viruses is required, to meet EU regulations.

6.6 Contribution to knowledge

Overall this work has contributed to the identification of mechanisms involved in bio-struvite biomineralization in synthetic solutions and wastewater and explored its potential application to the wastewater industry. Table 6-1 summarizes the contributions to knowledge that this PhD.

Table 6-1 Contributions to knowledge presented by the research work

	What has been confirmed	What has been developed	What has advanced knowledge
Theoretical knowledge	• *B. antiquum* produces urease (Chapter 2) • *B. antiquum*, *H. salinarum* cannot use carbohydrates directly, as carbon sources (Chapter 2) • *I. loihiensis* were adapt to grow in 3.5% w/v NaCl (Chapter 2) • All the microorganisms could use protein/amino acid as organic carbon source and grew under mesophilic temperature (22-34 °C) (Chapter 2) • The microorganisms investigated could biodegrade proteins to	• *H. salinarum* grew in <0.5% w/v NaCl. (Chapter 2) • Growth rates of the selected microorganisms were 0.16-0.28 1/h in synthetic B41 media (Chapter 3), and 0.02 to 0.08 1/h in wastewater (Chapter 4). • Bio-struvite (>10 μm) production was 1481-1567 mg /L in B41 media (Chapter 3) and 93 - 154 mg/L in wastewater (Chapter 4). • The bio-struvite and abiotic struvite recovered from wastewater were of similar content of P (11.9-12.7%), N(5.2-5.8%), Mg (9.3-9.8%)	• *B. pumilus*, *M. xanthus* and *H. salinarum* produced urease (Chapter 2) • Calcium (27.8 mg/L) hindered *M. xanthus* growth (Chapter 2) • *I. loihiensis* was facultative anaerobe and used NO_3-N as an electron accepter (Chapter 2) • *I. loihiensis* was grew in mild alkaline pH, and in the presence of Ca^{2+} (27.8 mg/L) (Chapter 2) • *I. loihiensis* lacks urease and cannot use ornithine as carbon source (Chapter 2) • *H. salinarum, B. pumilus* and *M. xanthus* produced bio-struvite through BIM in synthetic media and municipal wastewater (Chapter 3 and 4) • *B. antiquum* and *I. loihiensis* produced bio-struvite through BCM in synthetic media and municipal wastewater (Chapter 3 and 4) • Bio-struvite occurred in synthetic solution and

	release NH_4-N and raise the pH to create mild alkaline conditions for bio-struvite formation (Chapter 3 and 4)	and heavy metals, which met EU standard (Chapter 5)	wastewater when $SI_{struvite}$ reached 0.6 - 0.8 (Chapter 3 and 4) • The bio-struvite recovered from synthetic solution and wastewater contained Mg^{2+}, PO_4-P and NH_4-N in equal molar concentrations. (Chapter 3, 4 and 5)
Empirical evidence	• Morphology of bio-struvite crystals include coffin-lid shape, long bar shape and trapezoidal-platy shape, with and without truncated apices (Chapter 2, 3 and 4) • The microorganisms investigated could influence the crystal morphology (Chapter 3 and 4) • *B. antiquum* produced vesicle-like structure enclosing electron-dense	• *I. loihiensis* produced bio-struvite crystals of Dv_{90} >200 μm in liquids containing 0.8-1.0 % w/v NaCl (Chapter 3 and 4). • The initial NH_4-N, PO_4-P and $SI_{struvite}$ had positive relationship with the P removal efficiency, crystal production and size distribution. (Chapter 5) • The tested microorganisms were capable to produce bio-struvite in wastewater containing PO_4-P ≥19.7 mg/L	• Formation of bio-struvite only occurred under aerobic conditions. (Chapter 2) • There was no significant increase of P removal efficiency when initial PO_4-P concentration increased from 19.7 mg/L to 62.4 mg/L. (Chapter 5) • There was no significant increase of bio-struvite production and Dv_{50} when initial PO_4-P concentration increased from 33.9 mg/L to 62.4 mg/L. (Chapter 5) • Initial NH_4-N presented significant positive effect on Dv_{50}, and large crystal groups (Dv_{50} ≥100 μm) were obtained at initial NH_4-N ≥180 mg/L. (Chapter 5) • P removal efficiency by *B. antiquum* from

	granules which were associated with BCM bio-struvite (Chapter 3 and 4)	(Chapter 5) • *B. antiquum* removed P from wastewater to achieve a final PO_4-P concentration < 1 mg/L (Chapter 5) • P removal efficiency by *B. antiquum* from wastewater was relative stable (67-97%) within PO_4-P concentrations from 5.4 to 62.4 mg/L. (Chapter 5)	wastewater was independent on the initial PO_4-P, NH_4-N and $SI_{struvite}$ (Chapter 5) • Observation of vesicle-like structure enclosing electron-dense material in *I. loihiensis* cultures. (Chapter 3 and 4) • *B. pumilus* produce crusted cell/cell clusters, which may relate to epicellular biomineralization. (Chapter 3 and 4) • The estimated intracellular $SI_{struvite}$ of *B. antiquum* and *I. loihiensis* correlated to the observation of intracellular vesicles with granules/material. (Chapter 3)
Methodology		• Transmission electron microscopy methods with no staining could be used to examine intracellular vesicles. (Chapter 3 and 4)	• Flow cytometer could be used to identify intact cell and inorganic particles by SG-PI co-staining methods. (Chapter 3 and 4) • Mastersizer methods were developed to measure bio-struvite particle size and identify the heterogeneity/heterogeneous in crystal size. (Chapter 3 and 4)

6.7 Future work

This section concludes with the suggestions of further work arising from this PhD thesis.

Investigate interaction between organic substance (e.g. cell membrane, EPS matrix) and bio-struvite biomineralization in controlled conditions and in wastewater streams

Results in Chapter 2, 3, 4 and 5 showed the microbial capability to produce bio-struvite in controlled condition and in wastewater streams. These results indicated the possibility of organic substances (cell membrane, EPS matrix) contribute to the biomineralization process, as previously reported (Frankel and Bazylinski, 2003). *M. xanthus, I. loihiensis and H. salinarum* were reported produce EPS matrix in synthetic media (González-Muñoz et al., 2008, 2010; Merroun et al., 2003). Dead *M. xanthus* cells, irrespective of the cells entire or disrupted, were observed capable to induce bio-struvite biomineralization (González-Muñoz et al., 2010).

Identify the factor that limited the growth of the investigated microorganisms and the environmental influence on bio-struvite biomineralization to maximum bio-struvite production in municipal wastewater

The results of Chapter 2, 3 and 4 indicated that the aerobic metabolism of nitrogenous compounds was linked to bio-struvite biomineralization, and bio-struvite yield reduced with growth rate decreasing. In particular, the limited microbial growth in synthetic solution and wastewater was probably due to lack of essential vitamins and micronutrients, but this requires further investigation to identify the factor that limited the growth. Furthermore, presence of specific compounds (e.g. NaCl) was reported to hinder the bio-struvite production (Simoes et al., 2017). Thus bio-struvite production can be affected by metabolic pathway, microbial growth and other environmental influences. To maximize the

bio-struvite production in wastewater, a solution needs to be found to balance the effect from these three aspects.

Evaluate potential use of *B. pumilus* and *B. antiquum* cells recovered from wastewater as bio-seeds for bio-struvite biomineralization.

Results in Chapter 5 indicated the microbial capability of *B. antiquum* and *B. pumilus* to recover PO_4-P from wastewater containing low PO_4-P (5.4 mg/L), with 87- 97% and 51- 65%, respectively. The occurrence of crusted *B. pumilus* cell/cell clusters and intracellular vesicles within *B. antiquum* cells were described in Chapter 3 and 4. These specific cell structures/organic molecules were associated with the mechanisms involved in bio-struvite biomineralization and may have potential to be used as bio-seeds for P recovery. The application of such bio-seeds can facilitate the nucleation of bio-struvite formation in solution and promote crystal growth within metastable zone.

Assess the microbial capability for P removal, bio-struvite production and quality of the recovered bio-struvite using different wastewater streams to confirm the application of bio-struvite biomineralization in wastewater industry

The results of Chapter 5 showed the microbial capability to remove and recover P by bio-struvite from wastewater containing PO_4-P of 5.4 to 62.4 mg/L, whereby the microorganism were suggested have potential use using different wastewater streams for bio-struvite production process. The microbial strains to be applied varied with PO_4-P and the wastewater characteristic such as ammonia concentration, temperature, pH, DO, depended on their biochemical property and capability to remove and recover P from the wastewater.

6.8 References

Ariyanto, E. et al. (2014) ‘The influence of various physico-chemical process parameters on kinetics and growth mechanism of struvite crystallisation’, *Advanced Powder Technology*, 25(2) The Society of Powder Technology Japan, pp. 682–694.

Bailey, J. V. et al. (2007) ‘Evidence of giant sulphur bacteria in Neoproterozoic

phosphorites', *Nature*, 445(7124), pp. 198–201.

Cornel, P. and Schaum, C. (2009) 'Phosphorus recovery from wastewater: needs, technologies and costs', *Water Science and Technology*, 59(6), pp. 1069–1076.

Le Corre, K.S. et al. (2009) 'Phosphorus recovery from wastewater by struvite crystallization: a review', *Critical Reviews in Environmental Science and Technology*, 39(6), pp. 433–477.

De-Bashan, L.E. and Bashan, Y. (2004) 'Recent advances in removing phosphorus from wastewater and its future use as fertilizer (1997-2003)', *Water Research*, 38(19), pp. 4222–4246.

ESPP (2015) *Proposed E.U., fertiliser regulation criteria for recovered struvite*. Available at: https://phosphorusplatform.eu/images/download/ESPP struvite FR criteria proposal sent 24-4-15.pdf (Accessed: 1 February 2018).

FOMA (2014) *Comments heavy metals limits on fertilising materials*. Available at: http://ec.europa.eu/transparency/regexpert/index.cfm?do=groupDetail.groupDetailDoc&id=13108&no=5 (Accessed: 1 February 2018).

Frankel, R.B. and Bazylinski, D.A. (2003) 'Biologically induced mineralization by bacteria', *Reviews in Mineralogy and Geochemistry*, 54(1), pp. 95–114.

FWG (2014) *Essential safety and quality requirements for fertilising materials Fertilisers Working Group meeting General principles : safety*. Available at: http://ec.europa.eu/transparency/regexpert/index.cfm?do=groupDetail.groupDetailDoc&id=12426&no=7 (Accessed: 1 February 2018).

Galbraith, S.C. and Schneider, P.A. (2010) 'A review of struvite nucleation studies', in *Nutrient Recovery from Wastewater Streams*. , pp. 69–78.

González-Muñoz, M.T. et al. (2008) 'Ca-Mg kutnahorite and struvite production by *Idiomarina* strains at modern seawater salinities', *Chemosphere*, 72(3), pp. 465–472.

González-Muñoz, M.T. et al. (2010) 'Bacterial biomineralization: new insights from *Myxococcus*-induced mineral precipitation', *Geological Society, London, Special Publications*, 336(1), pp. 31–50.

Grover, J.E. et al. (1997) 'The occurrence of biogenic calcian struvite, $(Mg,Ca)NH_4PO_4.6H_2O$, as intracellular crystals in *Paramecium*', *Journal of Eukaryotic Microbiology*, 44(4), pp. 366–373.

Henze, M. and Comeau, Y. (2008) 'Wastewater characterization', in *Biological wastewater treatment: principles modelling and design*. IWA publishing, pp. 33–52.

Kemacheevakul, P. et al. (2015) 'Effect of magnesium dose on amount of pharmaceuticals in struvite recovered from urine', *Water Science and*

Technology, 72(7), pp. 1102–1110.

Liu, Y. et al. (2013) ‘Magnesium ammonium phosphate formation, recovery and its application as valuable resources: a review’, *Journal of Chemical Technology and Biotechnology*, 88(2), pp. 181–189.

Mann, S. (2001) *Biomineralization : principles and concepts in bioinorganic materials chemistry*. Oxford University Press.

Merroun, M.L. et al. (2003) ‘Lanthanum fixation by *Myxococcus xanthus*: cellular location and extracellular polysaccharide observation’, *Chemosphere*, 52(1), pp. 113–120.

Simoes, F. (2017) *A new route to recover phosphorus from waste water: biological struvite production School*. Cranfield University.

Simoes, F. et al. (2017) ‘Understanding the growth of the bio-struvite production *Brevibacterium antiquum* in sludge liquors’, *Environmental Technology*, Taylor & Francis, pp. 1–10.

Sinha, A. et al. (2014) ‘Microbial mineralization of struvite: a promising process to overcome phosphate sequestering crisis’, *Water Research*, 54, pp. 33–43.

Smirnov, A. et al. (2005) ‘Formation of insoluble magnesium phosphates during growth of the archaea *Halorubrum distributum* and *Halobacterium salinarium* and the bacterium *Brevibacterium antiquum*’, *FEMS Microbiology Ecology*, 52(1), pp. 129–137.

Smolke, C. (ed.) (2009) *The metabolic pathway engineering handbook: fundamentals (Vol. 1)*. CRC press.

Tansel, B. et al. (2018) ‘Struvite formation and decomposition characteristics for ammonia and phosphorus recovery: a review of magnesium-ammonia-phosphate interactions’, *Chemosphere*, 194, pp. 504–514.

Ulrich, J. and Stelzer, T. (2011) ‘Crystallization’, in *Kirk-Othmer Encyclopedia of Chemical Technology*. 4th edn. , pp. 1–63.

7 Conclusions

The overall conclusions of this project are presented with respect to the PhD objectives.

Objective A: Identify the factors that impact the growth of the selected microorganisms and bio-struvite production.

- Bio-struvite biomineralization only occurred under aerobic condition, and depended on the microbial growth.
- The microbial growth of the tested microorganisms took place to mesophilic range of temperatures (22-34°C), at neutral to mild alkaline pHs (7-8), and protein/amino acids were the preferred carbon source. *I. loihiensis* growth adapted to 3.5% w/v NaCl and with the presence of Ca^{2+}, while the other microorganisms preferred NaCl at concentrations less than 1% w/v.

Objective B: Understand the mechanisms of bio-struvite biomineralization in synthetic solutions and municipal wastewater and investigate the influence of wastewater on bio-struvite biomineralization.

- The tested microbial strains biodegraded nitrogenous organic compounds to release NH_4-N and raise the pH to create mild alkaline conditions for bio-struvite formation in synthetic solution and municipal wastewater.
- *H. salinarum, B. pumilus* and *M. xanthus* produced bio-struvite through BIM process. Occurrence of crusted *B. pumilus* cell structures was associated with epicellular biomineralization.
- *B. antiquum* and *I. loihiensis* produced bio-struvite crystals of homogeneous size and morphology with high reproducibility, as a result of high cellular control during the biomineralization. Electron-dense granules/materials enclosed in membrane-bound compartments (intracellular vesicles) were observed in the cytoplasm. Hence *B. antiquum* and *I. loihiensis* produced bio-struvite through BCM process.
- The mechanisms involved in bio-struvite biomineralization in municipal wastewater were similar as in synthetic solution. However, wastewater

affected microbial growth and changed the bio-struvite morphology by enhancing specific crystal faces.

Objective C: Evaluate the potential application of bio-struvite biomineralization process to wastewater treatment plants and potential use of bio-struvite as inorganic fertiliser.

- The PO_4-P removal efficiency, crystal production and Dv_{50} presented a positive relationship with the initial nutrient concentrations within the investigated range. The selected microorganisms were capable to produce bio-struvite in wastewater at initial PO_4-P concentrations of ≥19.7 mg/L. A significant PO_4-P level for P removal efficiency was 19.7 mg/L, and for bio-struvite production and Dv_{50} was 33.9 mg/L, respectively. The initial NH_4-N concentration had significantly positive effect on Dv_{50}. When compared with abiotic struvite precipitation, bio-struvite biomineralization had potential to be applied in wastewater with lower and wider P range concentrations.
- The P removal efficiency by *B. antiquum* was maintained at relatively stable high level, and presented less dependence on initial NH_4-N, PO_4-P and $SI_{struvite}$. *B. antiquum* removed PO_4-P from initial concentrations of 5.4 mg/L to less than 1 mg/L, thus it has the potential to be applied to remove P from raw municipal wastewater.
- Bio-struvite recovered from municipal wastewater was of high purity and contained extremely low heavy metal content. It met the European standard with respect to P, N and heavy metal content, indicating its potential use as an alternative of P and N fertilizer.